Instituto Universitário de Lisboa

Department of Information Science and Technology

Superchannel Transmission over Flexible-Grid Optical Networks

Paulo José da Costa Marinho Pereira

A Dissertation presented in partial fullfillment of the requirements
for the Degree of
Master in Telecommunications and Computer Engineering

Supervisor
Prof. Dr. João Rebola, Assistant Professor
ISCTE - Instituto Universitário de Lisboa
Co-Supervisor
Prof. Dr. Luis Cancela, Assistant Professor
ISCTE - Instituto Universitário de Lisboa

October 2019

Acknowledgements

Quero agradecer ao ISCTE-IUL, ao Instituto de Telecomunicações e aos meus orientadores a oportunidade de fazer esta dissertação no domínio da comunicação óptica, e também pelo trabalho que tiveram em analisar as versões que lhes apresentei.

Quero agradecer à minha esposa, Engª. Conceição Pereira, e à minha filha, Drª. Helena Pereira, que sempre me apoiaram em todos os momentos. Além de que elas dispensaram-me de muitas tarefas para que eu dispusesse de todo o tempo possível para me dedicar a fazer o presente trabalho. Foram incontáveis serões, fins-de-semana e muitos dias de férias dedicados a estudar comunicação óptica, a desenvolver o simulador que permitiu obter os resultados aqui apresentados e, por fim, a escrever esta dissertação. Sem elas este trabalho não existiria, e por isso lhes fico eternamente grato.

Resumo

O uso de super-canais tem sido proposto como uma boa relação custo-benefício para suportar a futura procura de capacidade de dados nas redes de transporte a longa distância. Contudo, nos super-canais, o espectro dos sub-canais está muito compactado e a interferência entre sub-canais pode tornar-se uma limitação.

Enquanto atravessa a rede óptica, um super-canal passa através de vários multiplexadores ópticos reconfiguráveis de inserção e extracção (ROADMs, em inglês). O efeito acumulado da filtragem de uma cascata de filtros baseados em comutadores selectivos no comprimento-de-onda (WSS em inglês) que se encontram dentro dos ROADMs, reduz a largura-de-banda disponível e causa distorção no sinal óptico. A performance dos sub-canais é significativamente dependente do espaçamento entre sub-canais, da interferência entre sub-canais e da filtragem nos WSS's.

Neste trabalho, avalia-se exaustivamente a penalidade na relação sinal-ruído óptica (OSNR, em inglês) devido a filtragem óptica e interferência entre sub-canais, usando diferentes formatos de modulação *M*-QAM, ritmos de símbolos, factores de excesso de banda, número de WSS's, larguras-de-banda dos WSS's, número de sub-canais e espaçamento entre portadoras. Fornece-se um procedimento para obter valores optimizados para estes parâmetros que garantem que a penalidade na OSNR é menor que 1.5 dB em todos os sub-canais depois de 20 WSS's.

Comparam-se também dois modelos espectrais para o filtro WSS, denominados analítico e super-Gaussiano. Investiga-se o uso da penalidade da EVM, computacionalmente muito mais rápida, como métrica de desempenho e conclui-se que fornece resultados mais pessimistas que a penalidade da OSNR para estimar a distorção da cascata de filtros.

Palavras-Chave: comutadores selectivos no comprimento-de-onda; interferência entre sub-canais; penalidade na magnitude do vector de erro; penalidade na relação sinal-ruído óptica; rede óptica com grelha flexível; super-canais

.

Abstract

Superchannels have been proposed as a cost-effective solution to cope with the future data capacity demand in long-haul transport networks. However, in superchannels, the spectrum of the subchannels is tightly packed and the crosstalk between subchannels can become a performance constraint.

Along its path in the optical network, a superchannel passes through several reconfigurable optical add-drop multiplexers (ROADMs). The cumulative filtering effect of the cascaded wavelength selective switches (WSSs), inside the ROADMs, reduces the available bandwidth and leads to signal distortion. The subchannels performance is significantly dependent on the intercarrier spacing. If too large, the edge subchannels suffer a higher distortion from the filtering cascade. If too narrow, it creates a considerable intercarrier crosstalk between the subchannels.

In this work, we perform the exhaustive assessment of the optical signal-to-noise ratio (OSNR) penalties due to the optical filtering and intercarrier crosstalk between subchannels using different *M*-ary quadrature amplitude modulation (*M*-QAM) formats, symbol rates, roll-off factors, number of traversed WSSs, WSS bandwidths, number of subchannels and intercarrier spacing. We provide a procedure to obtain optimized values of these parameters that guarantee an OSNR penalty below 1.5 dB for all subchannels after 20 WSSs.

Two WSS filter spectral models are compared, named analytical and super-Gaussian. We have shown the use of the computationally much faster performance metric, the error vector magnitude (EVM) penalty, and concluded that it provides a more pessimistic performance estimate than the OSNR penalty, to estimate the distortion due to the filters cascade.

Keywords: error vector magnitude penalty; flexible-grid optical network; intercarrier crosstalk; optical signal-to-noise ratio penalty; superchannel; wavelength selective switch.

Contents

List of Figures

List of Tables

List of Acronyms

4-QAM	Quadrature Amplitude Modulation with 4 constellation points
8-QAM	Quadrature Amplitude Modulation with 8 constellation points
16-QAM	Quadrature Amplitude Modulation with 16 constellation points
ADC	Analog-to-Digital Converter
ASE	Amplified Spontaneous Emission
ASK	Amplitude-Shift Keying
AWG	Arrayed-Waveguide Gratings
AWGN	Additive White Gaussian Noise
B2B	Back-to-Back
BER	Bit Error Rate
DAC	Digital-to-Analog Converter
DEC	Direct Error Count
DSP	Digital Signal Processing
EDFA	Erbium-Doped Fiber Amplifier
EON	Elastic Optical Network
EVM	Error Vector Magnitude
FEC	Forward Error Correction
FPGA	Field Programmable Gate Array
ICI	Inter-Channel Interference
IQ	In-phase/Quadrature
ISI	Intersymbol Interference
ITU-T	International Telecomunication Union, Telecommunication Sector
LCoS	Liquid Crystal on Silicon
LPF	Low-Pass Filter
MEMS	Micro-Electromechanical System
M-QAM	*M*-ary Quadrature Amplitude Modulation
OQF	Optical Quadrature Front-End
OSNR	Optical Signal-to-Noise Ratio
OTF	Optical Transfer Bandwidth
OTN	Optical Transport Network
PBC	Polarization Beam Combiner
PBS	Polarization Beam Splitter
PDF	Probability Density Function
PM	Polarization Multiplexing
PSD	Power Spectral Density
PSK	Phase-Shift Keying
ROADM	Reconfigurable Optical Add-Drop Multiplexer
RC	Raised Cosine

RRC	Root Raised Cosine
RWA	Routing and Wavelength Assignment
SE	Spectral Efficiency
TLD	Tunable Laser Diode
WDM	Wavelength-Division Multiplexing
WSS	Wavelength Selective Switch

List of Symbols

a_k	Symbol amplitude in the I or Q component
B	-6dB bandwidth of the WSS filter
B_{eq}	Noise-equivalent bandwidth
B_{mdB}	Bandwidth of the super-Gaussian filter at the *m dB* power level
B_{otf}	OTF bandwidth
B_{RC}	RC filter bandwidth
B_{ref}	Reference bandwidth
d_{th}	Threshold distance
E	Energy of a symbol in the constellation
E_b	Average energy per bit
E_s	Average energy per symbol
evm	Error vector magnitude
EVM	Error vector magnitude in dB
$evm_{filtering}$	EVM due to filtering
$EVM_{filtering}$	EVM due to filtering in dB
evm_{noise}	EVM due to noise
EVM_{noise}	EVM due to noise in dB
evm_{RMS}	Root-mean square of the error vector magnitude
evm_{total}	Total EVM due to noise and filtering
EVM_{total}	Total EVM due to noise and filtering in dB
g	Amplifier power gain
h	Planck constant
$H_N(f)$	Transfer function of the Nyquist filter
$h_{RC}(t)$	Raised-cosine pulse
$H_{RC}(f)$	RC transfer function
$h_{RRC}(t)$	Impulse response function of the RRC filter
$H_{RRC}(f)$	Transfer function of a RRC filter
M	Modulation format order
m	Power level in dB
n	Noise power
N_a	Number of samples per symbol
N_{ASE}	PSD of the ASE noise
N_{ch}	Number of subchannels
N_o	Power spectral density of noise
N_t	Number of transmitted symbols
n_{sg}	Order of the super-Gaussian filter
n_{sp}	Spontaneous noise emission factor
$osnr$	Optical signal-noise ratio
$OSNR$	Optical signal-noise ratio in dB
P	Symbol error probability
P_b	Bit error probability

P_s	Average symbol error probability
$R(f)$	Transfer function of the LCoS matrix
R_b	Bit rate
R_S	Symbol rate
s	Signal power
$S(f)$	WSS transfer function in the analytical model
$S_{0,k}$	Transmitted symbols in the complex plane
S_k	Received symbols in the complex plane
$S_{sg}(f)$	Transfer function of the super-Gaussian filter
SE	Spectral efficiency
snr	Signal-noise ratio
SNR	Signal-noise ratio in dB
T_d	Propagation delay
T_s	Symbol duration
$x(t)$	Sequence of pulses applied to the RRC filter
$y(t)$	Signal at optical transmitter output
$z(t)$	Signal at optical receiver input
$\delta(t)$	Dirac function
Δf	Intercarrier spacing
ν_0	Carrier frequency
ρ	Roll-off factor of the RRC filter
σ	Confinement parameter
σ_N^2	Noise power in an additive white Gaussian noise channel
σ_{sg}	Standard deviation of the super-Gaussian filter

Chapter 1

Introduction

1.1. Motivation

It is well known that the ever-increasing need for capacity in long-haul transport networks is primarily related to the expansion of the Internet traffic worldwide. It is vital to find the most cost-effective solution to cope with the present and perceived future demand, preferably postponing large investments in new fiber and new erbium-doped fiber amplifiers (EDFAs) deployments and new reconfigurable optical add-drop multiplexers (ROADMs) to deal with more connections and more transmission capacity.

For transparent optical paths in an optical network with ROADMs, only the traffic that is dropped or added to the network needs optical/electrical conversion, which is expensive and limited to a specific symbol rate and modulation format. The pass-through traffic remains in the optical domain and, if needed, it can be amplified (or attenuated for power equalization). The reconfiguration ability of the ROADMs allows the network operator to change the optical path as required by the traffic.

Furthermore, it would be desirable to decrease the operational cost of the existing optical networks, namely the cost of manually reconfiguring the ROADMs connections, because there are ROADMs that are not fully remotely reconfigurable and are not colourless, directionless and contentionless and manual reconfiguration is easily prone to errors leading to a network downtime increase. In addition, the ROADMs were designed for a fixed grid, *i.e.*, with a fixed interchannel spacing of 100 GHz or 50 GHz.

Nowadays, many deployed long-haul optical links still use a bit rate of 100 Gb/s (of payload) per channel with symbol rates between 28 and 35 GBd due to limitation in the electronic equipment in the transceivers.

The next generation of optical transport networks (OTN) will be using the concept of elastic optical network (EON). The main features are the use of superchannels, bandwidth variable wavelength selective switches (WSSs) inside the ROADMs, and the use of improved routing and spectrum assignment algorithms. The EON allows keeping the existing fiber deployed in the field but requires upgrading the ROADMs. The EON

has been widely accepted by industry and academia [1], because it will provide the ability to increase the capacity of the current optical links. Nowadays, each fiber can transport 100, 150, 200 Gb/s using polarization multiplexing quadrature amplitude multiplexing with 4 constellation points (PM-4QAM), PM-8QAM and PM-16QAM, [2], [3], with about one hundred wavelength-division multiplexing (WDM) channels [4].

The idea behind the EON is to allow superchannels with different bandwidths within a flexible-grid optical network. A superchannel is made of several modulated optical carriers, usually named subchannels, whose bandwidth depends on the traffic that the electronic router feeds into the ROADM or extracts from the ROADM. An experimental study has shown [4], if the whole bandwidth of the C-band was assigned to a comb of superchannels, each one with 1 Tb/s of capacity, the fiber would be able to transport 24 Tb/s instead of 9.6 Tb/s using traditional WDM channels, for a transmission distance of around 1571 km using PM-16QAM. This shows how the spectral efficiency (SE) can be increased from 2 bit/s/Hz to 5 bit/s/Hz when using superchannels or even more if higher order modulations formats are used [4].

In another experimental study [5], a 10-carrier superchannel with 1 Tb/s of capacity was able to reach a distance of 2300 km using PM-4QAM.

Capacity and SE of a superchannel are limited by the number of subchannels in each superchannel and is related the intercarrier crosstalk and cost [3], [4].

When there is an add/drop at the ROADM, all the optical subchannels in a superchannel are routed as one entity. As a result, there is no need for guard-bands between the subchannels because each subchannel is not routed individually so the subchannels can be tightly packed. Nevertheless, the crosstalk between subchannels [3] becomes a concern that must be addressed, because it creates an optical signal-to-noise ratio (OSNR) penalty that must be assessed thoroughly.

When the optical signal passes through several ROADMs in the network, it must go through several WSSs. The cumulative effect of the cascaded WSS filtering results in waveform distortion and reduced bandwidth available to the signal in the optical path, with the corresponding OSNR penalty, which must also be assessed.

Since the bandwidth of a superchannel can be changed by changing the number of subchannels and the intercarrier spacing, the WSS bandwidth must be able to change in the same way. The variable bandwidth WSS manufacturing is nowadays based on liquid crystal on silicon (LCoS) with electric remote control. The frequency slot width

granularity of the WSS is 12.5 GHz, which means that a superchannel can change its bandwidth in integral multiples of 12.5 GHz. This is also the value of the frequency slot width granularity of the flexible-grid optical network defined in [6]. The center frequency of the carrier can be displaced in integral multiples of 6.25 GHz [1] allowing that the spectrum will be used more efficiently when several superchannels, with different bandwidths, are generated in the optical network. However, with the different bandwidth superchannels and variable bandwidth WSSs, the allocation/deallocation/reallocation of spectrum can create a defragmentation that can result in unused spectrum. To solve this problem the need for routing and spectrum assignment algorithms comes into play. The network operator must be able to find a contiguous spectrum along the entire optical path.

Additionally, the modulation format must be chosen knowing the required reach and desired transmission capacity. At the expense of cost and complexity in the transceivers, we can increase the SE of a single channel, but the goal is to increase the SE of the whole C-band. For this, we need to use superchannels so that no spectrum will be wasted with band-guards between subchannels, as explained above, but also we need to use a possibility offered by the flexible-grid to reduce the bandwidth in use. Instead of a fixed grid of 50 GHz for each channel, we can have bandwidths as integer multiples of 12.5 GHz saving spectrum whenever possible, depending on the symbol rate and modulation format of the signals in the subchannels and on the number of subchannels, *e.g.*, a 75 GHz bandwidth for a superchannel with 2 subchannels instead of 2 channels with 100 GHz total bandwidth.

In optical links is always essential to consider the reach, *i.e.*, the distance that the signal can travel while the receiver is still able to recover the transmitted symbols and bits. Nowadays, with coherent-detection and digital signal processing, it is possible to modulate the amplitude and phase of the optical signal and even multiplex/demultiplex its polarization. Several *M*-QAM modulations formats are available and if one increases the number of bits per symbol, hence increasing the SE, one should expect an increase of the required OSNR at the optical receiver and, consequently and a reduced link reach [7]. On the other hand, if the fiber span is short, the measured OSNR may allow higher order modulation formats that have higher required OSNR [1]. Hence, the choice of the modulation order can be adaptative.

Since the EON will use different bandwidth superchannels [8], which allow different symbol rates and modulation formats to coexist in the same fiber link, the

transceivers must be able to generate and detect them in accordance with the link capacity and reach needed.

Recent proposals from the industry allow to double the symbol rate currently in use from 32.5 to 65 GBd in each optical channel [9], but, at the same time, force to double the bandwidth consumed by each optical channel. This is a welcomed development which does not hurt the idea of the use of superchannels because superchannels aggregate channels that must be routed as an entity allowing to eliminate the guard-bands between these channels and increasing SE. The superchannels, nowadays, are used mainly in situations where there is no dynamic variation of the number of subchannels due to the difficulty in finding spectral contiguity whenever necessary [10]. Nonetheless, the superchannels can aggregate more than just two subchannels allowing a significant increase of SE.

An extensive and rigorous assessment of the OSNR penalties due to the optical filtering and intercarrier crosstalk in optical network links using superchannels with different *M*-QAM modulation formats and symbol rates is essential to perform an accurate optimization of the optical network resources [3], [4].

1.2. Objectives

In this work we assess the performance of an optical superchannel through the use of the error vector magnitude (EVM) penalty and of the OSNR penalty associated to the inter-subchannel crosstalk and optical filtering of a cascade of ROADMs based on WSSs when using superchannels in the flexible grid using different scenarios:

a) Different modulation formats (4-QAM, 8-QAM, 16-QAM)

b) Different symbol rates

c) Different roll-off factors

d) Different number of WSSs

e) Different WSS bandwidths

f) Different number of carriers

g) Different intercarrier spacing

h) Compare two WSS spectral models: analytical and super-Gaussian models

i) Study the impact a frequency offset between the carriers frequency and the center frequency of the WSSs, within the ITU-T maximum tolerance (± 1.5 GHz)

j) Compare the EVM and OSNR penalties in terms of accuracy

1.3. Research method

As always when dealing with telecommunication technology, we have to balance performance, reach and cost. In our case, we need to transmit optical signals using the most spectrally efficient format for the required transmission capacity and reach, at an affordable cost.

To conduct the research needed for this work, we use the MATLAB software to develop a Monte Carlo simulation of the optical signal path. The whole optical path should be modelled and implemented in software, namely, optical transmitter, optical fiber, optical coherent receiver, optical amplifier and WSS-based ROADMs.

Several physical aspects of the optical communication system will be studied and presented, like the power spectral density (PSD) of the signals, eye-patterns, the constellations of the signals from different modulation formats and the WSS transfer functions. To account for the amplified spontaneous emission (ASE) noise from the EDFAs, we do noise loading at the receiver so that we can estimate the OSNR.

Regarding the performance metrics, we can compare the constellation points representing the symbols transmitted and received, and calculate the error vector magnitude (EVM). We implemented the direct error count (DEC) to obtain directly the bit error rate (BER) in the simulator. To study the optical filter bandwidth narrowing effect, we also use extensively the EVM and OSNR penalties.

With these tools, developed in this work, the studies proposed in the objective topics will be performed, discussed and important conclusions will be provided.

1.4. Dissertation organization

In Chapter 2, we present the model of the optical network with its several components and the type of signals used in this work, *i.e.*, the quasi-Nyquist WDM superchannels and how to generate them. We present and compare the analytical model and the super-Gaussian model for spectrally modelling of the WSS. We demonstrate how to make the super-Gaussian model filtering effects to approach those from the analytical model. We describe the general structure of the simulator built in MATLAB, which is able to perform Monte Carlo simulations. Next, we evoke the relationships between BER, EVM and OSNR and present the performance metrics EVM penalty and OSNR penalty used in this work. For illustration purposes and for selected scenarios,

we present the constellation points and eye-patterns, at the optical receiver input, of several modulation formats, symbol rates and roll-off factors used in this work and we relate these results with the WSS filtering effect.

In Chapter 3 we study the performance of an independently routed channel with and without the presence of side-channels in its spectral vicinity using the simulator. We start with an isolated channel to show the EVM dependences on the symbol rate and WSS bandwidth as we change the number of WSS in the cascade, without the presence of ASE noise. Then, in the presence of ASE noise, we use the EVM penalty alongside with the OSNR penalty to study how the WSS filtering can affect the optical signal for 4-QAM, 8-QAM and 16-QAM modulation formats, the symbol rates of 28 and 32.5 GBd and the roll-off factors of 0.1 and 0.3. Afterwards, we study the impact, on the system performance, of the presence of a frequency offset between the channel carrier and the WSSs center frequency. Next, we consider a channel with two side-channels and perform similar studies of performance using the EVM and OSNR penalties and also perform the frequency offset impact analysis.

In Chapter 4, we optimize the WSS bandwidth and the intercarrier spacing that guarantees OSNR penalties below 1.5 dB in all subchannels and hence provide a good quality of service for the superchannel transmission. The optimization is performed by using the OSNR penalty as performance metric to study the filter bandwidth narrowing and crosstalk effects on the optical superchannel, in center and edge subchannels, after a cascade of 20 WSSs. We also study the impact on center and edge subchannels, of the existence of a frequency offset between the WSSs center frequency and the subchannels carriers. We also investigate how the variation of the number of subchannels affects the transmission performance. Then, we calculate and study the SE of the channels and superchannels and compare several transmission scenarios. Finally, we compare a superchannel with 2 subchannels of 32.5 GBd with a single channel with twice the symbol rate.

In Chapter 5, we present the main conclusions and future work.

1.5. Dissertation main contributions

This work has the following main contributions:

- We show how the analytical model and super-Gaussian model can be used to model the WSS filter. We show how to make the super-Gaussian model similar to the

analytical model in terms of EVM penalty, OSNR penalty and PSD of the signal at the optical receiver.

- We show that the EVM and the OSNR penalties have a similar behaviour as a function of the number of cascaded WSSs, however, EVM penalty always estimates higher penalties that can reach 0.8 dB difference in relation to the OSNR penalty for OSNR penalties below 1.5 dB. For higher OSNR penalties the difference can reach 2 dB.
- We show that a frequency offset, between the subchannel carriers and the WSSs center frequency creates a significant impact on the edge frequencies of a superchannel.
- We show how the intercarrier spacing variation, can lead to increased crosstalk and distortion due to enhanced WSS filtering.
- We present a procedure to obtain the optimized WSS bandwidths and intercarrier spacings that should be used in superchannels with 2 up to 10 subchannels, so that all subchannels have an OSNR penalty below a specified threshold, after a certain number of WSSs.
- We calculate the increase in the SE and capacity when using superchannels in comparison to the scenario of independently routed channels.
- We present a performance comparison between a superchannel with 2 subchannels with a single channel with twice the symbol rate (and the same capacity) and we show that both options are similar and, hence, the choice is dependent on the network operator preferences.

References

[1] M. Jinno, "Elastic optical networking: roles and benefits in beyond 100-Gb/s era (Invited Tutorial)," *Journal of Lightwave Technology,* Vol. 35, No. 5, pp. 1116-1121, March 1, 2017.

[2] G. Bosco, V. Curri, A. Carena, P. Poggiolini and F. Forghieri, "On the performance of Nyquist-WDM terabit supechannels based on PM-QPSK, PM-8QAM or PM-16QAM subcarriers," *Journal of Lightwave Technology,* Vol. 29, No. 1, pp. 53-58, January 1, 2011.

[3] J. Pedro, "Designing transparent flexible-grid optical networks for maximum spectral efficiency (Invited)," *Journal of Optical Communications and Networking,* Vol. 9, No. 4, pp. C35-C40, April, 2017.

[4] T. Rahman *et al.*, "Long-haul transmission of PM-16QAM-,PM-32QAM-, and PM-64QAM-based terabit superchannels over a field deployed legacy fiber," *Journal of Lightwave Technology,* Vol. 34, No. 13, pp. 3071-3076, July 1, 2016.

[5] G. Gavioli *et al.*, "Ultra-Narrow-Spacing 10-Channel 1.12 Tb/s D-WDM Long-Haul Transmission Over Uncompensated SMF and NZDSF," *EEE Photonics Technology Letters,* Vol. 22, No. 19, pp. 1419-1421, October 1, 2010.

[6] ITU-T, "Recommendation ITU-T G.694.1 Edition 2.0," pp. 6-7, 2012.

[7] G. Bosco, "Chapter 4, Spectrally efficient multiplexing: Nyquist-WDM," in *Enabling technologies for high spectral-efficiency coherent optical communication networks,* Xiang Zhou, Chongjin Xie (Eds.), John Wiley & Sons, 2016, pp. 123-150.

[8] A. Napoli, *et al.*, ""Chapter 5, Transmission in elastic optical networks", in Víctor López, Luis Velasco (Eds.)," in *Elastic optical networks: architectures, technologies, and control,* Springer, 2016, pp. 123-156.

[9] Coriant Inc., "The role of higher baud rates in evolving coherent transport", white paper, Coriant Inc., 2018, pp. 6-15.

[10] T. Zami, B. Lavigne, and M. Bertolini, "How 64 GBaud optical carriers maximize the capacity in core elastic WDM networks with fewer transponders per Gb/s," *Journal of Optical Communications and Networking,* Vol. 11, No. 1, pp. A20-A30, January 2019.

Chapter 2

Model of an optical communication system with cascaded WSS-based ROADMs

2.1. Introduction

In this chapter, we describe the model of the optical communication system with coherent detection and with cascaded WSS-based ROADMs. The signals used in this work and the transfer functions for the WSS models, namely, the WSS analytical model and the WSS super-Gaussian model, are also presented. In this work, a MATLAB simulator of the optical path has been developed, which estimates several performance metrics and outputs several data and graphics such as eye-patterns, signal constellations and PSDs for its analysis.

In Section 2.2, we present the optical components of the optical network used in this work. In Section 2.3, we characterize the optical transmitter. In Subsection 2.3.1 we describe the modulation formats used and in Subsection 2.3.2 we define the type of signals considered in this work, the quasi-Nyquist WDM signals. In Subsection 2.3.3 we show how to generate the signal for each subchannel. In Section 2.4, we present the optical path with its main components. In Subsection 2.4.1, we characterize the optical fiber connecting the optical components and in Subsection 2.4.2 we explain the physical principles of the WSS and present two models to obtain its spectral shape. In Subsection 2.4.3, we describe succinctly the EDFA model. In Section 2.5, we describe the optical coherent receiver model and the subchannels detection from the superchannels. In Section 2.6, we present the simulator implemented in MATLAB including a simulation flow-chart. In Section 2.7, we describe the performance metrics used in this work to study the optical communication system. In Section 2.8, we compare the analytical model and the super-Gaussian model of the WSS filter and validate these models. In section 2.9, we present the conclusions of the chapter.

2.2. Model of the optical network

The model of the optical network used in this work is shown in Figure 2.1 with its main components: the optical transmitter, the WSSs placed along the optical path, which are inside the ROADMs, the optical coherent receiver and the optical fiber. The optical transmitter generates the superchannels considering the modulation formats and symbol rates in the subchannels, the intercarrier spacing and number of subchannels. The optical signals exit from the transmitter and enter the optical network and travel through optical fibers and WSSs in the optical nodes until they reach the optical coherent receiver. Along the optical path, the signals are subject to amplification of the EDFAs, which also adds ASE noise to the signal. In our model, we use a noise loading approach at the end of the optical path instead of considering all the distributed noise sources along the optical path. Hence, in this work, we can focus our analysis on the crosstalk between subchannels and on the filtering penalty that the WSSs impose on the optical signal. The BER, OSNR penalty and EVM penalty, due to crosstalk and WSS filtering, are calculated as performance metrics.

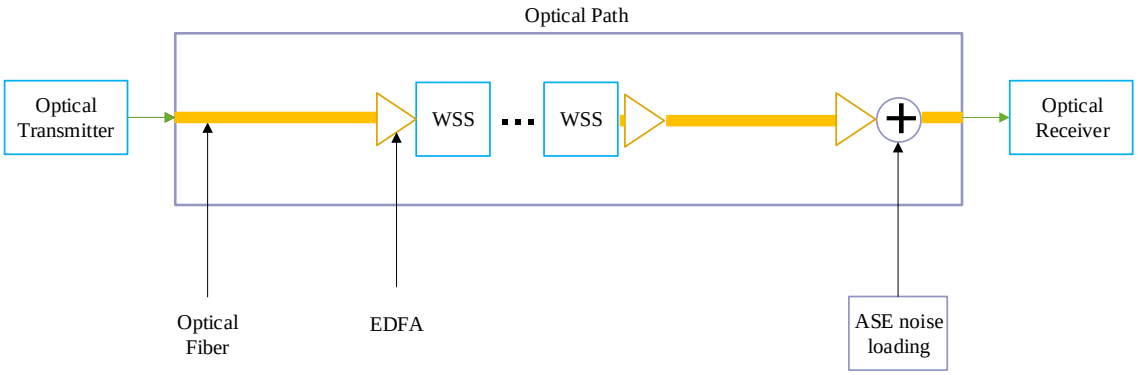

Figure 2.1 *Schematic model of an optical path inside of an optical network.*

2.3. Optical transmitter

When we have several channels, connecting the same endpoints in the optical network, we can aggregate them in a superchannel [1]. One of the techniques to generate a superchannel is the Quasi-Nyquist-WDM technique. The channels that are aggregated are called subchannels and the intercarrier spacing is the frequency spacing Δf between the subchannel carriers.

The capacity of the superchannel is the sum of the capacity of the subchannels. If we need to increase the capacity of the superchannel, we can pack more subchannels in the superchannel or use a higher modulation format. Packing more subchannels in a

superchannel can increase interchannel crosstalk. A higher modulation format reduces the length of the optical path because a higher modulation format increases the required optical signal noise ratio (OSNR) at the optical receiver to guarantee a specific quality of service [2].

In Figure 2.2, we can see a schematic of the optical transmitter that generates a superchannel with *N* subchannels [3]. It is composed of *N* sub-transmitters, one for each subchannel. In each sub-transmitter, the digital data to be transmitted enters into a digital signal processing (DSP) block where symbols are generated from groups of bits (mapping) and then a digital filter shapes the signal bandwidth for each of the in-phase and quadrature signal components. The digital signal is then applied to each digital-to-analog converter (DAC) and the analog signal then controls the in-phase/quadrature (IQ) modulators to modulate the optical wave generated from a tunable laser diode (TLD). Each polarization direction, x or y, is modulated separately and then combined by a polarization beam combiner (PBC). The optical coupler aggregates the different subchannels and launches them into the fiber as a superchannel with tightly packed subchannels.

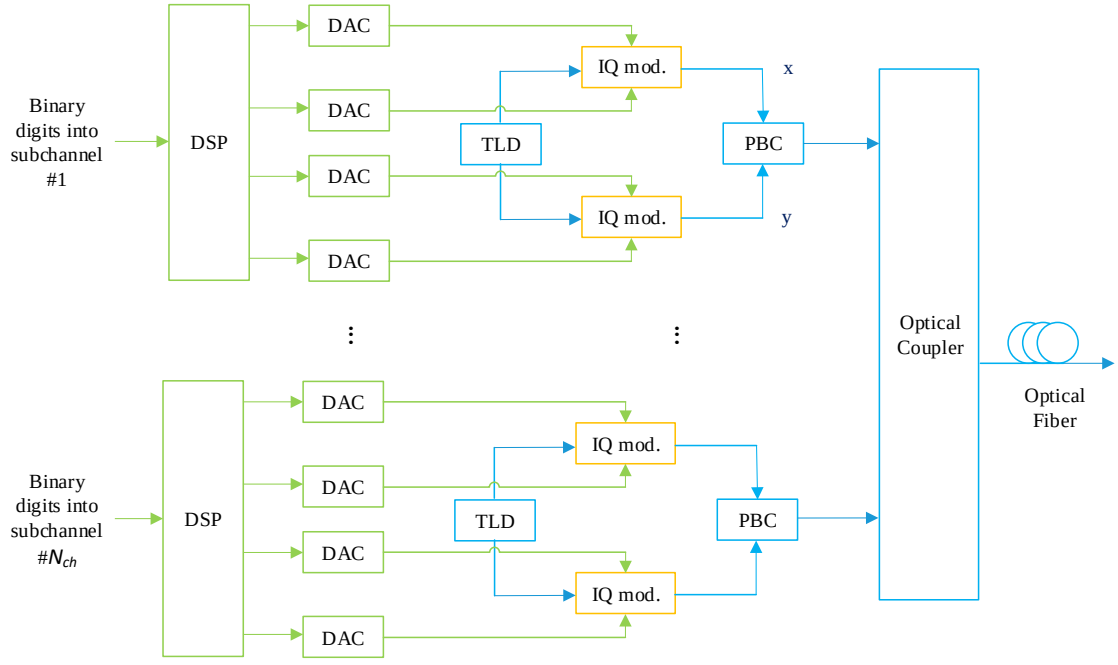

Figure 2.2 *Generation of subchannels in a superchannel based on Nyquist-WDM, where TLD is a tunable laser diode and PBC is a polarization beam combiner. The digital domain is in green and the optical domain is in blue. The conversion from the digital domain to the optical domain is done in the orange blocks.*

2.3.1. Modulation formats

In this work, we consider three modulation formats, namely, 4-QAM, 8-QAM (2-ASK/4-PSK) and 16-QAM [4]. Tables 2.1-2.3 present the mapping used to convert groups of bits into symbols, where a Gray mapping has been assumed. For the 8-QAM (2-ASK/4-PSK) modulation format case, it is not possible to implement a Gray mapping between all symbols, namely, between symbols pairs (2,5), (1,6), (3,8) and (4,7).

Table 2.1 4-QAM mapping.

Symbol	Bits	mapped symbol
1	00	1+j
2	01	1-j
3	10	-1+j
4	11	-1-j

Table 2.2 8-QAM (2-ASK/4-PSK) mapping.

Symbol	Bits	mapped symbol
1	101	1+j
2	001	-1+j
3	010	-1-j
4	110	1-j
5	000	$-1-\sqrt{3}$
6	011	$j\cdot(1+\sqrt{3})$
7	111	$1+\sqrt{3}$
8	100	$-j\cdot(1+\sqrt{3})$

Table 2.3 16-QAM mapping.

Symbol	Bits	mapped symbol	Symbol	Bits	mapped symbol
1	0000	-3-3j	9	0001	3-3j
2	1000	-3-j	10	1001	3-j
3	0100	-3+3j	11	0101	3+3j
4	1100	-3+j	12	1101	3+j
5	0010	-1-3j	13	0011	1-3j
6	1010	-1-j	14	1011	1-j
7	0110	-1+3j	15	0111	1+3j
8	1110	-1+j	16	1111	1+j

In Figures 2.3-2.5, are displayed, for the three modulation formats, the constellations in a back-to-back (B2B) configuration (without ASE noise nor WSS filtering) with their corresponding mappings.

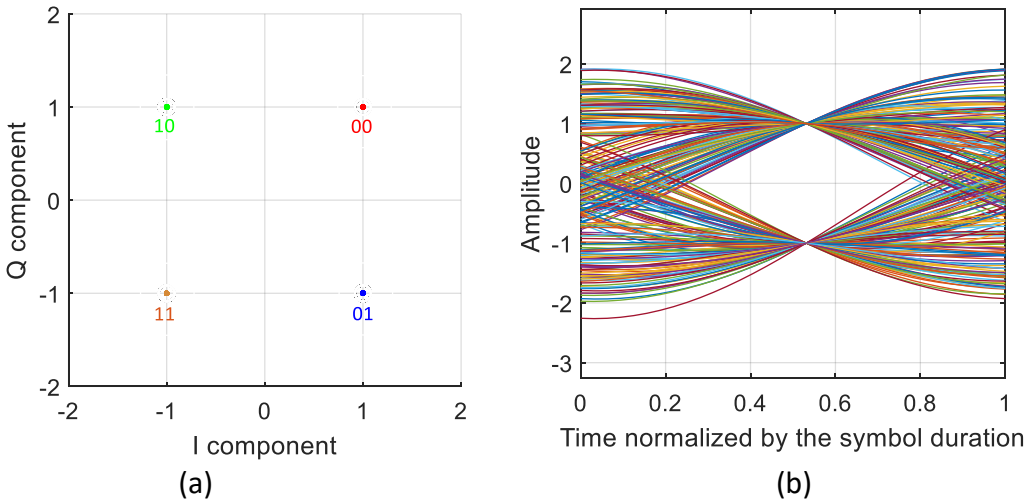

Figure 2.3 *Modulation format: 4-QAM. (a) In-phase and quadrature components of the constellation where each transmitted symbol has a different color and (b) normalized eye diagram for a 4-QAM RC signal.*

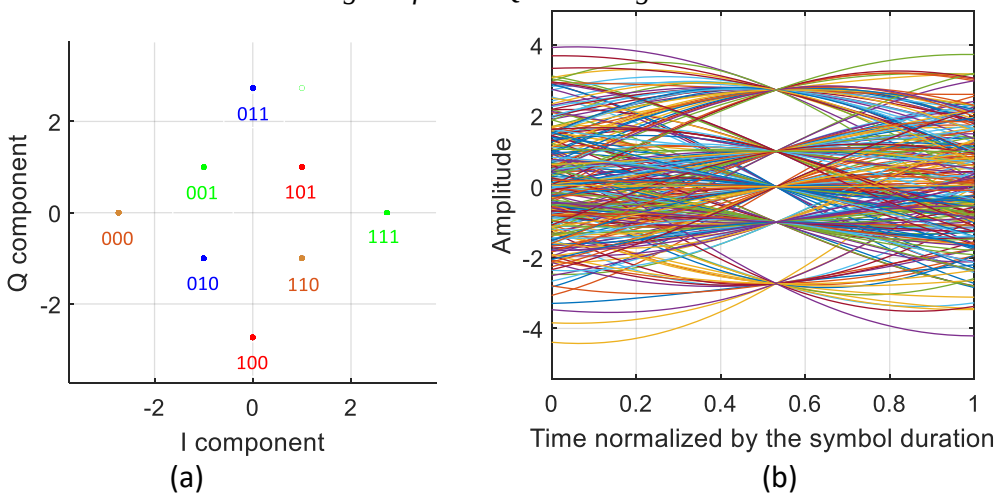

Figure 2.4 *Modulation format: 8-QAM (2-ASK/4-PSK). (a) In-phase and quadrature components of the constellation where each symbol has a different color which is different from neighboring symbols and (b) normalized eye diagram for a 8-QAM (2-ASK/4-PSK) RC signal.*

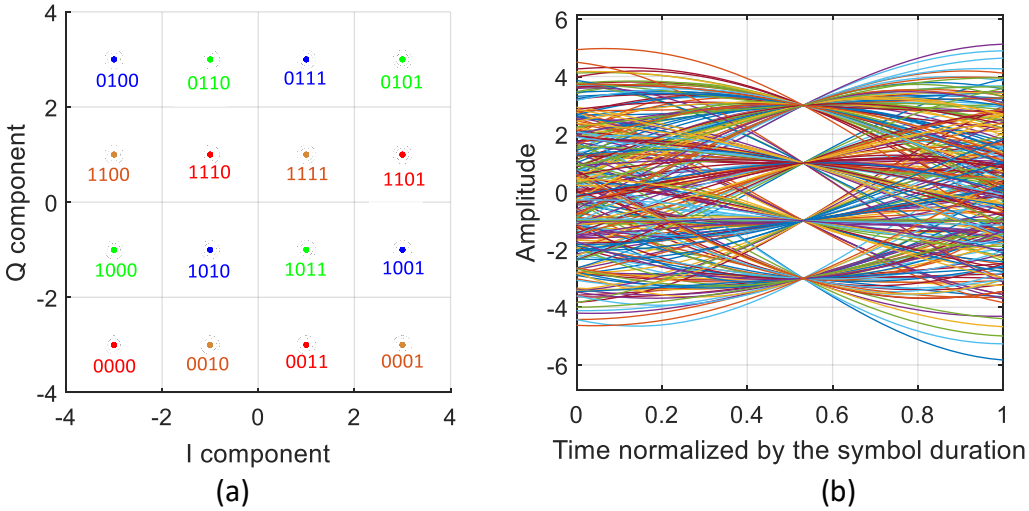

Figure 2.5 *Modulation format: 16-QAM. (a) In-phase and quadrature components of the constellation where each transmitted symbol has a different color which is different from the neighboring symbols and (b) normalized eye diagram for a 16-QAM RC signal.*

We use colored points to differentiate symbols from the neighboring symbols in all constellation figures in this work. The corresponding received eye-patterns of the I component with a raised-cosine (RC) pulse shape and a roll-off factor of ρ=0.1 is also depicted.

2.3.2. Quasi-Nyquist pulses

When using digital coherent optical communications, the available higher-order modulation formats used in conjunction with polarization multiplexing (PM), allow a higher SE and data transmission capacity, but a reduced reach because of the required OSNR [4]. We can reduce the spectral spacing between the subchannels in a superchannel to achieve a higher SE, and hence, a higher transmission capacity. The Quasi-Nyquist-WDM is a technique where the subchannels are packed together with a frequency spacing Δf between the carrier frequencies of adjacent subchannels which is larger than the symbol rate R_S of the subchannels [1]. We can shape the spectrum of the Quasi-Nyquist-WDM subchannels, by increasing or decreasing the roll-off factor ρ in the interval between 0 and 1, being 0 the Nyquist bandwidth limit. As we increase the roll-off factor, the less complex will be to implement a filter to shape the pulse spectrum, but more bandwidth is used. The value of the roll-off factors usually used in the literature for optical communications is 0.1, 0.2 [5] or 0.3 [6]. We can shape a Quasi-Nyquist pulse using raised-cosine pulses with different roll-off factors. In the time domain, the pulse is given by [1]

$$h_{RC}(t) = \frac{\sin\left(\frac{\pi t}{T_s}\right)}{\frac{\pi t}{T_s}} \frac{\cos\left(\frac{\pi \rho t}{T_s}\right)}{1-\left(\frac{2\rho t}{T_s}\right)^2} \tag{2.1}$$

where T_s is the symbol duration and t is the time. In the frequency domain, the RC transfer function is given by [1]

$$H_{RC}(f) = \begin{cases} T_s, & 0 \le |f| \le \frac{1-\rho}{2T_s} \\ \frac{T_s}{2}\left\{1+\cos\left[\frac{\pi T_s}{\rho}\left(|f|-\frac{1-\rho}{2T_s}\right)\right]\right\}, & \frac{1-\rho}{2T_s} \le |f| \le \frac{1+\rho}{2T_s} \\ 0, & |f| > \frac{1+\rho}{2T_s} \end{cases} \tag{2.2}$$

where f is the low-pass equivalent frequency.

The RC filter bandwidth B_{RC} is related to the symbol rate R_S and roll-off factor ρ by

$$B_{RC} = R_S \cdot (1 + \rho) \tag{2.3}$$

The raised cosine family of pulse shapes is an example of Quasi-Nyquist pulses. In the frequency domain, the pulse will have a shape almost like a rectangular form and, consequently, in the time domain, the pulse will look almost like a *sinc*.

Figure 2.6 displays the RC pulse in the time domain for the roll-off factors of 0.01, 0.1 and 0.3.

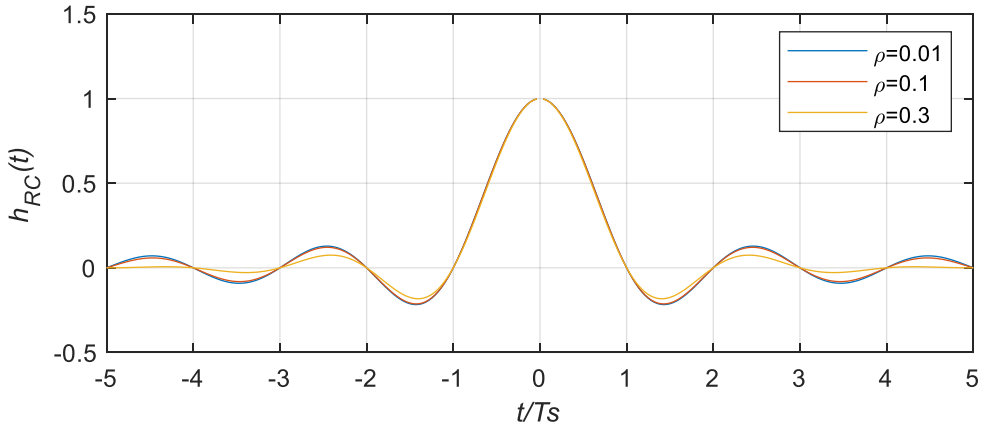

Figure 2.6 *RC pulse in the time domain for roll-off factors of 0.01, 0.1 and 0.3.*

In the time domain, the decay of the pulses outside their symbol time is important because, it can originate intersymbol interference (ISI) at the sampling instant, *i.e.*, the tailing oscillations of a symbol will be added to the oscillations of the adjacent symbols at that time instant. With faster pulse decay, the ISI will be smaller. In the case of a *sinc* pulse (ρ=0), a small error in the timing of the sampling would lead to a high ISI [7], [8]. The superposition of pulses and the consequent interference has another effect in the timing synchronization, named zero-crossing jitter, *i.e.*, a zero-crossing distortion, in the timing of the transition from a symbol to a different symbol. If we use a zero-crossing detection to get the symbol synchronization, the sampling time will be affected and will not be the optimum, and many erroneous symbols can be detected.

Typically, in communication systems the RC filter is split in two root raised-cosine (RRC) filters, one at the transmitter side and the other at the receiver side, with the same roll-off factor, because the receiver should have a transfer function matched to the spectrum of the signal, to achieve the best performance [9] [8].

Figure 2.7 displays the transfer function of a RRC filter $H_{RRC}(f) = \sqrt{H_{RC}(f)}$ for the roll-off factors of 0.01, 0.1 and 0.3 where we can see that the -3 dB bandwidth is independent of the roll-off factor, which when increased also enlarges the signal bandwidth.

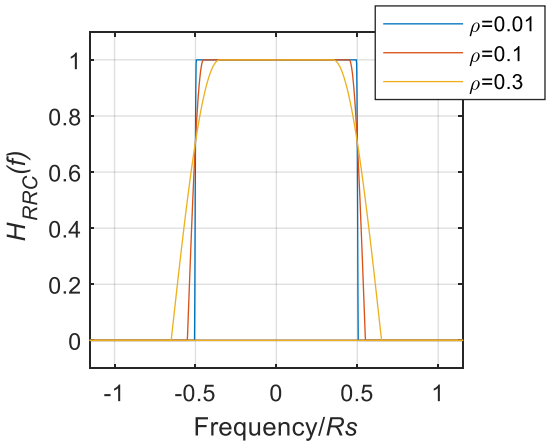

Figure 2.7 *RRC filter transfer function for roll-off factors of 0.01, 0.1 and 0.3.*

Typically, in the DSP blocks shown in Figure 2.2, the Nyquist shape of the pulses is implemented using a Nyquist filter, whose transfer function is given by [1]

$$H_N(f) = \sqrt{H_{RC}(f)} \quad \frac{\pi f T_s}{sin(\pi f T_s)} \tag{2.4}$$

In Figure 2.8 we can see the transfer function of the Nyquist filter and why a non-return-to-zero signal spectral shape can be transformed in a quasi-rectangular one [1].

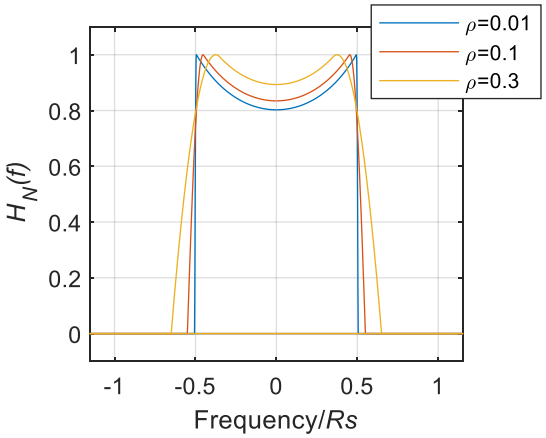

Figure 2.8 *Nyquist filter for roll-off factor of 0.01, 0.1 and 0.3.*

2.3.3. Generation of the transmitted optical signal

In this section, we describe the generation of the optical signal in our simulator for the several modulation formats used with a RRC pulse shape.

The sequence of pulses applied to the RRC filter input is expressed by

$$x(t) = \sum_{k=-\infty}^{+\infty} a_k \delta(t - kT_s) \tag{2.5}$$

where a_k is the symbol amplitude in the I or Q component and $\delta(t)$ is the Dirac function. The amplitudes a_k correspond to the real and imaginary parts of the amplitudes shown in Tables 2.1-2.3, where the real part of the complex symbol corresponds to the I component and the imaginary part corresponds to the Q component. At the optical transmitter output, we have:

$$y(t) = \sum_{k=-\infty}^{+\infty} a_k h_{RRC}(t - kT_s) \tag{2.6}$$

which corresponds to the QAM signal with RRC pulse shape and where the $h_{RRC}(t)$ is the impulse response function of the RRC filter. At the optical receiver input we have:

$$z(t) = \sum_{k=-\infty}^{+\infty} a_k h_{RRC}(t - T_d - kT_s) \tag{2.7}$$

where T_d is the propagation delay in a scenario without distortion due to filtering in the optical path, assuming that the optical fiber presents a flat spectral response and no phase distortion.

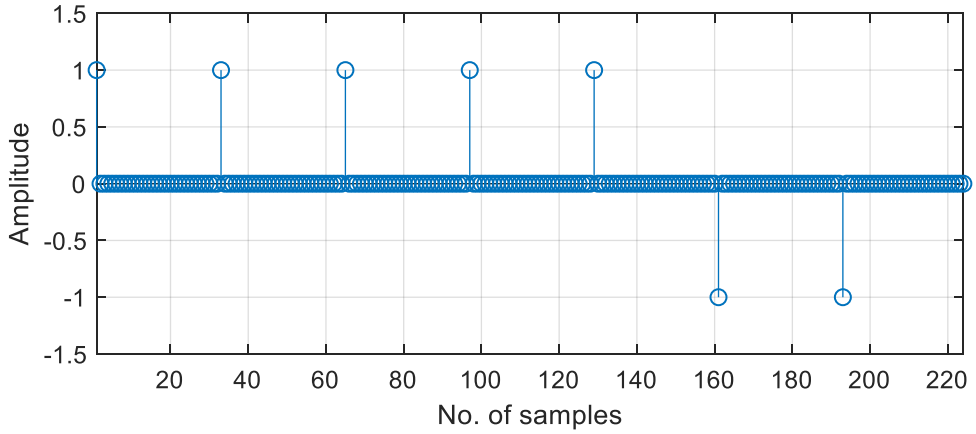

Figure 2.9 *Example of a vector of samples representing the in-phase component of 7 generated 4-QAM symbols.*

We implement the Nyquist pulse shaping in the simulator using equations (2.5) and (2.6). First, we generate one sample per symbol duration, emulating a Dirac pulse, as shown in Figure 2.9 for 7 generated 4-QAM symbols in the I component. The number of sampling points per symbol is set to 32. Then, the signal composed by the

comb of Diracs is applied to the RRC filter before transmission along the optical network using the fast Fourier transform (FFT). At the receiver the signal passes through another RRC filter.

As an example, the PSD of a transmitted signal with R_S=28 GBd after passing through the RRC filter with ρ=0.1, can be seen in Figure 2.10 where the signal has assumed the shape of the RRC filter and has a bandwidth of 28·(1+0.1)=30.8 GHz. The -3 dB bandwidth is 28 GHz. Figure 2.10 represents a signal with 4-QAM modulation format but for 8-QAM and 16-QAM, the PSDs are similar.

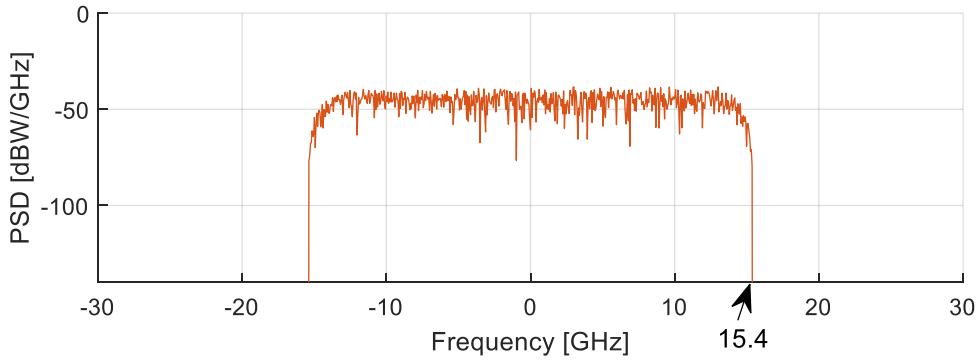

Figure 2.10 *PSD of the transmitted RRC signal with R_S=28 GBd and ρ=0.1 for a 4-QAM modulation format. This signal has been generated with a power of 0 dBm.*

Figure 2.11 represents a 28 GBd signal with 4-QAM that has assumed the shape of the RRC filter at its output with ρ=0.3. The signal has a -3 dB bandwidth of 28 GHz, but now the signal has a wider bandwidth of 28·(1+0.3)=36.4 GHz.

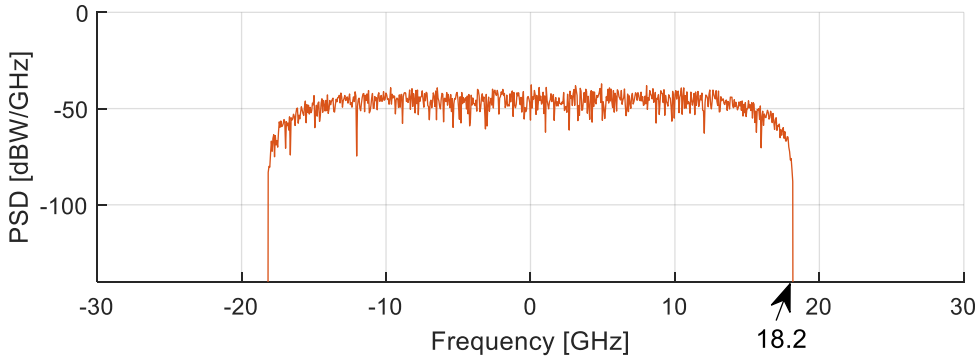

Figure 2.11 *PSD of the transmitted RRC signal with R_S=28 GBd and ρ=0.3 for a 4-QAM modulation format. This signal has been generated with a power of 0 dBm.*

2.4. Optical path

In this section we characterize the main components in the optical path: optical fiber, WSSs and EDFAs.

2.4.1. Optical fiber

The optical fiber is a dielectric transmission waveguide used for its very high transmission capacity. Its bandwidth is several orders of magnitude larger than electric transmission waveguides, around 4.8 THz in the C-band with 96 slots of 50 GHz and 128 slots of 37.5 GHz [5]. On the other hand, it presents a very low attenuation, about 0.2 dB/km, which allows a largely spaced deployment of optical signal amplifiers.

We must also consider in fiber transmission, the effects of the chromatic dispersion and polarization-mode dispersion. In coherent detection systems these impairments can be compensated or mitigated by the DSP at the receiver. The non-linear behavior of the fiber when in presence of high launched signal power can not be compensated effectively at the DSP [10].

Although in this work, we do not consider the effects on the optical signal due to the propagation in the fiber, since we want to study the filtering effect of the cascade of WSSs and the intercarrier crosstalk solely, we decided on the launch power based on fiber considerations. We choose to have 0 dBm launch power in each channel because it is a usual power for a 100 km span of SSMF (G.652) with a loss coefficient $\alpha = 0.22$ dB/km as can be seen in Figure 9 of [4], where an EDFA gain of 22 dB completely recovers the span loss. Although, we have chosen this value, the optimum transmitted power for maximum reach depends on the fiber type, on the span loss and on the type of optical network [4].

2.4.2. WSS filter

At each ROADM in the optical network, it is necessary to switch channels, *i.e.*, it is necessary to allow channels pass through the node (express signals) and others to be dropped from the fiber and new channels to be added to the fiber. There are several technologies to build the ROADMs. The huge majority [11] of the deployed ROADMs uses Arrayed-Waveguide Gratings (AWG) and WSS based on Micro-Electromechanical System (MEMS) devices that were designed to work in a fixed-grid network where channels are evenly spaced, and the WSSs have typically a frequency spacing of 100 GHz or 50 GHz [12]. Nowadays, the industry proposes ROADMs with LCoS-based WSSs, because its remotely controlled LCoS matrix can control on-the-fly the WSS bandwidth, which is crucial to implement a flexible-grid with a slot width granularity of 12.5 GHz [13]. This will allow a frequency slot of, *e.g.*, 37.5 GHz that could be used for

a 100 Gb/s PM-4QAM signal, instead of 50 GHz in the fixed-grid. When using superchannels with several subchannels, we consider frequency slots of hundreds of GHz, maintaining the same slot width granularity.

The device that is vital to the implementation of the flexible-grid is the WSS that is capable of acting as a variable bandwidth filter and the optical switching technology typically proposed is the LCoS. This technology is very important since it is considered as a programmable optical processor or even an optical Field Programmable Gate Array (FPGA) [11]. The main functionalities of a LCoS-based WSS are: multiple wavelengths routing and switching, power equalization of different wavelength channels, variable channel bandwidths, polarization-independent operation, compactness and millisecond reconfiguration times [11].

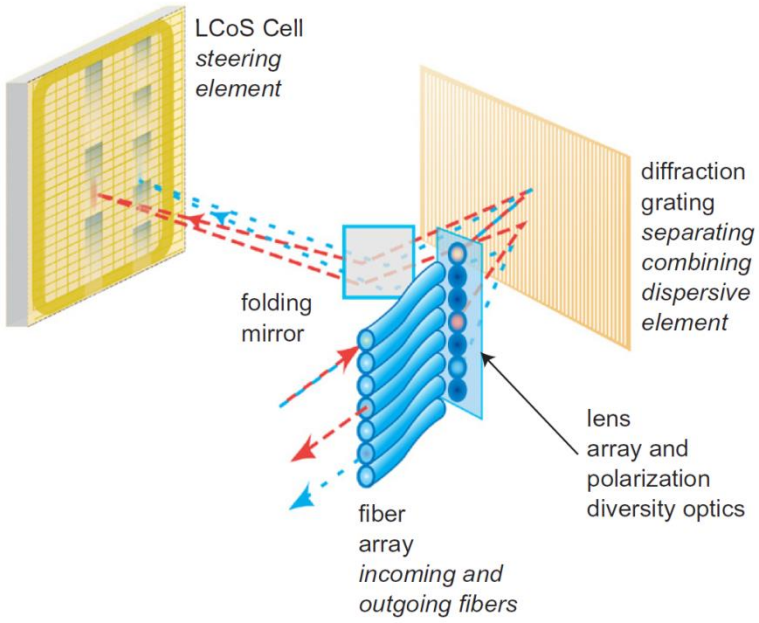

Figure 2.12 *General schematic of LCoS-based WSS operation [14]*

Figure 2.12 shows a schematic of the LCoS-based WSS operation. The WSS has a lens to concentrate the input beam coming from a fiber, into a diffraction grating that acts like a prism spreading the beam into the LCoS matrix. Each element of the matrix receives a slice of the beam and each element is programmed to act on it, whilst sending that slice into forming an output beam to another output fiber. Since we can program the behavior of each matrix element, we can change the bandwidth of filter to be in accordance with the ITU flexible-grid granularity.

The LCoS matrix can be characterized as a rectangular filter [15]:

$$R(f) = \begin{cases} 1, & -B/2 \le f \le B/2 \\ 0, & otherwise \end{cases} \tag{2.8}$$

where B is the rectangular bandwidth of the filter transfer function defined by the WSS matrix which corresponds to the -6 dB bandwidth of the WSS transfer function in the analytical model.

To model the transfer function of the LCoS-based WSS, some authors [16] and [17] choose a super-Gaussian function, but others authors [18], supported by [14] and [19], propose the analytical model that represents the underlying physical process inside the WSS, where its transfer function is given by:

$$S(f) = \frac{1}{2}\sigma\sqrt{2\pi}\left[\mathrm{erf}\left(\frac{B/2 - f}{\sqrt{2}\sigma}\right) - \mathrm{erf}\left(\frac{-B/2 - f}{\sqrt{2}\sigma}\right)\right] \tag{2.9}$$

where σ is the confinement parameter of the WSS and erf(x) is the error function. The WSS is characterized by its Optical Transfer Function (OTF), which is assumed to be Gaussian, and its -3 dB bandwidth, B_{otf}, can be related to the confinement parameter σ by [18]

$$\sigma = \frac{B_{otf}}{2\sqrt{2\ln 2}} \tag{2.10}$$

The OTF bandwidth is assumed to be constant over the frequency range of the WSS. A lower OTF bandwidth makes the laser beam to be focused onto a smaller spot size and the transfer function of the WSS approaches a more rectangular shape [18]. This model has been confirmed with measured data [15], [18] and [20] .

In the literature, several works use the super-Gaussian transfer function to model the response of a WSS. The transfer function of the super-Gaussian filter is given by [18]

$$S_{sg}(f) = \frac{1}{\sigma_{sg}\sqrt{2\pi}}\exp\left[-\left(f^2/2\sigma_{sg}^2\right)^{n_{sg}}\right] \tag{2.11}$$

where n_{sg} is the filter order, σ_{sg} is the standard deviation that is related to the m-dB bandwidth of the super-Gaussian filter by [21]

$$\sigma_{sg} = \frac{B_{mdB}}{2\left[2\left(\ln\sqrt{10^{m/10}}\right)^{1/n_{sg}}\right]^{1/2}} \tag{2.12}$$

where B_{mdB} is the m-dB bandwidth.

2.4.3. Optical Amplifier

The EDFA has a fiber that is doped with ions of a rare earth element, the erbium. The EDFA acts as an optical amplifier which uses light amplification by stimulated emission of radiation (LASER). The optical signal, when traverses the EDFA is amplified because it stimulates the decay of ions of Erbium (Er^{3+}) from a higher energy level to a lower energy level. This energy difference between these levels is precisely the energy of the photons of the incoming optical signal. At the output of the EDFA, we observe an increase of the number of photons and, hence, an amplification of the optical signal. To remove the ions from the lower energy level and replace them in the upper level of energy, the ions must be pumped with energy from an external light source.

If there is an ion spontaneous decay, then an undesired photon is emitted, which can be amplified. This generates an undesired effect called amplified spontaneous emission (ASE) which, for the optical communications, it is called ASE noise.

Hence, the EDFA can amplify an optical signal but with an accompanying noise with the PSD given by [22]

$$N_{ASE} = n_{sp} h\, \nu_0\, (g - 1) \tag{2.13}$$

where n_{sp} is the spontaneous noise emission factor, h is the Plank constant, ν_0 is the carrier frequency of the optical signal and g is the amplifier power gain.

The EDFA allows to amplify the optical signals in the 1.55 μm window, which is precisely the region of the spectrum where the optical fibers have the lowest attenuation. The EDFAs are usually placed at the input of each optical node to compensate the attenuation in the optical fiber link and at its output to compensate the power losses inside the optical node.

The amplification of the EDFA is called transparent since the EDFA amplifies an optical signal independently of the symbol rate, modulation format, single channel, WDM channels or superchannel.

After a certain number of amplifications, the noise can raise to a level that requires a signal regeneration. The optical signal is converted to a digital signal and after regeneration is converted again to an optical signal. Since the information in the signal leaves the optical domain to the digital domain and then again to optical domain, we do not have an all-optical path, so we can say that regenerators make the optical path non-transparent (opaque). These regenerators are expensive and dependent on the symbol rate and modulation format and, therefore, should be avoided whenever possible. When we have several channels in the optical fiber, and regeneration is needed, we must also have a number of regenerators equal to number of channels. The same is true for the subchannels in the superchannels.

2.5. Optical coherent receiver

At the end of the optical path, we can use a power splitter to distribute the power of the superchannel into the several sub-receivers. Each sub-receiver detects only one subchannel, although it receives at its input the whole superchannel as can be seen in Figures 2.13 and 2.*14*. In each sub-receiver, firstly, there is a polarization beam splitter (PBS) to split the two polarizations of the subchannel and then, after the TLD and the optical quadrature front-end (OQF), having a 2x4 90° hybrid and photodetectors, the optical signal is demodulated and becomes an electrical signal. This setup is duplicated because of the detection of two polarizations components of the optical signal. The analog signal is then converted to a digital signal by the analog-to-digital converter (ADC) and then is subject to signal processing in the DSP block.

Digital filters are placed inside the DSP and the coefficients of the filters can be updated to adapt to changes in the modulation format, symbol rate or in the optical channel [10]. The digital filters inside the DSP should be used to detect a specific subchannel because subchannels are tightly packed in the superchannel, without band-guards, and digital filters can provide a steep spectral shape. Since we are using the RRC shape at the transmitter, we should use a RRC filter in the receiver to shape the signal spectrum to a RC shape. The DSP performs polarization separation, polarization mode dispersion compensation, chromatic dispersion compensation, timing recovery, carrier phase recovery and inter-channel interference (ICI) cancelation [23] and intersymbol interference (ISI) mitigation [1].

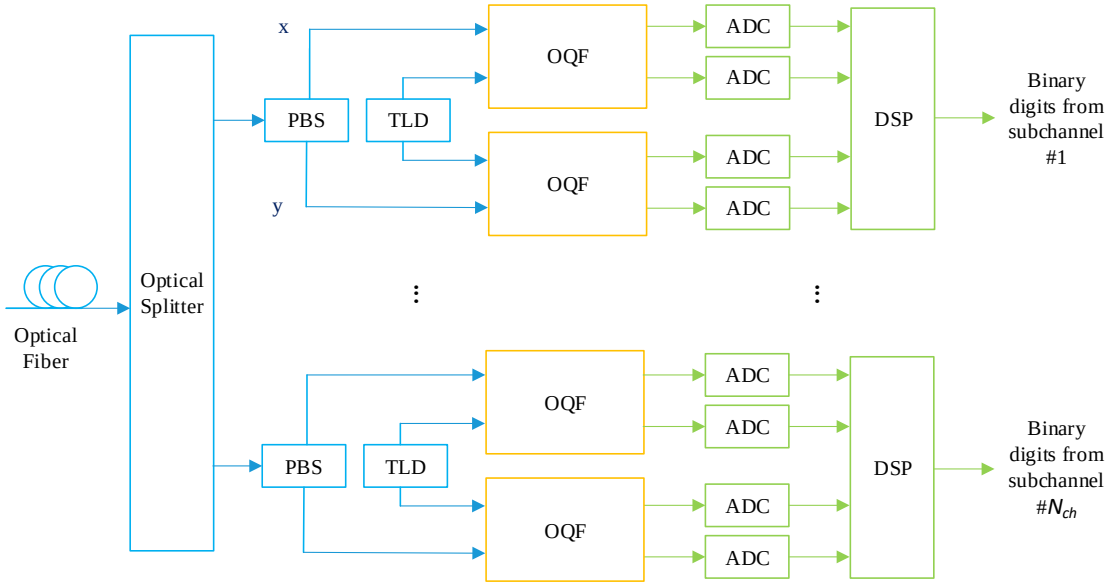

Figure 2.13 *Coherent detection of subchannels in a superchannel based on Nyquist-WDM, where PBS is a polarization beam splitter, TLD is a tunable laser diode and OQF is the optical quadrature front-end. The optical domain is in blue and the digital domain is in green. The conversion from the optical domain to the digital domain is done in the orange blocks.*

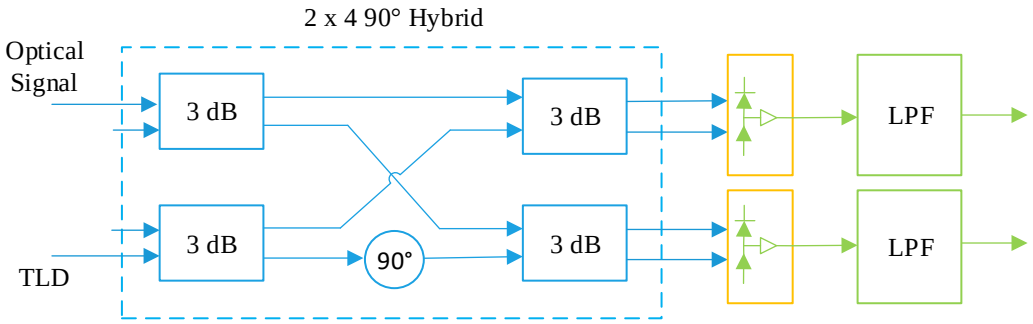

Figure 2.14 *Optical quadrature front-end with four power splitters, one 90° phase delay, two balanced photo-detectors, two trans-impedance amplifiers and two low-pass filter (LPF) . The optical domain is in blue and the digital domain is in green. The conversion from the optical domain to the digital domain is done in the orange blocks.*

2.6. Simulation model description

In our simulator, we consider that the transceivers are ideal [4] and that there is no frequency offset between the TLDs at the transmitter and at the receiver sides. When we study the effect of a frequency offset in the lasers, they all exhibit the same offset. We also consider that the optical fiber presents a flat spectral response and no phase distortion. We do not consider the transmission delay between transmitter and receiver

and its effect on the phase of the signal. We consider no phase distortion in the WSSs as in [6]. In the simulator we only consider a single polarization direction.

To clarify and explain the general structure of the simulator we present, in Figure 2.15, the simulator flow-chart. The transmitter, depicted in green, is composed by the symbols generator, the pulses generator with in-phase and quadrature generation, and finally the RRC filtering. The optical path, depicted in red, connecting the transmitter and the receiver is composed of several cascaded WSSs. At the optical receiver input, the simulator performs the noise loading of ASE noise arising from the EDFA amplification. The receiver, depicted in blue, has an optical quadrature front-end, a RRC filter and finally we mention the correlator in its usual position, although we do not make use of it because we are not considering the transmission delay in the optical fiber nor the phase delay in the filters.

The ASE noise sample functions are added to the signal and (after synchronization and correlation) the simulator checks if the number of bit errors is, or not, still below the defined errors threshold. If the condition is true, the simulator generates another noise sample function. When the threshold is surpassed, the simulator checks if the estimated BER is above the chosen target BER for the OSNR reference value, that depends on the symbol rate and modulation format selected. If so, the simulator increments the OSNR by 0.1 dB. The process of ASE noise samples function generation is started again for a lower noise power level at the receiver input while keeping constant the chosen signal power level at the transmitter. The BER is estimated until it is equal (or below) the target BER, and then the simulation ends.

At the receiver, the signals must go through the second RRC filter, and then we can see the eye-pattern, the constellation and the PSD of the received signal, with or without noise. In the simulator, we can use several performance metrics, EVM, EVM penalty, OSNR, OSNR penalty, signal power, maximum noise power and BER. To receive the signal and estimate the several performance metrics, the sampling instant to consider at the receiver must be chosen. Initially, we started by taking the sampling instant that leads to the largest eye opening of the eye-pattern, but we realized that the eye was totally closed after just a few WSSs, specially for the 8-QAM modulation format. We choose to rely on the EVM to find the best sampling instant. For each received signal, we calculate the EVM at every sampling instant and choose the sampling instant by the lowest EVM.

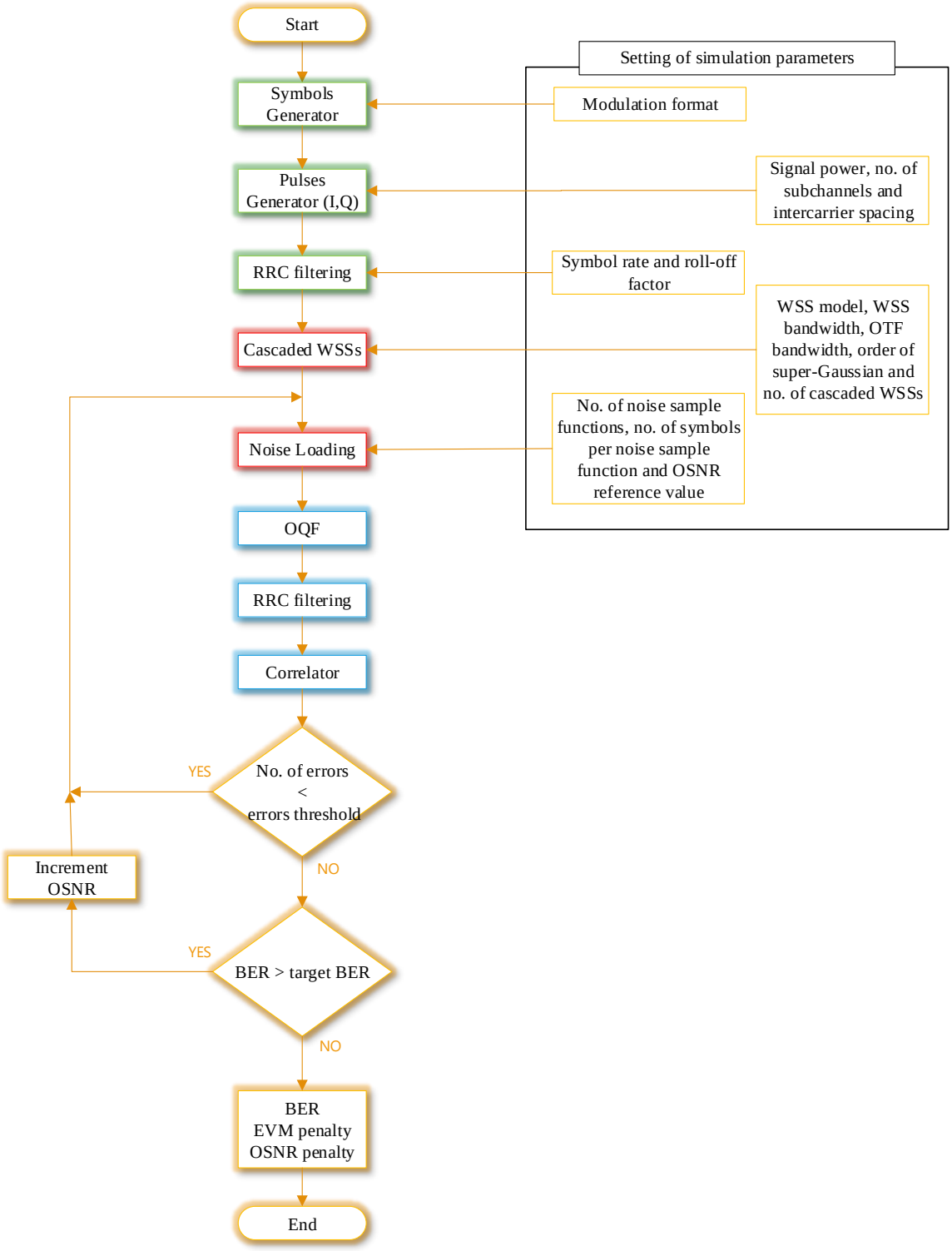

Figure 2.15 *Flow-chart of the Monte Carlo simulator used to estimate the BER, EVM penalty and OSNR penalty of the optical signal after a cascade of WSSs. The green blocks represent the optical transmitter, the red blocks, the optical path and the blue blocks, the optical receiver..*

In summary, the method to obtain the OSNR penalty is to repeatedly increase the OSNR by a small amount, by lowering the noise power at the optical receiver until we get, from the simulation, a BER equal to the reference BER in Tables 2.5 and 2.6.

To use the simulator, several parameters must be defined. In Table 2.4, the main parameters of the simulator and the values used in the present chapter are listed.

The simulator developed in this work allows us to use a Monte Carlo simulation to obtain the OSNR penalty performance metric, and the BER in presence of ASE noise. We simulate the noise as an additive white Gaussian noise (AWGN). Alternatively, we can choose to estimate only the EVM penalty, where the Monte Carlo simulation is not needed and the performance is only dependent on the waveform distortion.

Table 2.4 Main parameters of the simulator

N_a	Number of samples per symbol	32, 64
R_S	Symbol rate	28, 32.5, 65 GBd
ρ	Roll-off factor of the RRC filters	0.1, 0.3
B_{otf}	OTF bandwidth	8 GHz - 16 GHz
n_{sg}	Order of the super-Gaussian filters	3.5^{th} , 4.9^{th}
B	-6dB bandwidth of the WSS filters	37.5, 50 GHz
Δf	Intercarrier spacing	37.5, 50 GHz
N_{ch}	Number of subchannels in the superchannel	2 up to 10
	Type of modulation format	4,8,16-QAM
	Required OSNR	11.48 - 18.64 dB
	Target BER	10^{-2} (32.5 GBd) $4 \cdot 10^{-3}$ (28 GBd)
	Maximum number of cascaded WSSs in the optical path	20
	Signal power level at the transmitter, per subchannel	0 dBm
	Number of symbols in each noise sample function	512
	Minimum number of noise sample functions generated, to obtain an accurate OSNR	256
	Minimum number of errors to obtain an accurate BER	100

We started with 32 samples per symbol and afterwards we tested the simulator with 64. This increase has no significant change of the results to be presented.

The symbol rates of 28 and 32.5 GBd are equal to those used in [24]. For the two RRC filters, the roll-off factors are 0.1 or 0.3, which are typical found in the literature [5] [6]. If we decide to use the WSS analytical model, we must choose the bandwidth B_{otf} somewhere between 8 and 16 GHz in accordance with [18]. If we choose to use the super-Gaussian model, we can set, in the simulator, a fractional order. The -6 dB bandwidth of the WSS filters are equal to those used in [24], *i.e.*, 37.5 and 50 GHz for

the single routed channel scenario, which means that these -6 dB WSS bandwidths are equal to frequency slot for each channel. For the superchannel scenario we have to increase the bandwidth in accordance with the frequency slot granularity of the flexible grid and the intercarrier spacing. The type of modulations is equal to those used in [24], *i.e.*, 4-, 8- and 16-QAM. The values for the required OSNRs are calculated in Section 2.7. The target BERs and the maximum number of cascaded WSSs in the optical path were chosen to be equal to those used in [24]. The maximum number of subchannels in the superchannel is equal to those found in [4].

In computer simulations, it is necessary to choose how many bits are transmitted in each simulation iteration, to take into account rigorously the waveform distortion on the signal. The number of transmitted bits used in our simulations is equal to the one used in [4]. Each noise sample function affects a signal with 512 symbols, which means that each noise sample function affects a sequence of 1024, 1536 or 2048 bits, for 4-QAM, 8-QAM and 16-QAM, respectively, by generating 256 noise sample functions in each performance estimation, hence, the transmitted bits in one simulation run are $256 \cdot 512 \cdot 2$=262,144 bits for 4-QAM, $256 \cdot 512 \cdot 3$=393,216 bits for 8-QAM and $256 \cdot 512 \cdot 4$=524,288 bits for 16-QAM. These sequences of pseudo-random symbols are de Bruijn sequences generated using Galois Fields arithmetic [25]. For the other 2 adjacent subchannels of the subchannel under study, we use the MATLAB function *ltePRBS*, with different parameters, to generate other pseudo-random sequences so that they would not produce the same sequence for both adjacent subchannels.

The number of noise sample functions for estimating the OSNR is set to 256 [4]. Higher number of noise samples have been evaluated but the precision of the OSNR penalty has not been significantly changed and the simulation becomes unnecessarily more time consuming.

2.7. Performance metrics

There are several performance metrics typically used to evaluate the performance of an optical communication system with coherent detection and *M*-QAM modulation. In the following, the performance metrics used in this work are described, namely, EVM, EVM penalty, BER, OSNR and OSNR penalty.

The EVM is defined by the expression [26] [27]:

$$evm = \frac{\frac{1}{N_t}\sum_{k=1}^{N_t}\left|S_k - S_{0,k}\right|^2}{\frac{1}{N_t}\sum_{k=1}^{N_t}\left|S_{0,k}\right|^2} \tag{2.14}$$

$$EVM_{dB} = 10\log_{10} evm \tag{2.15}$$

where N_t is the number of symbols transmitted in one simulation run, S_k represents the received symbols in the complex plane, with waveform distortion and noise, and $S_{0,k}$ represents the transmitted symbols in the complex plane in a B2B configuration as given by Tables 2.1-2.3. The EVM allows us to evaluate how distant, in a Euclidian distance, are the received symbols from the transmitted symbols. The EVM is usually presented as a root mean square (RMS) value:

$$evm_{RMS} = \sqrt{\frac{\frac{1}{N_t}\sum_{k=1}^{N_t}\left|S_k - S_{0,k}\right|^2}{\frac{1}{N_t}\sum_{k=1}^{N_t}\left|S_{0,k}\right|^2}} \tag{2.16}$$

$$EVM_{dB} = 20\log_{10} evm_{RMS} \tag{2.17}$$

Another performance metric used in this work is the BER. To evaluate the BER, we use two different methods. One method is to use the direct error counting (DEC), *i.e.*, to count the number of received bit errors and dividing it by the total number of transmitted bits. Another method is to use the EVM obtained from the simulator, and calculate the BER analytically through theoretical formulas, which depend on the modulation format and are extracted from [7] and from the Appendixes A, B and C:

4-QAM: $$P_b = Q\left(\sqrt{\frac{s}{n}}\right) \tag{2.18}$$

8-QAM: $$P_b = \frac{4}{3}\,Q\left(\sqrt{\frac{2}{3+\sqrt{3}}\,\frac{s}{n}}\right) \tag{2.19}$$

16-QAM: $$P_b = \frac{3}{4}\,Q\left(\sqrt{\frac{1}{5}\,\frac{s}{n}}\right) \tag{2.20}$$

where [27] $$evm = \left(\frac{s}{n}\right)^{-1} \tag{2.21}$$

where P_b is the bit error probability which is an estimate of the BER, $Q(x)$ is the Q function, and s/n is the electric signal-to-noise ratio. In this work, the BER results presented correspond to the BER obtained from DEC, although equations (2.18)-(2.20) are also used for verification purposes.

Another performance metric used in this work is the OSNR. We simulate the ASE noise through a noise loading approach, on the Monte Carlo simulator. The OSNR is the ratio between the signal power and the noise power for a certain noise bandwidth in the optical domain at any point in the optical path. We measure the OSNR over the typical reference noise bandwidth 0.1 nm, *i.e.*, 12.5 GHz at 1.55 μm [28].

The OSNR relates to the SNR by

$$osnr = \frac{p\,R_s}{2\,B_{ref}}\,\frac{s}{n} \tag{2.22}$$

where p is 1 for single polarization multiplexing and 2 for dual polarization multiplexing and B_{ref} is the reference bandwidth which is equal to 12.5 GHz.

As we are considering polarization multiplexing, so we use Equations (2.23) and (2.24), to calculate the OSNR required at the receiver input and use this value as a reference value for estimating the OSNR penalty.

$$osnr = \frac{R_s}{B_{ref}}\frac{s}{n} \tag{2.23}$$

$$OSNR\,[dB] = 10\log_{10}\left(\frac{R_s}{B_{ref}}\right) + 10\log_{10}\left(\frac{s}{n}\right) \tag{2.24}$$

For a chosen BER and a specific modulation format, we can calculate the SNR analytically using Equations (2.18)-(2.20), and from these values we obtain the EVM values that we use as EVM reference values. This method follows a similar reasoning as the one presented in [29]. The EVM reference value for each modulation format is named evm_{total}.

$$evm_{total} = evm_{noise} + evm_{filtering} \tag{2.25}$$

$$EVM_{total}\,[dB] = 10\log_{10}(10^{EVMnoise\,[dB]/10} + 10^{EVMfiltering\,[dB]/10}) \tag{2.26}$$

The $evm_{filtering}$, which is the EVM due to filtering effect only, without the ASE noise, is obtained from simulation. Then the EVM penalty is calculated using Equations (2.27) and (2.28).

$$EVM_{noise}\ [dB] = 10\log_{10}(10^{EVMtotal\ [dB]/10} - 10^{EVMfiltering\ [dB]/10}) \quad (2.27)$$

$$EVM\ penalty\ [dB] = EVM_{total}\ [dB] - EVM_{noise}\ [dB] \quad (2.28)$$

To clarify how the EVM penalty is calculated, we present a numeric example. If we consider 4-QAM and BER= 10^{-2} from Equation (2.18), we get SNR=8.46 dB. From Equation (2.21), we get $EVM_{total}\ [dB]$= -8.46 dB. We consider this EVM to be our reference value. Then, in the simulator, we want to estimate the EVM penalty due to filtering $EVM_{filtering}\ [dB]$ in the absence of ASE noise. For 20 WSSs having each a -6 dB bandwidth of 37.5 GHz, we get $EVM_{filtering}\ [dB]$= -10.73 dB. Now, we use Equation (2.27) to calculate $EVM_{noise}\ [dB]$ which is this case is -12.35 dB. Finally, we calculate EVM penalty using (2.28) to obtain $EVM\ penalty\ [dB]$= 3.89 dB.

With the method present above, we can calculate the EVM penalty due to filtering without perform a time consuming Monte Carlo simulation, which includes the ASE noise generation to estimate the OSNR penalty. In this work, we compare the EVM penalty method with the usual OSNR penalty measured using a Monte Carlo simulation. The OSNR penalty is defined as the difference between the required OSNR at the receiver and the back-to-back required OSNR for the same target BER [30].

$$OSNR\ penalty\ [dB] = OSNR_{req}\ [dB] - OSNR_{B2B}\ [dB] \quad (2.29)$$

In this work, we have chosen to use 4-QAM, 8-QAM (2-ASK/4-PSK), 16-QAM, with a payload bit rate of 100 Gb/s, 150 Gb/s, 200 Gb/s, respectively, and to use polarization multiplexing. The next step is to decide if the DSP at the transceivers uses soft-decision (SD) or hard-decision (HD), the length of the forward error correction (FEC) and, as a consequence, the symbol rate. In our work, for the SD case, we consider a 32.5 GBd symbol rate with a pre-FEC BER of 10^{-2} and, for the HD case, we use 28 GBd with a pre-FEC BER of $4{\cdot}10^{-3}$ as in [24]. Table 2.5 shows the SNRs in dB calculated using Equations (2.18)-(2.20) for the two selected BERs, 10^{-2} for SD-FEC and $4{\cdot}10^{-3}$ for HD-FEC, and the selected modulation formats, 4-QAM, 8-QAM and 16-QAM. From these values, we obtain the EVM reference values, $EVM_{total}\ [dB]$.

Table 2.5 Theoretical reference SNR in dB for different modulation formats and BERs

Modulation format	BER= 10^{-2}	BER= $4 \cdot 10^{-3}$
4-QAM	7.33	8.46
8-QAM	11.45	12.53
16-QAM	13.90	15.14

From the calculated SNRs and for the two selected symbol rates, we calculate the reference OSNRs shown in Table 2.6 using Equation (2.24). Throughout this work, we use these BERs, EVMs and OSNRs, as reference values.

Table 2.6 Theoretical reference OSNR in dB for the different modulation formats, BERs and symbol rates

Modulation format	BER= 10^{-2} R_S= 32.5 GBd	BER= $4 \cdot 10^{-3}$ R_S= 28 GBd
4-QAM	11.48	11.97
8-QAM	15.60	16.03
16-QAM	18.05	18.64

Table 2.7 Simulated reference SNR in dB for different modulation formats and BERs

Modulation format	BER= 10^{-2}	BER= $4 \cdot 10^{-3}$
4-QAM	7.32	8.45
8-QAM	11.48	12.55
16-QAM	13.88	15.13

Table 2.8 Simulated reference OSNR in dB for the different modulation formats, BERs and symbol rates

Modulation format	BER= 10^{-2} R_S= 32.5 GBd	BER= $4 \cdot 10^{-3}$ R_S= 28 GBd
4-QAM	11.44	11.94
8-QAM	15.62	16.01
16-QAM	18.06	18.63

We checked the BER, SNR and OSNR estimation implemented in the simulator in a B2B configuration with 256 noise sample functions and we present the simulator results in Tables 2.7 and 2.8, which are in a very good agreement with the theoretical values shown in Tables 2.5 and 2.6, hence validating both performance metrics estimation in the simulation.

2.8. WSS performance analysis and simulator validation

In this section, we analyze the relation between the analytical model and the super-Gaussian model transfer functions.

In the analytical model of the WSS, for bandwidths greater than 30 GHz [15], we notice that the -6 dB bandwidth remains constant with the B_{otf} changing as we can see in

Figure 2.16. The -6 dB bandwidth is used in this work as the bandwidth of the analytical model, because it corresponds to the channel bandwidth of the WSS matrix.

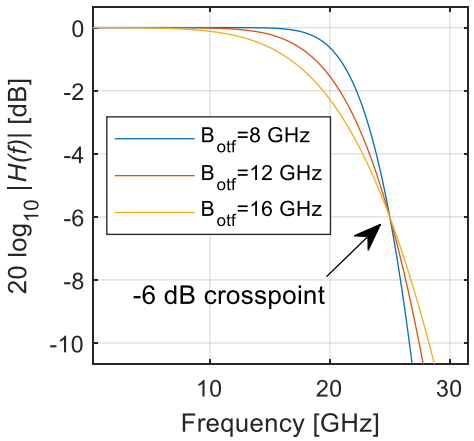

Figure 2.16 *Transfer function of the WSS analytical model for a 50 GHz -6 dB bandwidth for B_{otf}=8, 12 and 16 GHz.*

Figure 2.17 shows the -3 dB bandwidth and -6 dB bandwidth of the cascaded WSSs as a function of the number of WSSs for the analytical model, where each WSS has a 50 GHz -6 dB bandwidth, for several values of $B_{otf,}$ namely 8, 10, 12 and 14 GHz. It is clear that the filter bandwidth narrowing effect is enhanced with the increased number of cascaded WSSs. Figure 2.17 shows also that the higher the B_{otf} the more sensitive is the WSS to bandwidth narrowing effect, because its transfer function is further away from a rectangular shape as shown in Figure 2.16.

Figures 2.16 and 2.17 (a) have an excellent agreement with the results presented in Figures 2 and 10 of [21], respectively, which confirms that the transfer function of the analytical model, given by Equation (2.9), is reproduced faithfully. Likewise, we used the results presented in Figure 1 of [31] to verify the correctness of our simulator for the super-Gaussian model transfer function as given by Equation (2.11).

The next step is to compare both WSS models, analytical model and super-Gaussian model, for 20 cascaded WSSs. When comparing both models, for a certain B_{otf}, a careful choice of the order of the super-Gaussian filter must be made. First, we must choose at which power level value the transfer functions are equal between the two models, and then the filter order is tested for different values, with 0.1 increments, to determine the optimal fitting [32].

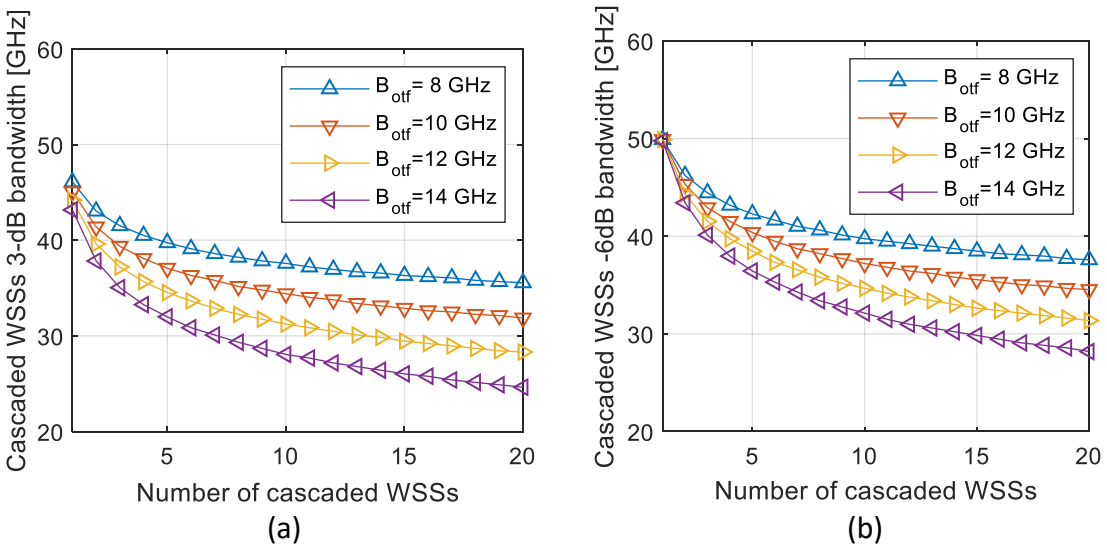

Figure 2.17 *Variation of the cascaded -3 dB bandwidth (a) and -6 dB bandwidth (b) as a function of cascaded WSSs for the analytical model with a 50 GHz -6 dB bandwidth WSS and using B_{otf} =8, 10, 12 and 14 GHz.*

In Figure 2.18, we can see the variation of the cascaded WSSs bandwidth up to 20 cascaded WSSs with B_{otf}=8.5 GHz for the analytical model. We choose this value for B_{otf} because it belongs to the interval of possible values indicated in [18], and we prefer a sharp filter instead of a smooth filter. For the super-Gaussian model, we consider filters with 50 GHz -6 dB bandwidth and a 4.9th super-Gaussian order and also 37.5 GHz -6 dB bandwidth with a 3.5th super-Gaussian order. We choose the -6 dB bandwidths to be equal for both filter models and to be equal to the frequency slot bandwidth [24]. If we used bandwidths equal for both filter models at another power level then we would have to use other values for the super-Gaussian order.

As can easily be seen in Figure 2.18, we can get a very good match between the analytical model and the super-Gaussian model, for the cascaded WSS bandwidth at the last WSS. It should be noted that the B_{otf} remains constant at 8.5 GHz while the super-Gaussian order change, depending on the WSS bandwidth.

Table 2.9 WSS bandwidths in GHz of each WSS for the analytical model and for the super-Gaussian model.

Power level [dB]	Bandwidth of each WSS [GHz]			
-3	Analytical	Super-Gaussian	Analytical	Super-Gaussian
	33.40	33.75	45.85	46.45
-6	37.5		50	

Table 2.9 we present the corresponding -3 dB bandwidths for each WSS model, where we can see that the two models have different transfer functions, since at -3 dB, the bandwidths are different even if at -6 dB they are equal.

As can easily be seen, in Figure 2.18, we can get a very good match, between the analytical model and the super-Gaussian model, for the cascaded WSS bandwidth at the last WSS. It should be noted that the B_{otf} remains constant at 8.5 GHz while the super-Gaussian order change, depending on the WSS bandwidth.

Therefore, we can conclude that for an adequate choice of the super-Gaussian order, the super-Gaussian model can appropriately approach the analytical model, as already concluded in [20]. The choice of the order depends on the level that the power transfer functions are equal between the two models. This level should not be higher than -6 dB [20].

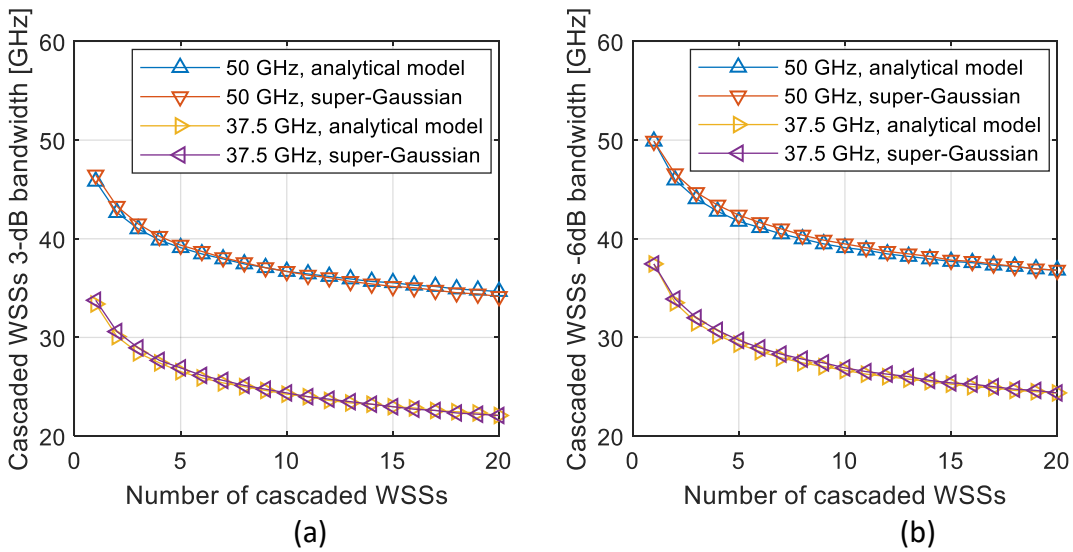

Figure 2.18 *Variation of the (a) -3 dB bandwidth and (b) -6 dB bandwidth as a function of cascaded WSSs for both models, using 4.9th super-Gaussian order for the 50 GHz -6 dB bandwidth for a single WSS and using 3.5th super-Gaussian order for the 37.5 GHz -6 dB bandwidth for a single WSS. In both cases, 50 GHz and 37.5 GHz, we consider B_{otf}=8.5 GHz.*

It must be emphasized that for the super-Gaussian model to successfully approach the analytical model, the order of the super-Gaussian must be increased for larger bandwidths of the WSS. In [18], for the case of a WSS with a B_{otf}=11.1 GHz and bandwidths of 82.5 GHz and 162.5 GHz, the authors set a super-Gaussian order of 9.8 and 22.3, respectively, to model appropriately the measured data. For a higher bandwidth, we must consider a higher super-Gaussian order.

The effect of the filter bandwidth narrowing after 20 cascaded WSSs in the signal PSD is shown in Figures 2.19 and 2.20 for 50 GHz and 37.5 GHz -6 dB bandwidths respectively. These PSDs can be compared with Figures 2.10 and 2.11, where the

transmitted signal is depicted. Figures 2.19 and 2.20 show PSD of signals with 4-QAM, but for 8-QAM and 16-QAM, the PSDs look similar.

Figures 2.19 and 2.20 show that the filter bandwidth narrowing effect over a signal with 28 GBd is much more significant in the case of the 37.5 GHz filter than with the 50 GHz filter and leads to a much higher signal distortion. The effect of the signal distortion due to the filtering effect can be seen in the received signal constellations. Figures 2.21 and 2.22 show the received signal constellations after a cascade of 20 WSSs for 50 GHz and 37.5 GHz -6 dB bandwidths. Figures 2.21 and 2.22 shows a scattering of the received symbols in the complex plane and the corresponding increase of the Euclidian distance between the transmitted symbols and the received symbols in comparison with Figures 2.3-2.5. We also see clearly, by the use of colored points, that there are errors in the detection of symbols, because some received symbols cross the decision threshold to another symbol decision region. The number of errors grows as the modulation order is increased.

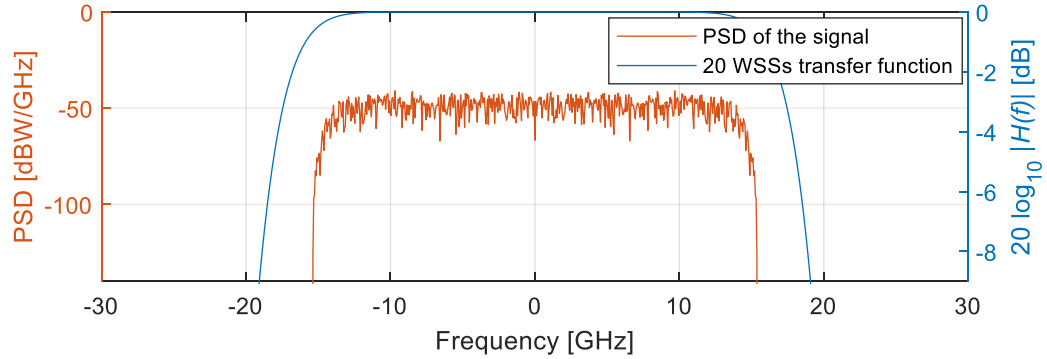

Figure 2.19 *Filtering transfer function after 20 cascaded WSSs at 50 GHz -6 dB bandwidth and PSD of the received signal with 28 GBd and ρ=0.1 for a 4-QAM modulation format. This signal has only one channel without side-channels and has a launch power of 0 dBm.*

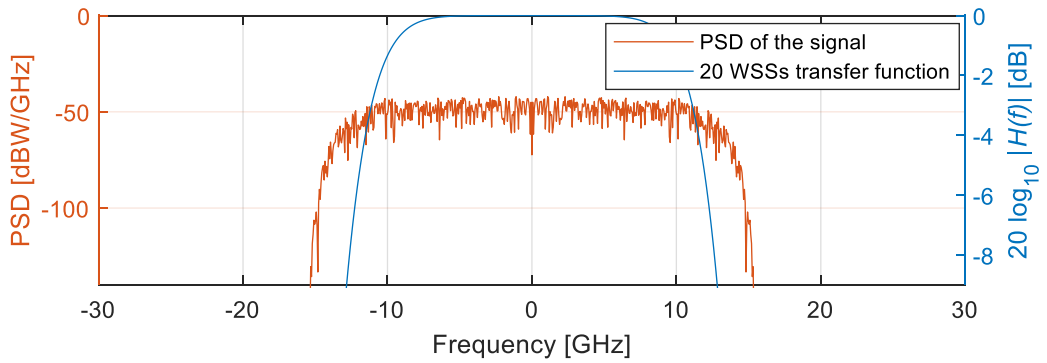

Figure 2.20 *Filtering transfer function after 20 cascaded WSSs at 37.5 GHz -6 dB bandwidth and PSD of the received signal with 28 GBd and ρ=0.1 for a 4-QAM modulation format.. This signal has only one channel without side-channels and has a launch power of 0 dBm.*

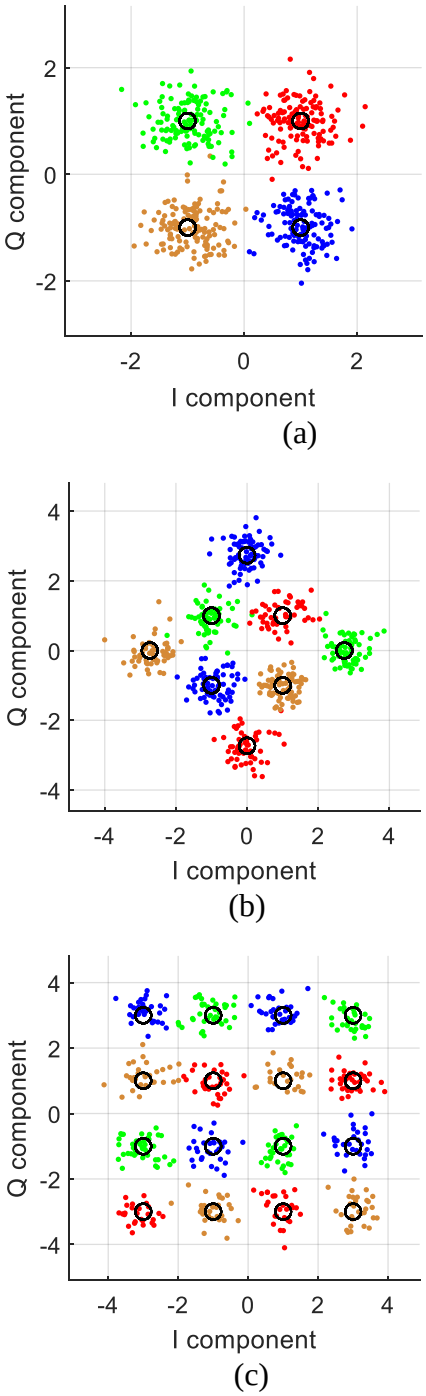

Figure 2.21 *Constellation after passing through 20 cascaded WSSs with 50 GHz -6 dB bandwidth using a signal in the presence of ASE noise with 28 GBd and ρ=0.1 and with modulation format (a) 4-QAM, (b) 8-QAM and (c) 16-QAM. Empty circles (original constellation) and i points (received constellation).*

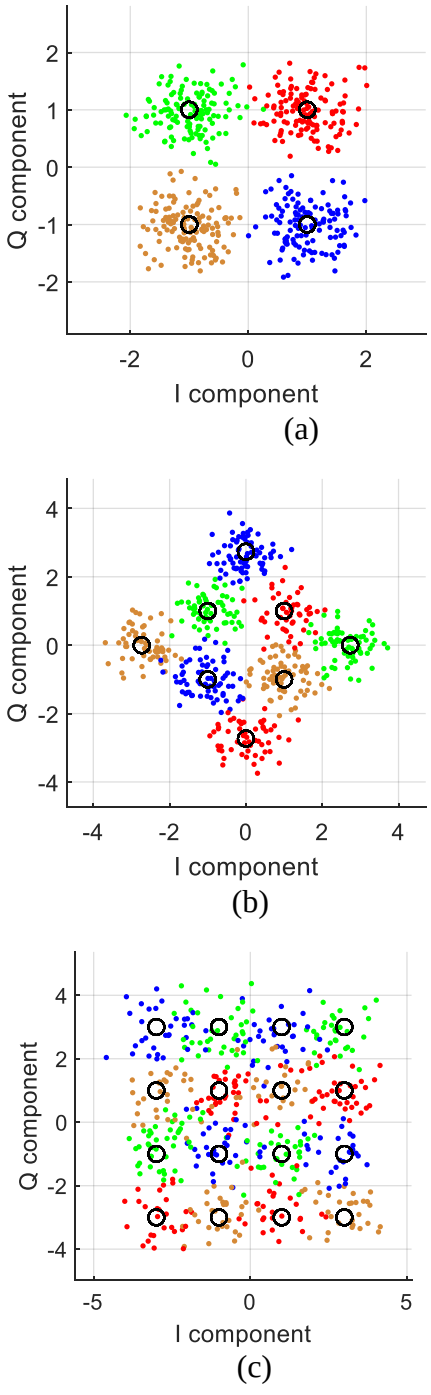

Figure 2.22 *Constellation after passing through (a) 20 (b) 15 (c) 8 cascaded WSSs with 37.5 GHz -6 dB bandwidth using a signal in the presence of ASE noise with 28 GBd and ρ=0.1 and with modulation format (a) 4-QAM, (b) 8-QAM and (c) 16-QAM. Empty circles (original constellation) and i points (received constellation).*

It should be noticed that the edge frequencies of the signal spectrum are more substantially affected by the filtering effect for the 37.5 GHz case, than for the 50 GHz case, as shown in Figures 2.19 and 2.20 which is then translated into signal distortion as shown in Figures 2.21 and 2.22. In Figure 2.22 it is important to notice the variation of the number of traversed WSSs. For the same performance criterion, higher modulation format orders reduce the number of traversed WSSs. In Figure 2.22 (b) and (c) after 15 and 8 WSSs, respectively, the OSNR penalty is above 6 dB, which is the upper limit chosen for the graphics in this work.

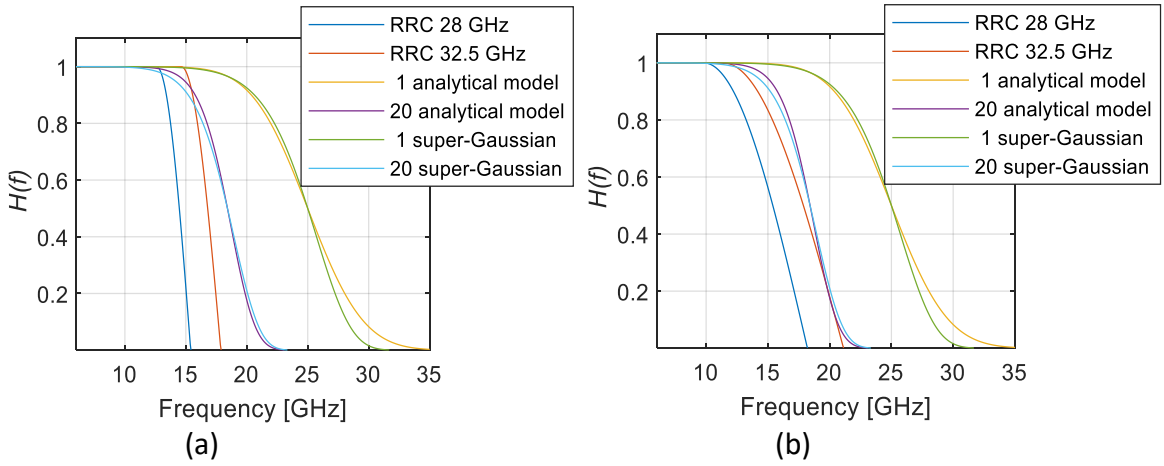

Figure 2.23 *Transfer functions after one WSS and 20 cascaded WSSs with 50 GHz -6 dB bandwidth with B_{otf}=8.5 GHz using a signal with 28 GBd and another with 32.5 GBd and ρ=0.1 (a) and ρ=0.3 (b) for the analytical and super-Gaussian models. The super-Gaussian filter order is 4.9th.*

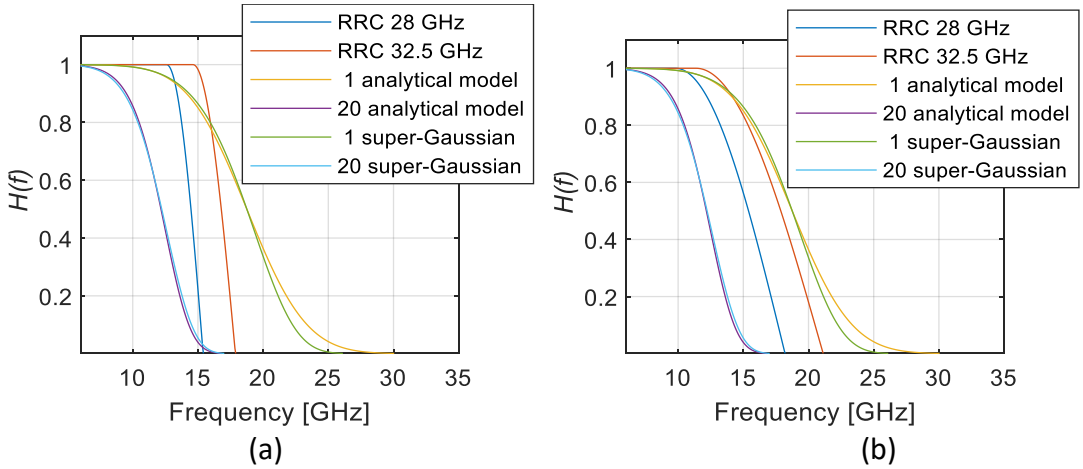

Figure 2.24 *Transfer functions after one WSS and 20 cascaded WSSs with 37.5 GHz -6 dB bandwidth and WSSs with B_{otf}=8.5 GHz using a signal with 28 GBd and another with 32.5 GBd and ρ=0.1 (a) and ρ=0.3 (b) for the analytical and super-Gaussian models. The super-Gaussian filter order is 3.5th.*

Another interesting analysis is to look at the transfer functions of the analytical model and super-Gaussian model. The idea is to compare them for one WSS and after 20 cascaded WSSs. Figures 2.23 and 2.24 show the transfer functions of one WSS and

of 20 cascaded WSSs with B_{otf}=8.5 GHz for the analytical model, and 4.9th super-Gaussian order for 50 GHz -6 dB bandwidth filter and 3.5th super-Gaussian order for 37.5 GHz -6 dB bandwidth filter for the super-Gaussian model. The RRC filters transfer function for a 28 GBd and 32.5 GBd signals with ρ=0.1 and ρ=0.3 are also shown.

In Figures 2.23 and 2.24, we see that the transfer functions after 20 WSS are similar between both models and they allow us to have a different awareness of the impact of the filter bandwidth narrowing effect when comparing one WSS with 20 cascaded WSS. In Figure 2.23, we see that the impact of one WSS on the signal is almost null because the RRC filter bandwidth with ρ=0.1 and ρ=0.3 is below the bandwidth of 1 WSS. Even for 20 WSSs, with ρ =0.1, the RRC filter and, consequently, the signal bandwidth is mostly below the filter bandwidth which leads to low distortion, in accordance with the constellations in Figure 2.21. For the 37.5 GHz case, in Figure 2.24, the effect of the narrowing of the filter is more pronounced than for the 50 GHz case in Figure 2.23, because the filter bandwidth for one WSS and for 20 WSSs is lower than the RRC filter bandwidth leading to higher signal distortion, in accordance with the constellations in Figure 2.22.

2.9. Conclusions

In this chapter, we describe the model of the optical communication system with coherent detection and with cascaded WSS-based ROADMs. We characterized the optical components of the optical network with detail: optical transmitter, optical fiber, WSS filter, EDFAs and optical coherent receiver.

Then, we explained how to generate superchannels by aggregating subchannels using quasi-Nyquist WDM signals having different modulation formats, symbol rates and roll-off factors.

We have presented the simulator implemented in MATLAB which performs a Monte Carlo simulation to evaluate the system performance considering all the modelled components in presence of ASE noise. We described the main parameters of the simulator.

We also described the performance metrics, BER, EVM penalty and OSNR penalty, which are extensively used in this work. We have showed a method to estimate the EVM penalty due to filtering and crosstalk in the simulation, without the need of generating ASE noise sample functions and we compared it with the OSNR penalty

from Monte Carlo simulation. Through simulation we have seen how computationally fast is the EVM penalty, when compared to the OSNR penalty.

Then, we have shown how the analytical model and super-Gaussian model can be used to model a WSS filter. We can choose either model, but the analytical model is said to provide a more accurate representation of the WSS device, which is characterized by the OTF bandwidth and can be used for whatever WSS bandwidth necessary. In contrast, if we choose to use the super-Gaussian model, than we need to set the filter order accurately, to model properly the measured WSS characteristics. If we know the OTF bandwidth, we can perform this choice by matching the analytical model transfer function to the super-Gaussian model transfer function, by selecting a level of the power filter response where both transfer functions are equal and, then, by optimizing the order that allows the best fitting. We found that for a certain OTF bandwidth, the super-Gaussian order that leads to the best fit depends on the WSS bandwidth. We saw also that the transfer functions after 20 WSS can be made similar between both spectral models, if we do a correct choice of the super-Gaussian filter order. We have concluded that the higher the WSS bandwidth, the higher the order of the super-Gaussian transfer function must be set.

We have shown that the filter bandwidth narrowing effect for a cascade of WSSs, each having a -6 dB bandwidth of 37.5 GHz, has a more harmful effect on the signal edge frequencies, than with a 50 GHz bandwidth filter. For a 32.5 GBd signal, this effect is more significant, because the signal has a larger bandwidth than for a 28 GBd signal.

The modulation format order also plays an important role because the higher the modulation format order, the higher is the distortion induced by the filtering, which can limit the number of traversed WSSs.

References

[1] G. Bosco, "Chapter 4, Spectrally efficient multiplexing: Nyquist-WDM," in *Enabling technologies for high spectral-efficiency coherent optical communication networks*, Xiang Zhou, Chongjin Xie (Eds.), John Wiley & Sons, 2016, pp. 123-150.

[2] J. Pedro, "Designing transparent flexible-grid optical networks for maximum spectral efficiency (Invited)," *Journal of Optical Communications and Networking*, Vol. 9, No. 4, pp. C35-C40, April, 2017.

[3] M. Jinno, "Elastic optical networking: roles and benefits in beyond 100-Gb/s era (Invited Tutorial)," *Journal of Lightwave Technology*, Vol. 35, No. 5, pp. 1119-1120, March 1, 2017.

[4] G. Bosco, V. Curri, A. Carena, P. Poggiolini and F. Forghieri, "On the performance of Nyquist-WDM terabit superchannels based on PM-BPSK, PM-QPSK, PM-8QAM or PM-16QAM subcarriers," *Journal of Lightwave Technology*, Vol. 29, No. 1, pp. 56-58, January 1, 2011.

[5] T. Rahman *et al.*, "Long-haul transmission of PM-16QAM-,PM-32QAM-, and PM-64QAM-based terabit superchannels over a field deployed legacy fiber," *Journal of Lightwave Technology*, Vol. 34, No. 13, pp. 3071-3076, July 1, 2016.

[6] T. Rahman *et al.*, "On the mitigation of optical filtering penalties originating from ROADM cascade," *IEEE Photonics Technology Letters*, Vol. 26, No. 2, pp. 154-155, January 15, 2014.

[7] A. B. Carlson, "Chapter 11, Baseband digital transmission," in *Communication Systems*, McGraw-Hill, 5th Edition, 2010, pp. 479-542.

[8] J. G. Proakis, "Chapter 9, Signal design for band-limited channels," in *Digital Communications*, Prentice Hall, 4th Edition, 2001, pp. 534-582.

[9] J. Wang, C. Xie, Z. Pan, "Matched filter design for RRC spectrally shaped Nyquist-WDM systems," *Photonics Technology Letters*, Vol. 25, No. 23, pp. 2263-2266, December 1, 2013.

[10] A. Napoli, *et al.*, ""Chapter 5, Transmission in elastic optical networks", in Víctor López, Luis Velasco (Eds.)," in *Elastic optical networks: architectures, technologies, and control*, Springer, 2016, pp. 83-116.

[11] A. Lord, Y. R. Zhou, R. Jensen, A. Morea, and M. Ruiz, "Chapter 2, Evolution from wavelength-switched to flex-grid optical networks," in *Elastic optical networks: architectures, technologies, and control*, Víctor López, Luis Velasco (Eds.), Springer, 2016, pp. 12-14.

[12] J. M. Fabrega, "On the filter narrowing issues in elastic optical networks," *Journal of Optical Communications and Networking*, Vol. 8, No. 7, pp. 1-2, July, 2016.

[13] ITU-T, "Recommendation ITU-T G.694.1 Edition 2.0," pp. 6-7, 2012.

[14] S. Frisken, I. Clarke, S. Poole, "Chapter 18, Technology and applications of liquid crystal on silicon (LCoS) in telecommunications, in Alan E. Willner, Tingye Li, Ivan P. Kaminow (Eds.)," in *Optical Fiber Telecommunications, Volume VI-a: Components and Subsystems*, Oxford Academic Press, 2013, pp. 721-723.

[15] C. Pulikkaseril, M. Roelens, J. Bolger, S. Poole, S. Frisken, "Filter bandwidth definition of the WaveShaper S-series programmable optical processor," White Paper, Finisar Corp., 2012, pp.1-2.

[16] T. A. Strasser, “Wavelength-selective switches for ROADM applications,” *IEEE Journal of Selected Topics in Quantum Electronics,* Vol. 16, No. 5, pp.1154-1155, September/October, 2010.

[17] S. Tibuleac, “Transmission impairments in DWDM networks with reconfigurable optical add-drop multiplexers,” *Journal of Lightwave Technology,* Vol. 28, No. 4, pp. 563-567, February 15, 2010.

[18] C. Pulikkaseril, *et al.*, “Spectral modeling of channel band shapes in wavelength selective switches,” *Optics Express,* Vol. 19, No. 9, pp. 4 and 11, April 2011.

[19] X. Zhou, *et al.*, “Bandwidth variable transceivers with artificial neural network-aided provisioning and capacity improvement capabilities in meshed optical networks with cascaded ROADM filtering,” *Optics Communications,* Vol. 409, pp. 23-25, September, 2017.

[20] J. Pan, C. Pulikkaseril, L. Stwart and S. Tibuleac, “Comparison of ROADM filter shape models for accurate transmission penalty assement,” *IEEE Photonics Conference (IPC),* pp. 550-551, Waikoloa, HI, USA, October, 2016.

[21] C. Pulikkaseril, *et al.*, “Spectral modeling of channel band shapes in wavelength selective switches,” *Optics Express,* Vol. 19, No. 9, pp. 3, April 2011.

[22] E. Desurvire, “Chaper 5, Gain, saturation and noise characteristics of erbium-doped fiber amplifiers,” em *Erbium-Doped Fiber Amplifiers*, John Wiley & Sons,1994, pp. 319-336.

[23] J. Pan *et al.*, “Inter-channel crosstalk cancellation for Nyquist-WDM superchannel applications,” *Journal of Lightwave Technology,* Vol. 30, No. 24, pp. 3994-3995, December 15, 2012.

[24] A. Morea, J. Renaudier, T. Zami, A. Ghazisaeidi, and O. Bertran-Pardo, “Throughput comparison between 50-GHz and 37.5-GHz grid transparent networks [Invited],” *Journal of Optical Communications Network,* Vol. 7, No. 2, pp. A293-A295 , February, 2015.

[25] M. Jeruchim, P. Balaban, K Shanmugan, "Simulation of communication systems: modeling, methodology, and techniques", Kluwer, 2nd Edition, 2000, pp.389-392.

[26] H. A. Mahmoud and H. Arslan, “Error vector magnitude to SNR conversion for nondata-aided receivers,” *IEEE Transactions on Wireless Communications,* Vol. 8, No. 5, pp. 2694-2704, May 2009.

[27] R. Shafik, S. Rahman, R. Islam, “On the extended relationships among EVM, BER and SNR as performance metrics,” *4th International Conference on Electrical and Computer Engineering,* pp. 409-410, Dhaka, Bangladesh, December, 2006.

[28] B. Nebendahl, *et al.*, “EVM as new quality metric for optical modulation analysis,” in *Electronics, Communications and Photonics Conference*, Fira, Greece, pp. 1-4, April, 2013.

[29] P. E. D. Cruz, T. M. F. Alves, and A. V. T. Cartaxo, “Theoretical analysis of the four-wave mixing effect in virtual carrier-assisted DD MB-OFDM ultradense WDM metropolitan networks,” *Journal of Lightwave Technology,* Vol. 34, No. 23, pp. 5707-5408, December, 2016.

[30] A. J. Stark, *et al.*, “System performance prediction with the gaussian noise model 100G PDM-QPSK coherent optical networks,” *Journal of Lightwave Technology,* Vol. 31, No. 21, pp. 3356-3367, November, 2013.

[31] A. Morea, J. Renaudier, T. Zami, A. Ghazisaeidi, and O. Bertran-Pardo, "Throughput comparison between 50-GHz and 37.5-GHz grid transparent networks [Invited]," *Journal of Optical Communications Network*, Vol. 7, No. 2, pp. A293-A300, February, 2015.

[32] J. Pan, C. Pulikkaseril, L. Stwart and S. Tibuleac, "Comparison of ROAD filter shape models for accurate transmission penalty assement," *IEEE Photonics Conference (IPC)*, pp.1-2, Waikoloa, HI, USA, October, 2016.

Chapter 3

Study of the transmission of a channel through a cascade of WSSs

3.1. Introduction

In this chapter, we study the behavior of an independently routed channel with and without side-channels, *i.e.*, channels in its spectral vicinity, when the channel goes through a cascade of WSSs emulating a transmission through an optical network, to assess the effect of optical filtering and crosstalk on the received signal performance.

In Section 3.2, we analyze the EVM dependence on the symbol rate when we increase the number of the WSSs in the cascade. In Section 3.3, we analyze the EVM dependence on the WSS bandwidth as we increase the number of the WSSs in the cascade. In these two sections, we consider that the system has no noise. In Section 3.4, we use the EVM penalty and OSNR penalty as performance metrics to study the degradation imposed on a 28 GBd isolated channel, *i.e.*, without out-of-band crosstalk, so that all penalties are due to the optical filtering of the cascaded WSSs. In Section 3.5, we analyze the impact on the signal performance, of the existence of a frequency offset between the channel optical carrier and the WSSs center frequency. In Sections 3.6 and 3.7, we perform studies for a 28 GBd signal, with side-channels, similar to the ones in the previous sections, to investigate the impact of possible crosstalk on the performance degradation. In Section 3.8, we study the effect of the variance of the optical transfer function bandwidth, B_{otf}, on the signal performance degradation. In Section 3.9, we present the conclusions of this chapter.

3.2. EVM dependence on the symbol rate

In this section, we are going to study the EVM dependence on the symbol rate, as the optical signal passes through a cascade of WSSs. Each WSS has a fixed -6 dB bandwidth of 37.5 GHz or 50 GHz. In this section, our study focus is on a single independently routed channel. We use a 4-QAM signal with ρ=0.1 and a symbol rate between 25 GBd and 35 GBd. To focus on this EVM dependence, we consider only the waveform distortion and neglect the ASE noise. We use the analytical model with

B_{otf}=8.5 GHz. This corresponds to a super-Gaussian model with a 3.5th order for the 37.5 GHz -6 dB bandwidth and 4.9th order for the 50 GHz -6 dB bandwidth. The WSS bandwidths chosen are equal to the frequency slot available to the channel [1]. In all results performed through the chapter, we obtained a similar network performance from the analytical model and from the super-Gaussian model. Hence, we only present results for the analytical model.

In Figure 3.1, we can see the EVM contour in dB as a function of the number of cascaded WSSs using a 4-QAM signal with a symbol rate between 25 GBd and 35 GBd, with ρ=0.1, where each -6 dB WSS bandwidth is a) 50 GHz and b) 37.5 GHz.

From Figure 3.1, we can conclude that, if we increase the number of cascaded WSSs in the optical path, to maintain the same EVM, then the symbol rate must be reduced. For the 50 GHz case, when compared to the 37.5 GHz case, we observe lower values of the EVM, which is expected since the filter bandwidth narrowing effect has a lower impact on the signal, because of the wider bandwidth of each WSS, for the same symbol rate and roll-off factor. In Figure 3.1, the EVM is between [-76.5, -25.5] dB for the scenario of 50 GHz and [-36, -8] dB for the scenario of 37.5 GHz.

If we increase the roll-off factor from 0.1 to 0.3, the signal launched on the optical path has a larger bandwidth and it is expected that the EVM will be more degraded when the number of cascaded WSSs is increased. Figure 3.2 shows the EVM contour in dB as a function of the number of cascaded WSSs and of the symbol rate for a 4-QAM signal with ρ=0.3. In Figure 3.2, we can see the EVM in an interval of [-72,-24] dB for the scenario of 50 GHz and [-34.2,-7.6] dB for the scenario of 37.5 GHz.

When we compare Figures 3.1 and 3.2, we observe clearly the impact of the larger signal bandwidth, degrading the EVM for the signal with ρ=0.3.

The values of the EVM shown in Figures 3.1 and 3.2 are much lower than the reference values obtained in Chapter 2. These low values are explained by the absence of ASE noise, since we wanted to focus only on the waveform distortion from WSS filtering.

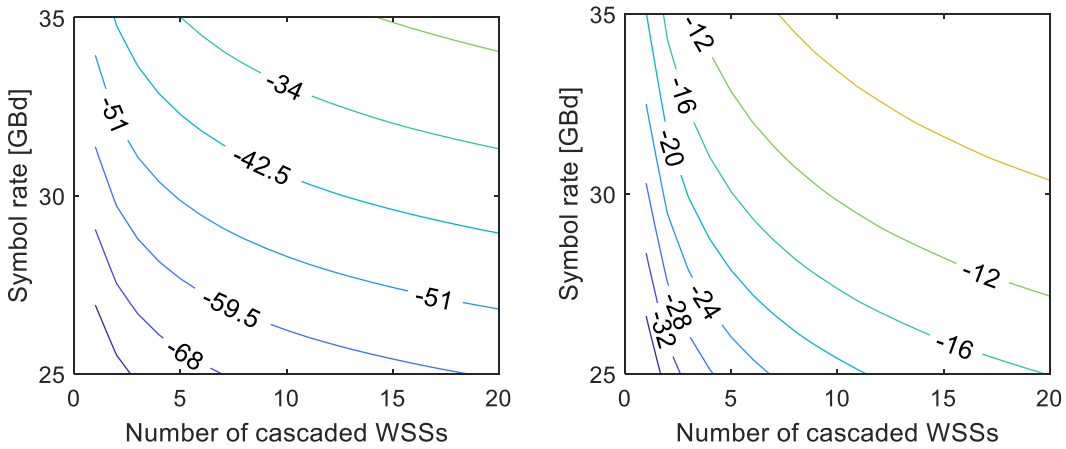

(a) (b)

Figure 3.1 *EVM contour in dB as a function of the number of cascaded WSSs and of the symbol rate for a 4-QAM signal with ρ=0.1. The -6 dB bandwidth of each WSS filter is (a) 50 GHz and (b) 37.5 GHz.*

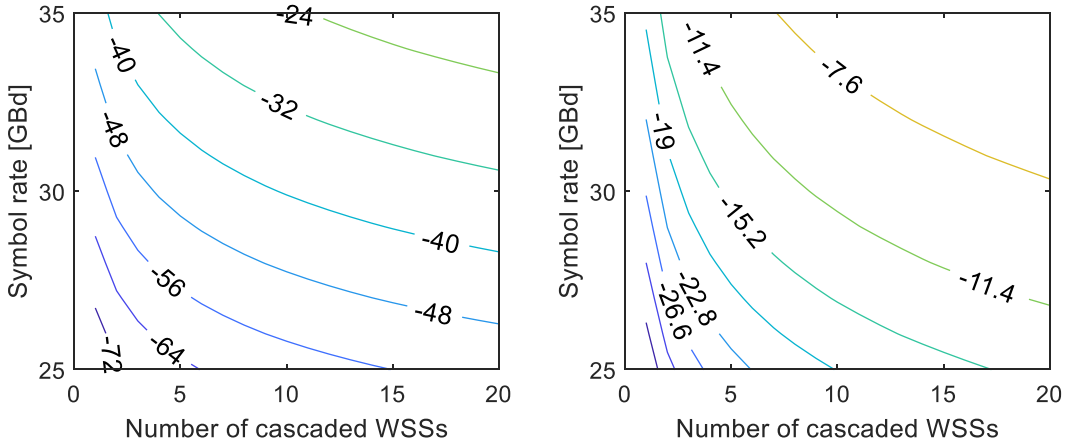

(a) (b)

Figure 3.2 *EVM contour in dB as a function of the number of cascaded WSSs and of the symbol rate for a 4-QAM signal with ρ=0.3. The -6 dB bandwidth of each WSS filter is (a) 50 GHz and (b) 37.5 GHz.*

3.3. EVM dependence on the WSS bandwidth

In this section, we study the EVM dependence on the WSS bandwidth as a function of the number of cascaded WSSs for a fixed signal symbol rate. To focus on this dependence, we consider only the waveform distortion and neglect the ASE noise, similarly to what is done in the previous section.

Figure 3.3 shows the EVM contour in dB as a function of the number of cascaded WSSs and of the -6 dB bandwidth of each WSS, for the symbol rate of a) 28 GBd and b) 32.5 GBd, with ρ=0.1.

From Figure 3.3, we can conclude that if we increase the number of cascaded WSSs, and need to maintain the same EVM, the bandwidth of each WSS must be increased, to reduce the optical filtering effect.

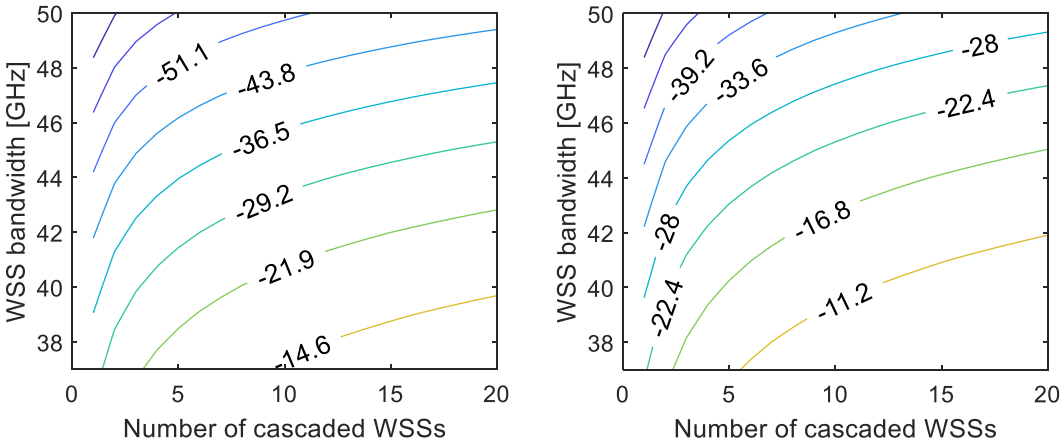

Figure 3.3 *EVM contour in dB as a function of the number of cascaded WSSs and of the -6 dB bandwidth of each WSS with (a) 28 GBd and (b) 32.5 GBd with ρ=0.1.*

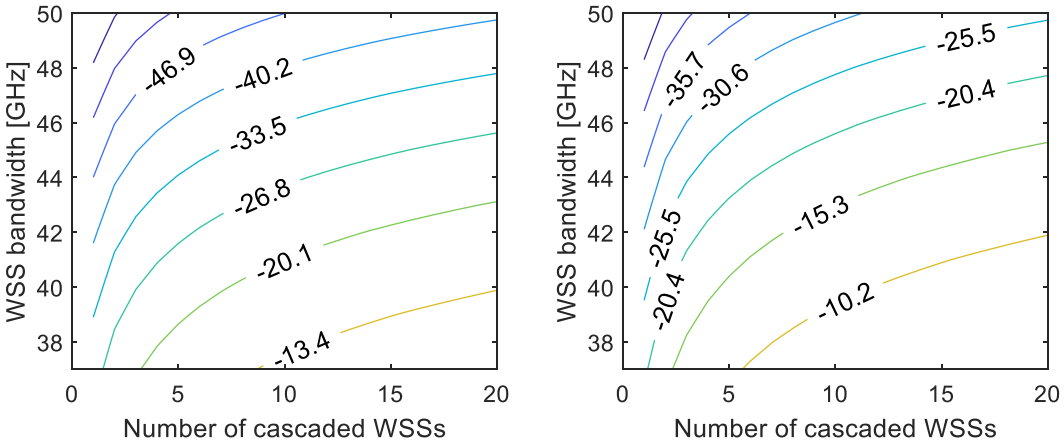

Figure 3.4 *EVM contour in dB as a function of the number of cascaded WSSs and of the -6 dB bandwidth of each WSS with (a) 28 GBd and (b) 32.5 GBd with ρ=0.3.*

For the 28 GBd case, when compared to the 32.5 GBd case, we observe a lower EVM degradation, which is expected since the filter bandwidth narrowing effect of the WSS cascade has a lower impact on the narrower bandwidth of the 28 GBd signal than on the 32.5 GBd signal, for the same WSS bandwidth and signal roll-off factor. In Figure 3.3, the EVM values are in the interval of [-65.7, -14.6] dB for the scenario of 28 GBd and in the interval of [-50.4,-11.2] dB for the scenario of 32.5 GBd.

To obtain the results shown in Figure 3.3, we use the analytical model with the same B_{otf} for all WSSs, which is independent of the WSS bandwidth. If we use the

super-Gaussian model, we have to change the order of the super-Gaussian each time the WSS bandwidth is changed.

Figure 3.4 shows the EVM contour in dB as a function of the number of cascaded WSSs and of the -6 dB bandwidth of each WSS, for the symbol rate of a) 28 GBd and b) 32.5 GBd, with ρ=0.3.

If we compare Figures 3.3 and 3.4, when we increase the roll-off factor from 0.1 to 0.3, the signal uses more bandwidth and the EVM is degraded due to the enhanced filtering effect. The EVM values in Figure 3.4 are in the interval of [-60.3,-13.4] dB for the scenario of 28 GBd and in the interval of [-45.9,-10.2] dB for the scenario of 32.5 GBd.

3.4. EVM and OSNR penalties for a single channel

In this section, the EVM and the OSNR penalties due to a cascade of WSS filters are studied for 32.5 GBd and 28 GBd signals with ρ=0.1 and 0.3, for the 4-QAM, 8-QAM and 16-QAM modulation formats. In the present and subsequent sections, the ASE noise is considered in the system using the optical network model presented in Figure 2.1.

Figures 3.5-3.7 show the (a) EVM penalty and (b) OSNR penalty for 4-QAM, 8-QAM and 16-QAM modulation formats, respectively, as a function of the number of cascaded WSSs. The roll-off factor is 0.1 and two symbol rates are considered, 28 GBd and 32.5 GBd, and the –6 dB bandwidths of each WSS filter are 37.5 GHz and 50 GHz.

In these figures, we can see that the penalty is higher for the 37.5 GHz WSS filters cascade in comparison with the 50 GHz WSS filters cascade, especially for the 32.5 GBd signal case. Considering the same WSS bandwidth for each WSS in the cascade, the penalty is higher if the R_S =32.5 GBd because the signal has a larger bandwidth than the signal with 28 GBd. We also see that a higher QAM modulation order is more sensitive to the filtering effect, since for the same power at the transmitter, the constellation points are closer and more prone to an error in detection, as already shown in Chapter 2. For example, for the 4-QAM modulation format with 28 GBd, ρ=0.1 and each WSS with a -6 dB bandwidth of 37.5 GHz, after 15 WSSs the OSNR penalty is 1.2 dB. For the 8-QAM, after 10 WSSs the OSNR penalty is 1.5 dB. For the 16-QAM, after 5 WSSs, the OSNR penalty is 1.2 dB.

We can also see that for the 50 GHz case, the penalties are practically null because the bandwidth of the signal is clearly lower than the bandwidth of the cascaded WSSs.

From the results presented in Figures 3.5-3.7, the EVM and the OSNR penalties show a similar behavior with the increase of the number of WSSs, although the EVM penalty predicts higher values when compared with the OSNR penalty. For example, for the 4-QAM, 28 GBd, ρ=0.1, 37.5 GHz, after 15 WSSs, the difference is 1.1 dB between the two metrics. For the 8-QAM after 10 WSSs, the difference is 1.2 dB. For the 16-QAM after 5 WSSs, the difference is 0.8 dB.

The EVM is similar to the SNR only when the distortion is negligible when compared with the noise [1]. Since in this work, we have distortion due to the filter bandwidth narrowing effect, differences in the penalties estimated from the EVM and OSNR are expected. Hence, in this work, we evaluate if, at least, we can have a rough estimate of the performance of the signal as it traverses a cascade of WSSs using the EVM penalty. This can be important, because the OSNR penalty consumes too much computational time, if extensive optimization of the optical communication system is to be performed.

We set that the OSNR penalty must be lower than 1.5 dB [2]. By considering this limit for a cascaded WSSs having each a -6 dB bandwidth of 37.5 GHz and considering a 28 GBd signal with ρ=0.1, from Figures 3.5-3.7 for 4-QAM, 8-QAM and 16-QAM modulation formats, the optical path can have 15, 9 and 5 WSSs in a cascade, respectively. If we increase the symbol rate to 32.5 GBd while keeping ρ=0.1, then for 4-QAM, 8-QAM and 16-QAM modulation formats, the optical path can have 6, 4 and 2 WSSs in a cascade, respectively.

Figures 3.8 and 3.9 present the PSD of the signal at the optical transmitter and at the optical receiver after 20 cascaded WSSs with each WSS with a -6 dB bandwidth of 37.5 GHz and 50 GHz, respectively, for a signal with R_S =28 GBd and ρ=0.1. The figures show also the signal after the RRC filter at the receiver and the RRC filter transfer function. When comparing Figures 3.8 (a) and 3.9 (a), we notice that Figure 3.8 (a) shows a lower bandwidth for the first WSS. After cascading 20 WSSs, the effect of the filter bandwidth narrowing, shown in Figure 3.8 (b), is enhanced and leads to a higher distortion in the signal spectrum, when compared with the PSD of the signal shown in Figure 3.9 (b).

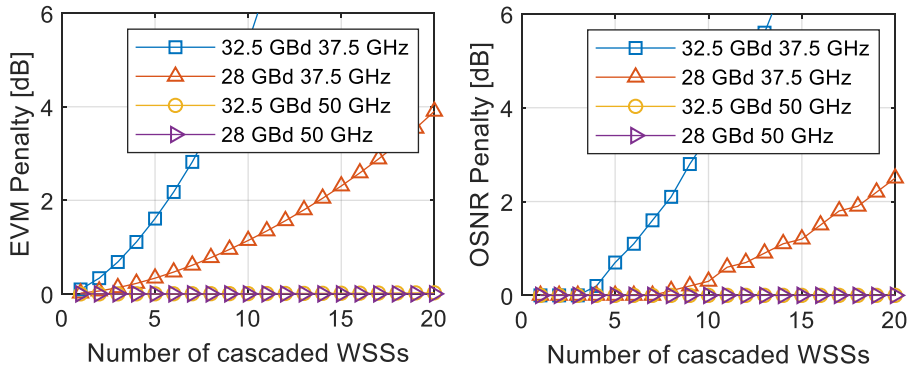

Figure 3.5 *(a) EVM penalty and (b) OSNR penalty as a function of the number of cascaded WSSs. The -6 dB bandwidths of each WSS are 37.5 GHz and 50 GHz. The symbol rate is 28 GBd and 32.5 GBd with ρ=0.1, for the 4-QAM modulation format.*

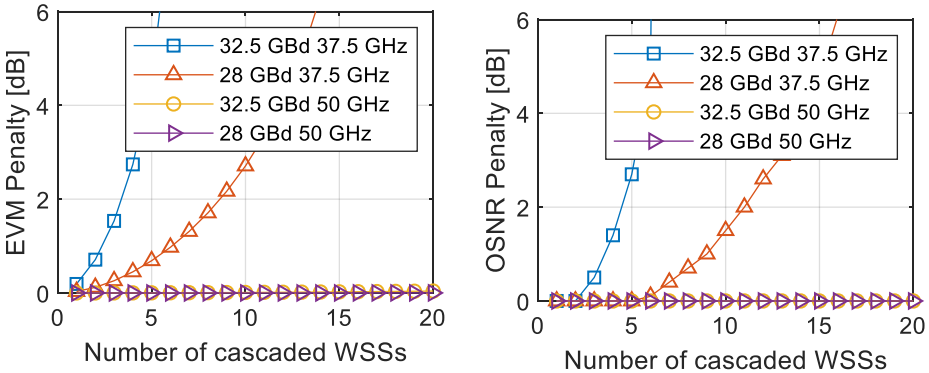

Figure 3.6 *(a) EVM penalty and (b) OSNR penalty as a function of the number of cascaded WSSs. The -6 dB bandwidths of each WSS are 37.5 GHz and 50 GHz. The symbol rate is 28 GBd and 32.5 GBd with ρ=0.1 for 8-QAM modulation format.*

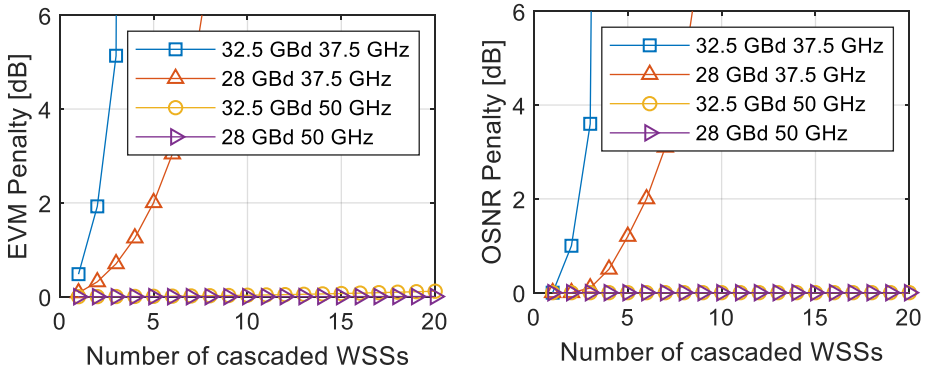

Figure 3.7 *(a) EVM penalty and (b) OSNR penalty as a function of the number of cascaded WSSs. The -6 dB bandwidths of each WSS are 37.5 GHz and 50 GHz. The symbol rate is 28 GBd and 32.5 GBd with ρ=0.1 for 16-QAM modulation format.*

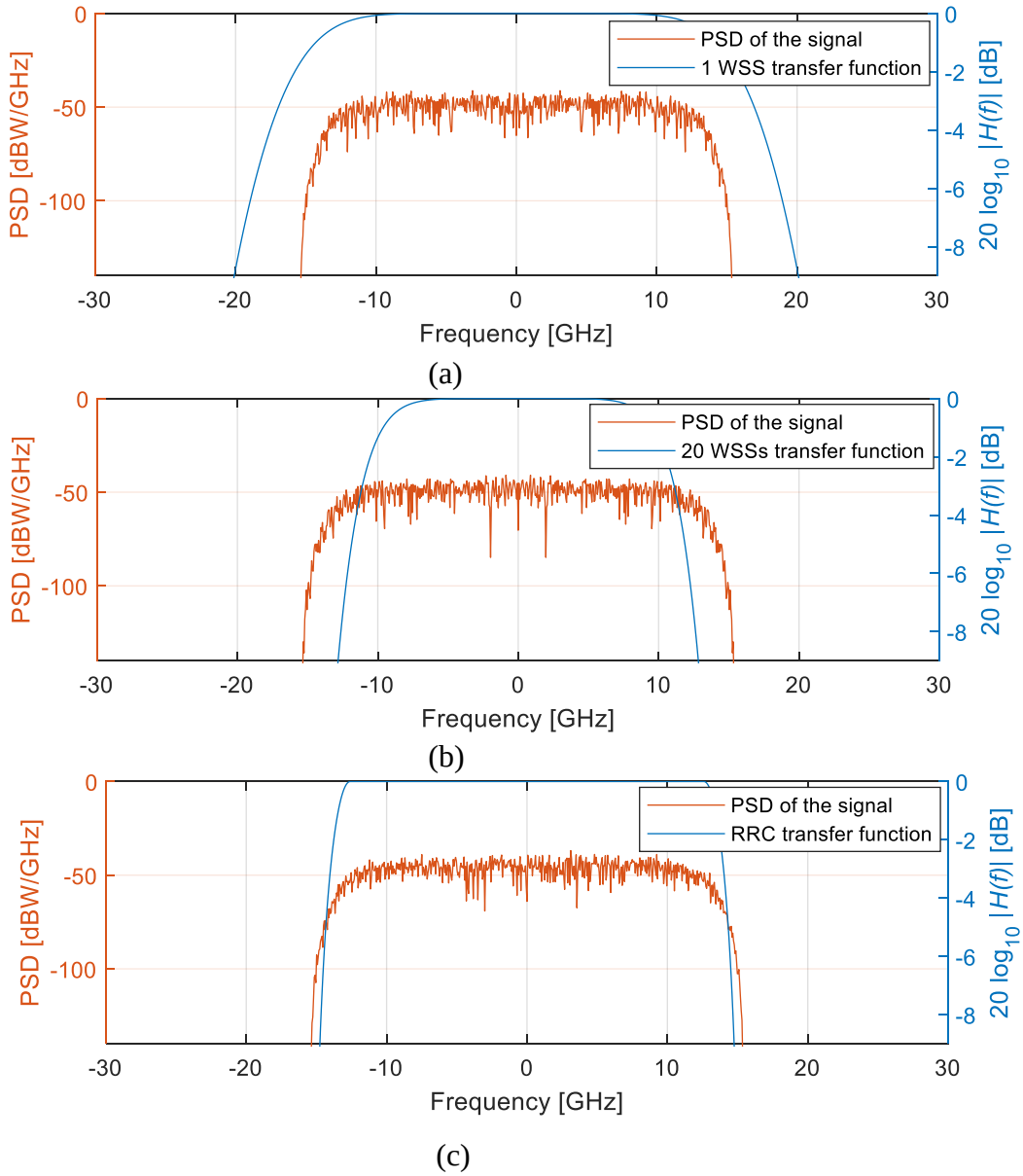

Figure 3.8 *PSD of the signal for the 4-QAM modulation format, R_S =28 GBd with ρ=0.1. The -6 dB bandwidth of each WSS is 37.5 GHz. (a) the PSD of the signal at the optical transmitter output and filter transfer function after the first WSS, (b) the PSD of the signal at the optical receiver input and transfer function of 20 cascaded WSSs, (c) the PSD of the signal after the RRC filter at the receiver and transfer function of the RRC filter.*

For WSSs with a -6 dB bandwidth of 37.5 GHz, the -6 dB bandwidth reduces to 24.34 GHz after 20 cascaded WSSs. The bandwidth is reduced to 64.9% of its initial value. For WSSs with a -6 dB bandwidth of 50 GHz, the -6 dB bandwidth narrows to 36.82 GHz after 20 cascaded WSSs. The cascaded bandwidth is 73.6% of its initial value. The reason for this higher percentage is because, as we increase the bandwidth of each WSS, the transfer function of the cascade tends to approach a more rectangular shape, which reduces the filter bandwidth narrowing effect.

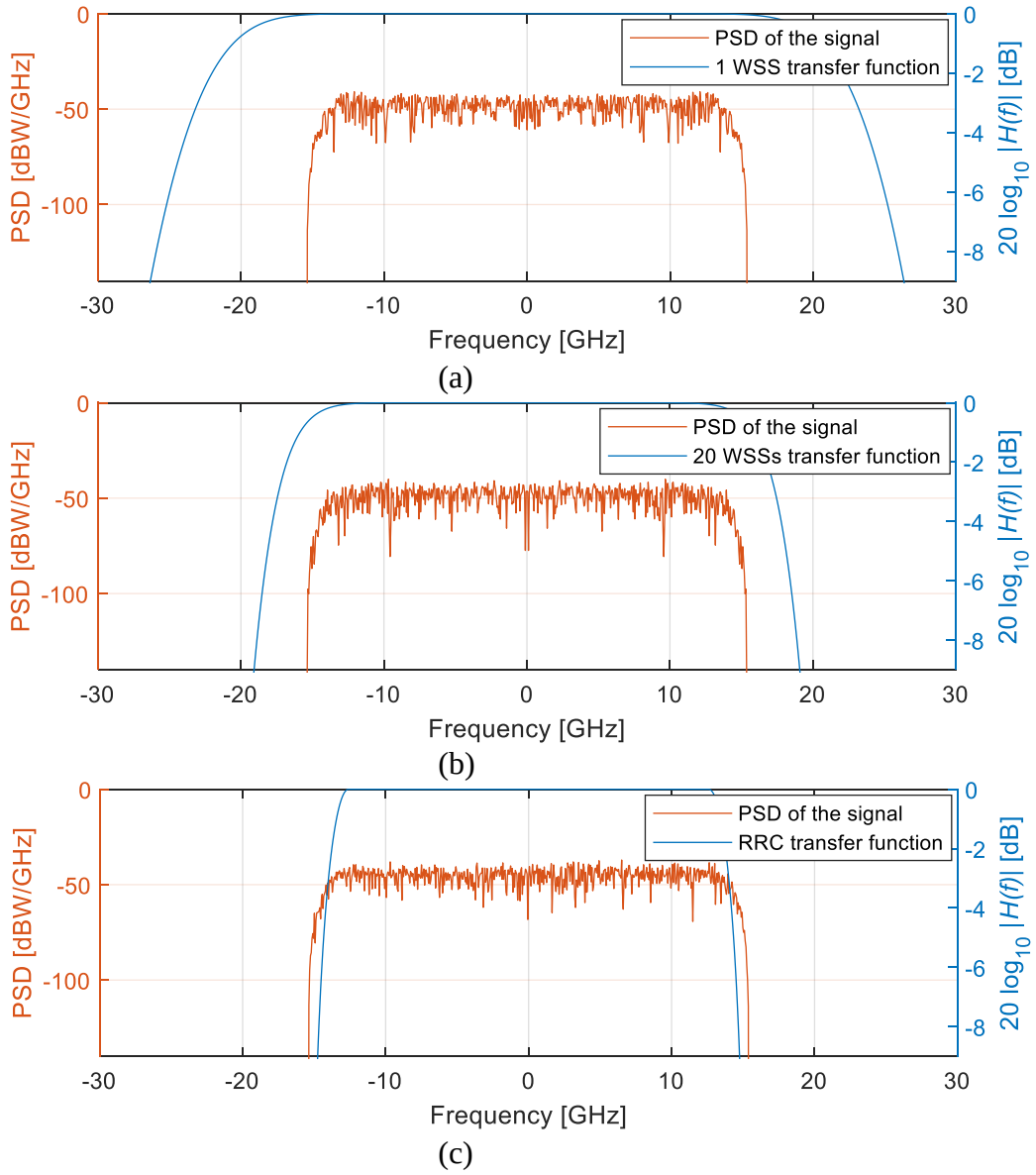

Figure 3.9 *PSD of the signal for the 4-QAM modulation format, R_S =28 GBd with ρ=0.1. The -6 dB bandwidth of each WSS is 50 GHz. (a) the PSD of the signal and the filter transfer function after the first WSS, (b) the PSD of the signal at the optical receiver input and transfer function of 20 cascaded WSSs, (c) the PSD of the signal after the RRC filter at the receiver, and transfer function of the RRC filter.*

Another way to realize that the transfer function of the WSS cascade becomes more rectangular with increased bandwidth of each WSSs in the cascade is to think that the order of an equivalent super-Gaussian filter should be increased to provide the same results with the filter cascading, which makes the WSS transfer function more rectangular and, subsequently, also the cascade of WSSs. For WSSs with the -6 dB bandwidth of 50 GHz, with 28 GBd or 32.5 GBd, the cascade practically does not affect the PSD of the signal.

The EVM penalty and OSNR penalty in Figures 3.5-3.7 are consistent with the results presented in Figures 3.8 and 3.9.

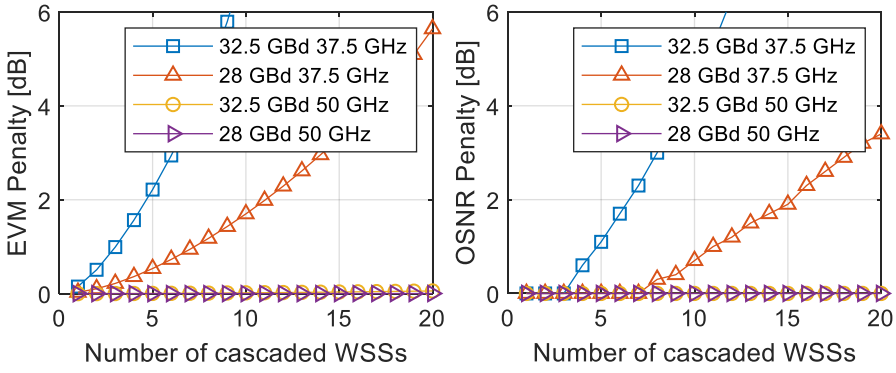

Figure 3.10 *(a) EVM penalty and (b) OSNR penalty as a function of the number of cascaded WSSs. The -6 dB bandwidths of each WSS are 37.5 GHz and 50 GHz. The symbol rate is 28 GBd and 32.5 GBd with ρ=0.3 and 4-QAM modulation format.*

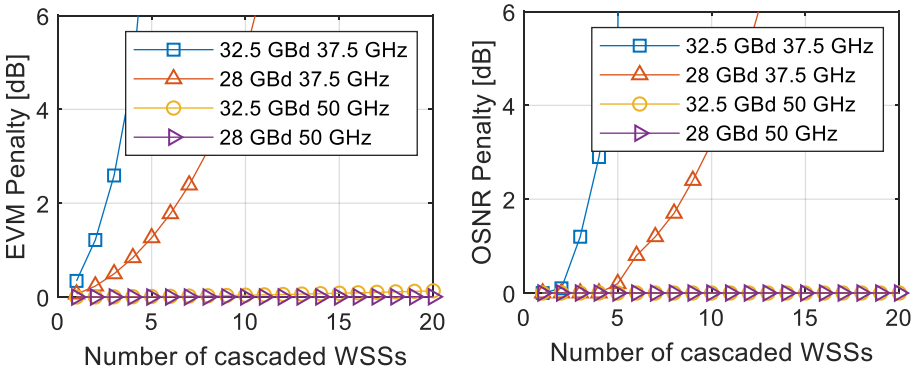

Figure 3.11 *(a) EVM penalty and (b) OSNR penalty as a function of the number of cascaded WSSs. The -6 dB bandwidths of each WSS are 37.5 GHz and 50 GHz. The symbol rate is 28 GBd and 32.5 GBd with ρ=0.3 and 8-QAM modulation format.*

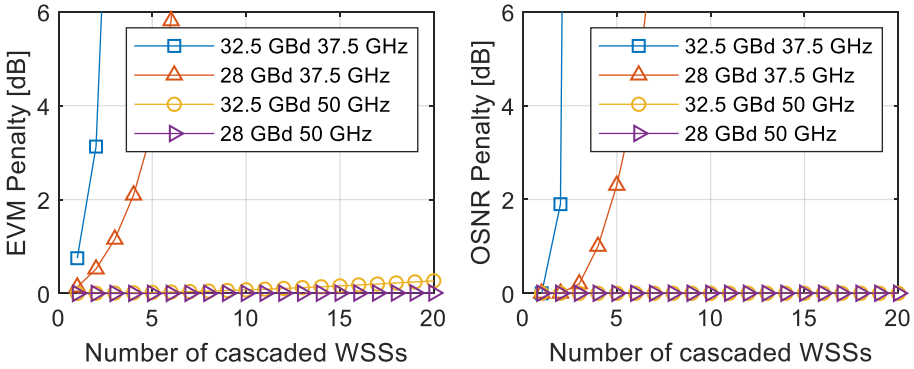

Figure 3.12 *(a) EVM penalty and (b) OSNR penalty as a function of the number of cascaded WSSs. The -6 dB bandwidths of each WSS are 37.5 GHz and 50 GHz. The symbol rate is 28 GBd and 32.5 GBd with ρ=0.3 and 16-QAM modulation format.*

Figures 3.10-3.12 show the (a) EVM penalty and (b) OSNR penalty for the 4-QAM, 8-QAM and 16-QAM modulation formats, respectively, as a function of the number of WSSs in the cascade. Two symbol rates are considered, 28 GBd and

32.5 GBd, for a roll-off factor of 0.3 and the –6 dB bandwidths of each WSS filter are 37.5 GHz and 50 GHz.

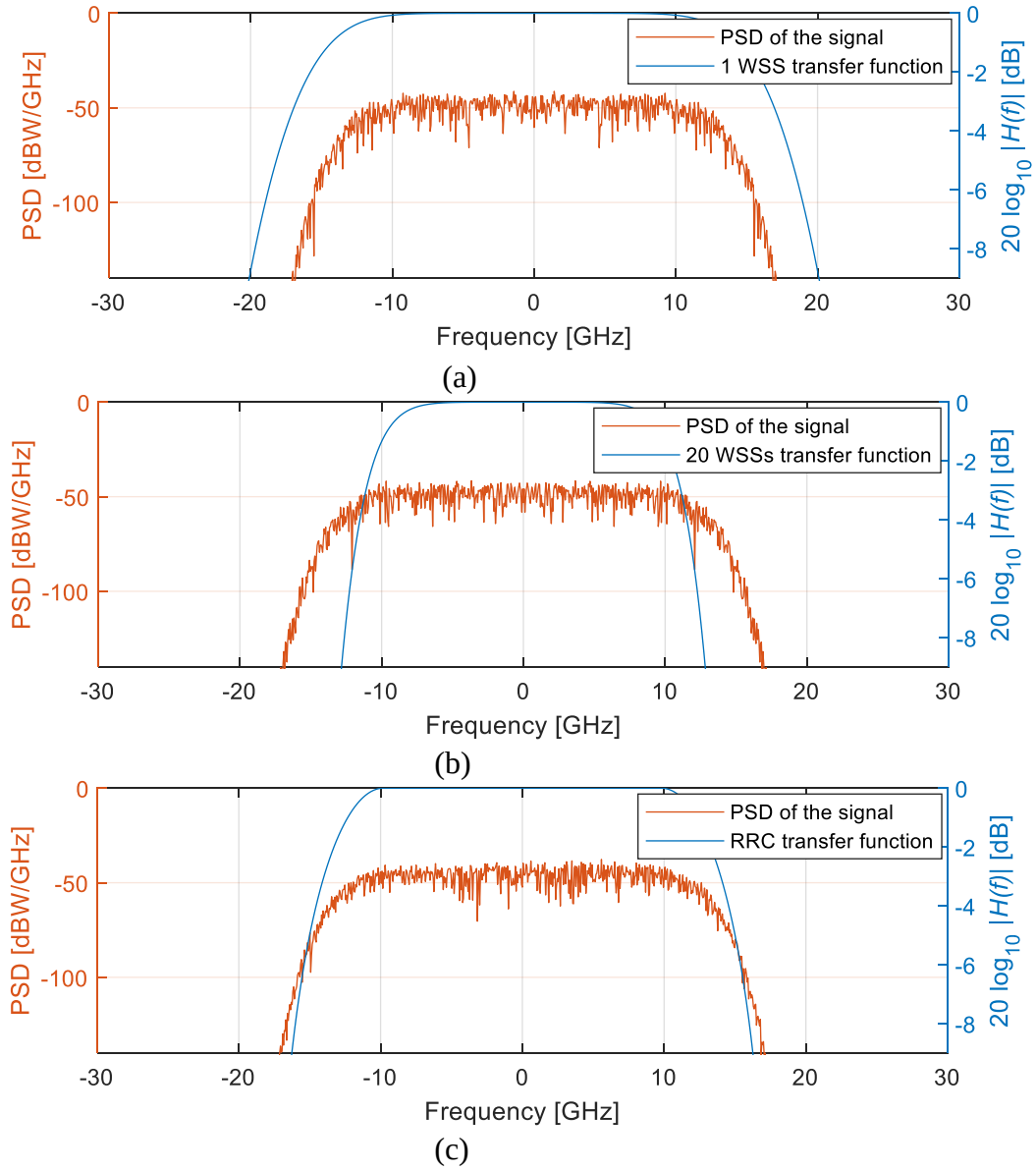

Figure 3.13 *PSD of the signal for the 4-QAM, R_S =28 GBd with ρ=0.3. The -6 dB bandwidth of each WSS is 37.5 GHz. In (a) the PSD of the signal and the filter transfer function after the first WSS. In (b) the PSD of the signal at the optical receiver and the transfer function of 20 cascaded WSSs. In (c) the PSD of the signal after the RRC filter at the receiver, and the transfer function of the RRC filter.*

When comparing Figures 3.10-3.12 with Figures 3.5-3.7, we observe that the penalties have increased, as expected because a RRC signal with a higher roll-off factor has a higher bandwidth. For example, for the 4-QAM, 28 GBd, ρ=0.3, 37.5 GHz, after 15 WSSs, the OSNR penalty increase is 0.7 dB. For the 8-QAM, after 10 WSSs the OSNR penalty increase is 1.7 dB. For the 16-QAM, after 5 WSSs, the OSNR penalty increase is 1.1 dB.

From the results presented in Figures 3.10-3.12, EVM penalty and the OSNR penalty show similar behaviors with the increase of the number of WSS, although the EVM penalty predicts higher values when compared with the OSNR penalty. For example, for the 4-QAM, 32.5 GBd, ρ=0.3, 37.5 GHz, after 15 WSSs, the difference is 1.4 dB. For the 8-QAM, after 10 WSSs, the difference is 2.0 dB. For the 16-QAM, after 5 WSSs, the difference is 1.2 dB.

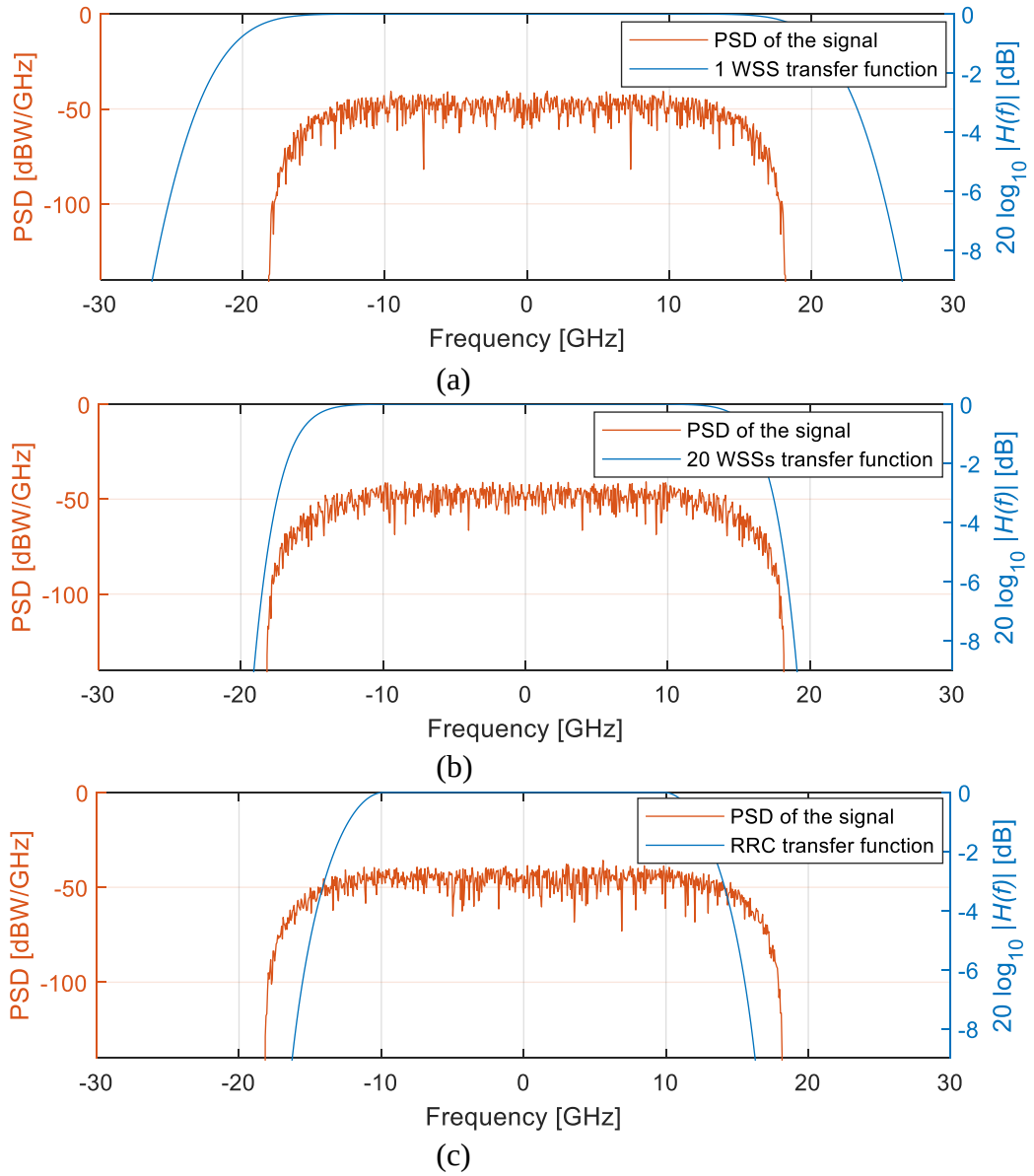

Figure 3.14 *PSD of the signal for the 4-QAM, R_S =28 GBd with ρ=0.3. The -6 dB bandwidth of each WSS is 50 GHz. In (a) the PSD of the signal and the filter transfer function after the first WSS. In (b) the PSD of the signal at the optical receiver and the transfer function of 20 cascaded WSSs. In (c) the PSD of the signal after the RRC filter at the receiver, and the transfer function of the RRC filter.*

By assuming that the OSNR penalty must be lower than 1.5 dB [3], for cascaded WSSs having each a -6 dB bandwidth of 37.5 GHz, and considering a 28 GBd signal

with ρ=0.3, from Figures 3.10-3.12 for 4-QAM, 8-QAM and 16-QAM modulation formats, the optical path can reach 12, 7 and 4 WSSs in a cascade, respectively. If we increase the symbol rate to 32.5 GBd while keeping ρ=0.3, then for 4-QAM, 8-QAM and 16-QAM modulation formats, the optical path can have only 5, 3 and 1 WSSs in a cascade, respectively.

Figures 3.13 and 3.14 present the PSDs of the signal at the optical transmitter and at the optical receiver after 20 cascaded WSSs with each WSS with -6 dB bandwidth of 37.5 GHz and 50 GHz, respectively, for a signal with R_S =28 GBd and ρ=0.3. The figures show also the signal after the RRC filter at the receiver and its transfer function.

When comparing Figures 3.13 (a) and 3.14 (a), we notice that the first figure shows a much lower WSS bandwidth. After cascading 20 filters, the effect of filter bandwidth narrowing effect shown in Figure 3.13 (b), leads to a higher distortion in the signal spectrum, when compared with Figure 3.14 (b).

The EVM penalty and OSNR penalty shown in Figures 3.10-3.12 are consistent with the observations taken from the PSDs shown in Figures 3.13 and 3.14, since the penalties due to filtering are increased for the signal with the larger bandwidth.

3.5 Frequency offset for a single channel

In this section, we study the impact on the signal performance of the existence of a frequency offset, within the ITU-T maximum tolerance, between the channel optical carrier and the WSSs center frequency. This is important because tunable laser sources used at the transmitter and at the receiver may show a frequency drift with time [5]. We consider that all lasers have the same behavior and exhibit the same frequency drift with time. The maximum tolerance recommended by the ITU-T is ±1.5 GHz, so we simulate the scenario where the frequency of the laser is shifted by +1.5 GHz. We also consider that all WSS filters are perfectly aligned throughout the optical path.

Figures 3.15-3.17 show the impact of the frequency offset on the EVM penalty and OSNR penalty, as a function of the number of cascaded WSSs, for 32.5 GBd and 28 GBd signals with ρ=0.1 for the 4-QAM, 8-QAM and 16-QAM modulation formats.

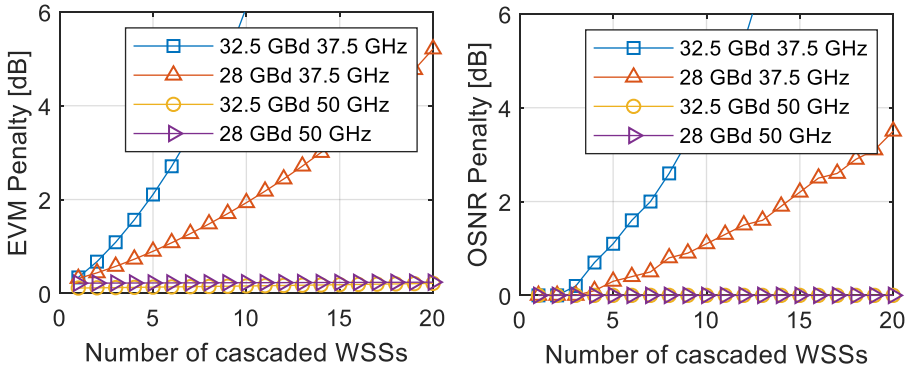

Figure 3.15 *(a) EVM penalty and (b) OSNR penalty as a function of the number of cascaded WSSs. The -6 dB bandwidths of each WSS are 37.5 GHz and 50 GHz. The symbol rate is 28 GBd and 32.5 GBd with ρ=0.1 using the 4-QAM modulation format. The signal carrier is shifted by +1.5 GHz relative to the WSSs center frequency.*

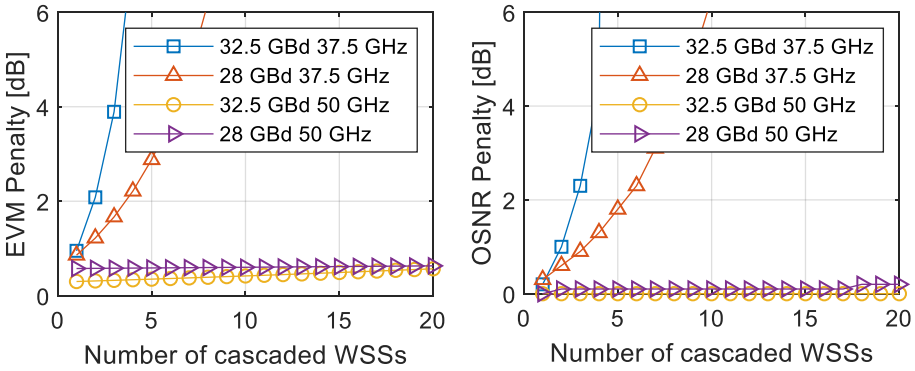

Figure 3.16 *(a) EVM penalty and (b) OSNR penalty as a function of the number of cascaded WSSs. The -6 dB bandwidths of each WSS are 37.5 GHz and 50 GHz. The symbol rate is 28 GBd and 32.5 GBd with ρ=0.1 using the 8-QAM modulation format. The signal carrier is shifted by +1.5 GHz relative to the WSSs center frequency.*

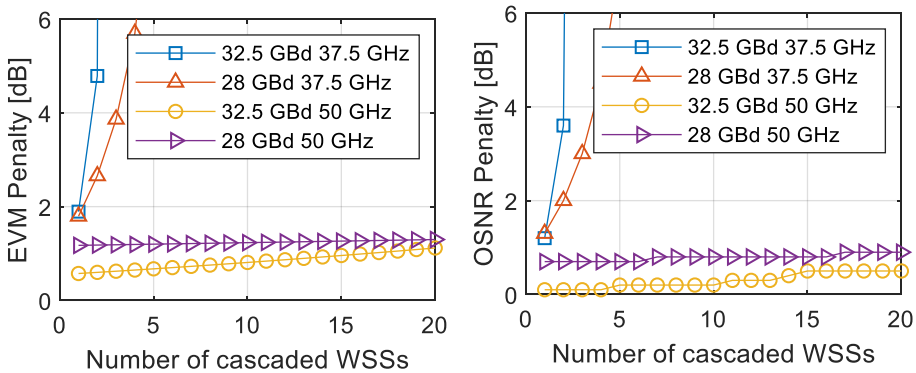

Figure 3.17 *(a) EVM penalty and (b) OSNR penalty as a function of the number of cascaded WSSs. The -6 dB bandwidths of each WSS are 37.5 GHz and 50 GHz. The symbol rate is 28 GBd and 32.5 GBd with ρ=0.1 using the 16-QAM modulation format. The signal carrier is shifted by +1.5 GHz relative to the WSSs center frequency.*

Again, by considering that the OSNR penalty must be lower than 1.5 dB, for cascaded WSSs having each a -6 dB bandwidth of 37.5 GHz, and considering a 28 GBd

signal with ρ=0.1, from Figures 3.15-3.17 for 4-QAM, 8-QAM and 16-QAM modulation formats, the optical path can have 11, 4 and 1 cascaded WSSs, respectively. If we increase the symbol rate to 32.5 GBd while keeping ρ=0.1, then for 4-QAM, 8-QAM and 16-QAM modulation formats, the optical path can only reach 5, 2 and 1 WSSs, respectively. The number of WSSs is lower than the ones we have obtained without the frequency offset from Figures 3.5-3.7.

Another interesting analysis is to look at the OSNR penalty, which is 2.2 dB, after 15 WSSs, with the frequency offset, for 4-QAM, 28 GBd, ρ=0.1 and 37.5 GHz. The penalty is even higher for higher order modulation formats. For 8-QAM, after 9 WSSs the OSNR penalty is 5.0 dB. For 16-QAM, after 4 WSSs the OSNR penalty is 4.5 dB.

The higher order modulation formats are more impacted by the frequency offset, as can also be seen for the 50 GHz case, because when we increase the modulation format order, we observe that the OSNR penalty becomes not null and almost constant with the number of cascaded WSS..

We can conclude that the frequency offset of +1.5 GHz increases the OSNR penalty, because the frequencies on the right edge of the signal are more distorted by the WSS filtering than in the frequency offset absence.

3.6. EVM and OSNR penalties for a channel with side-channels

In this section, we study the behavior of a single channel with side-channels, with a fixed intercarrier spacing, when it goes through a cascade of WSSs. Each of these 3 channels is considered to be routed independently of the others. The presence of the side-channels may create inter-channel crosstalk between the center channel and the side-channels. The intercarrier spacing is set to 37.5 GHz, so that each channel uses a 37.5 GHz frequency slot in the flexible grid. We choose the 37.5 GHz slot, because it is a more demanding scenario than the 50 GHz scenario. In this section, each -6 dB WSS bandwidth is 37.5 GHz and the signal has R_S =28 GBd with ρ=0.1 and ρ=0.3.

We simulate a center channel with two side-channels each transmitting symbols from a different pseudo-random binary sequence. Each channel corresponds to a signal with R_S =28 GBd, ρ=0.1 and an intercarrier spacing Δf=37.5 GHz. A signal with 0 dBm launch power is transmitted in each of the 3 channels. Figure 3.18 shows the PSD of the signal in the center channel and in the side-channels at the optical transmitter output for the 4-QAM modulation format.

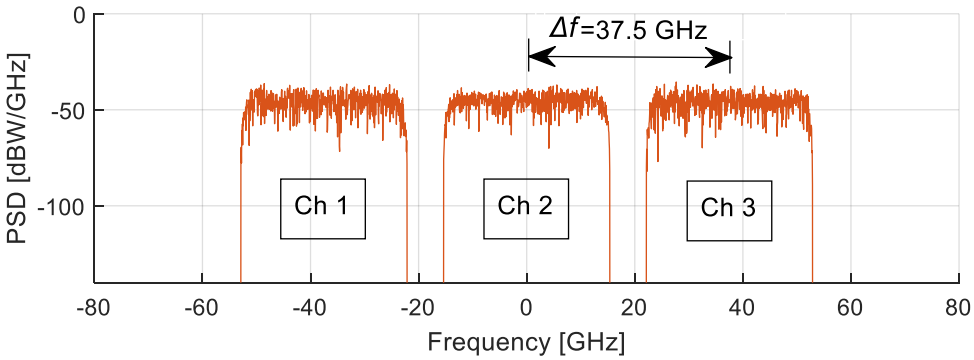

Figure 3.18 *PSD of the signal at the optical transmitter output for three independently routed channels with 4-QAM modulation format. The R_S =28 GBd with a ρ=0.1 and Δf =37.5 GHz.*

In Figure 3.19 (a) we can see the PSD of the center channel and the side-channels after the first WSS and the transfer function of the first WSS. In Figure 3.19 (b), is displayed the PSD of the signal at the optical receiver input and also the transfer function, both after 20 cascaded WSSs, and we can see that the side-channels have been practically filtered out. Figure 3.19 (c) shows the PSD of the signal after the filtering by the RRC filter and the RRC transfer function.

We can see the filter bandwidth narrowing effect by looking at Figure 3.19 (a) and (b), where the WSSs transfer function shows a reduced bandwidth and the PSD of the signal is clearly distorted. Figure 3.19 indicates that with ρ=0.1, the spectrum of the signals in the side-channels do not overlap with the spectrum of the signal in the center channel, and the crosstalk is negligible. Hence, the whole OSNR penalty to be observed must come from the filtering in the cascaded WSSs and not from the crosstalk.

Figure 3.20 shows the (a) EVM penalty and the (b) OSNR penalty as a function of the number of cascaded WSSs, for the 4-QAM, 8-QAM and 16-QAM modulation formats with ρ=0.1 in the presence of side-channels. Again, we observe that the higher order modulations formats are less robust to the filtering effect of the cascade of WSSs.

To have the OSNR penalty below 1.5 dB, we can have, from Figure 3.20 and for 4-QAM, 8-QAM and 16-QAM, 15, 9 and 5 WSSs, respectively. The increase in the penalty on the signal in the center channel is caused by the filter bandwidth narrowing effect of the cascaded WSSs, since the higher modulation format are more sensitive to distortion. When we presented in Section 3.4, the performance metrics studies for 1 channel without side-channels, we already concluded the need of an increase in the required OSNR at the receiver, for a higher modulation format for the same target BER.

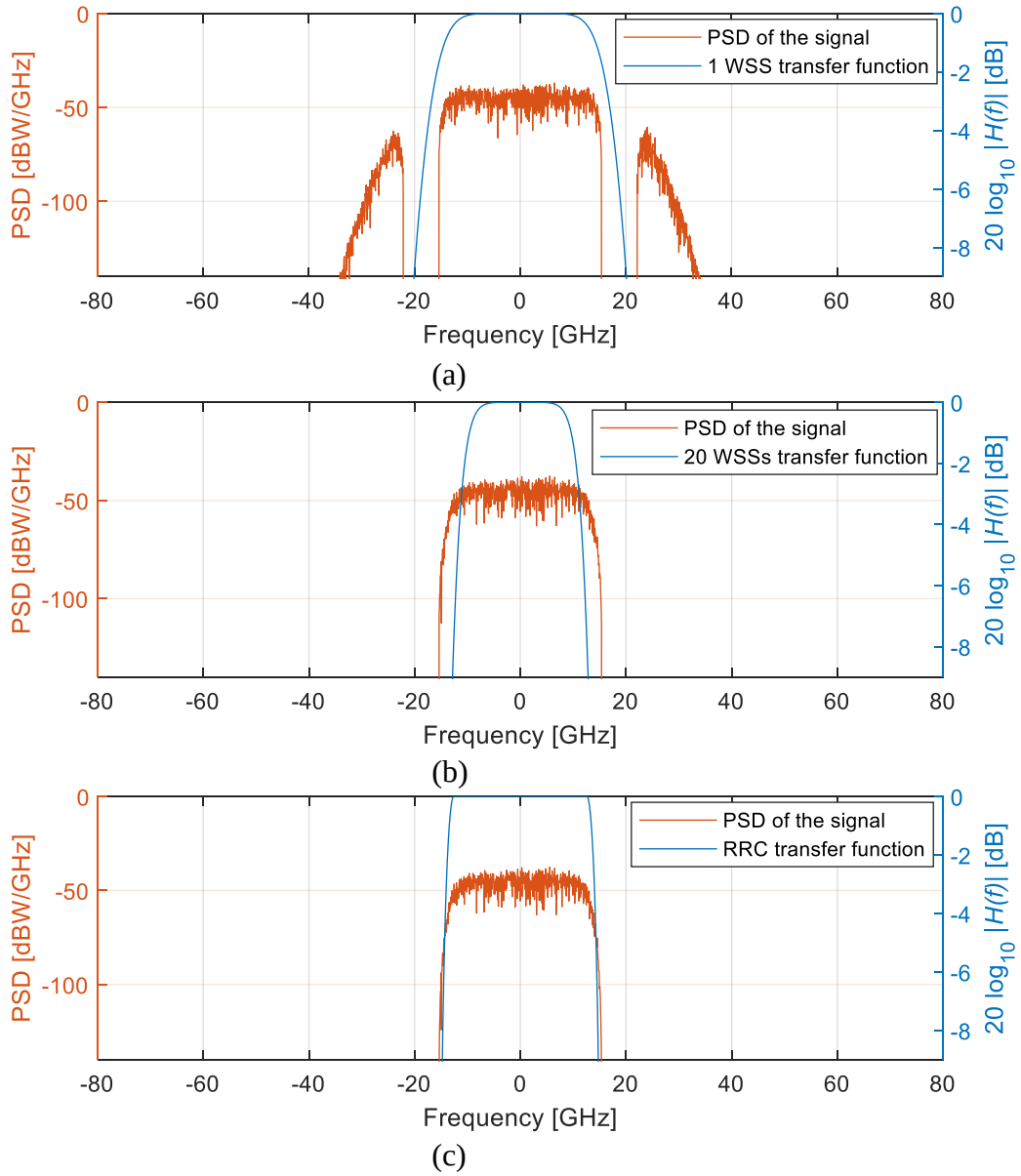

Figure 3.19 *PSD of the signal for the 4-QAM modulation format. The R_S =28 GBd with ρ=0.1 and the Δf=37.5 GHz. The -6 dB bandwidth of each WSS is 37.5 GHz. In (a) the PSD of the signal and the filter transfer function after the first WSS (b) the PSD of the signal at the optical receiver input and also the transfer function of 20 cascaded WSSs. In (c) the PSD of the signal after the RRC filter at the receiver, and the transfer function of the RRC filter.*

If we compare Figure 3.20 with Figures 3.5-3.7 we conclude that with ρ=0.1, the penalty is practically the same, because the spectra of the channels do not overlap.

In Figure 3.21, we can see the PSD of the center channel and the side-channels at the optical transmitter output with 4-QAM modulation format, and Δf=37.5 GHz. Each channel has R_S =28 GBd with ρ=0.3.

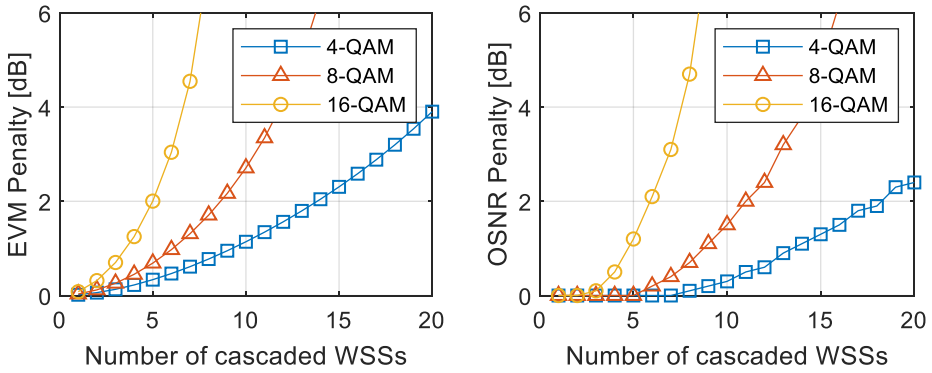

(a) (b)

Figure 3.20 *EVM penalty (a) and OSNR penalty (b) of the center channel as a function of the number of cascaded WSSs. The -6 dB bandwidth of each WSS is 37.5 GHz. The R_S =28 GBd with ρ=0.1 using the 4-QAM, 8-QAM, and 16-QAM modulation formats and Δf =37.5 GHz.*

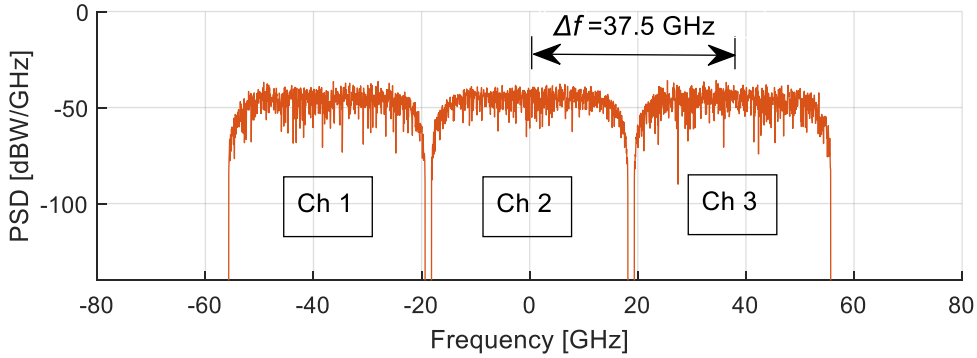

Figure 3.21 *PSD of the signal at the optical transmitter output for three independently routed channels with 4-QAM modulation format for R_S =28 GBd, ρ=0.3 and Δf =37.5 GHz.*

When we compare Figures 3.21 and 3.18, it should be noticed that now the channels are closer in frequency, but still do not overlap, and probably no crosstalk will be observed after the cascaded WSSs. Hence, similarly to the ρ=0.1 case, with ρ=0.3 the whole OSNR penalty to be observed must come from the filtering in the cascaded WSSs and not from the crosstalk.

In Figure 3.22 (a), the PSD of the center channel and the side-channels after the first WSS and the transfer function of the first WSS are depicted for ρ=0.3. In Figure 3.22 (b), it is displayed the PSD of the signal at the optical receiver input and also the transfer function, both after 20 cascaded WSS, and we can see that the side-channels have been practically filtered out. Figure 3.22 (c) shows the signal after the filtering by the RRC filter and the RRC transfer function.

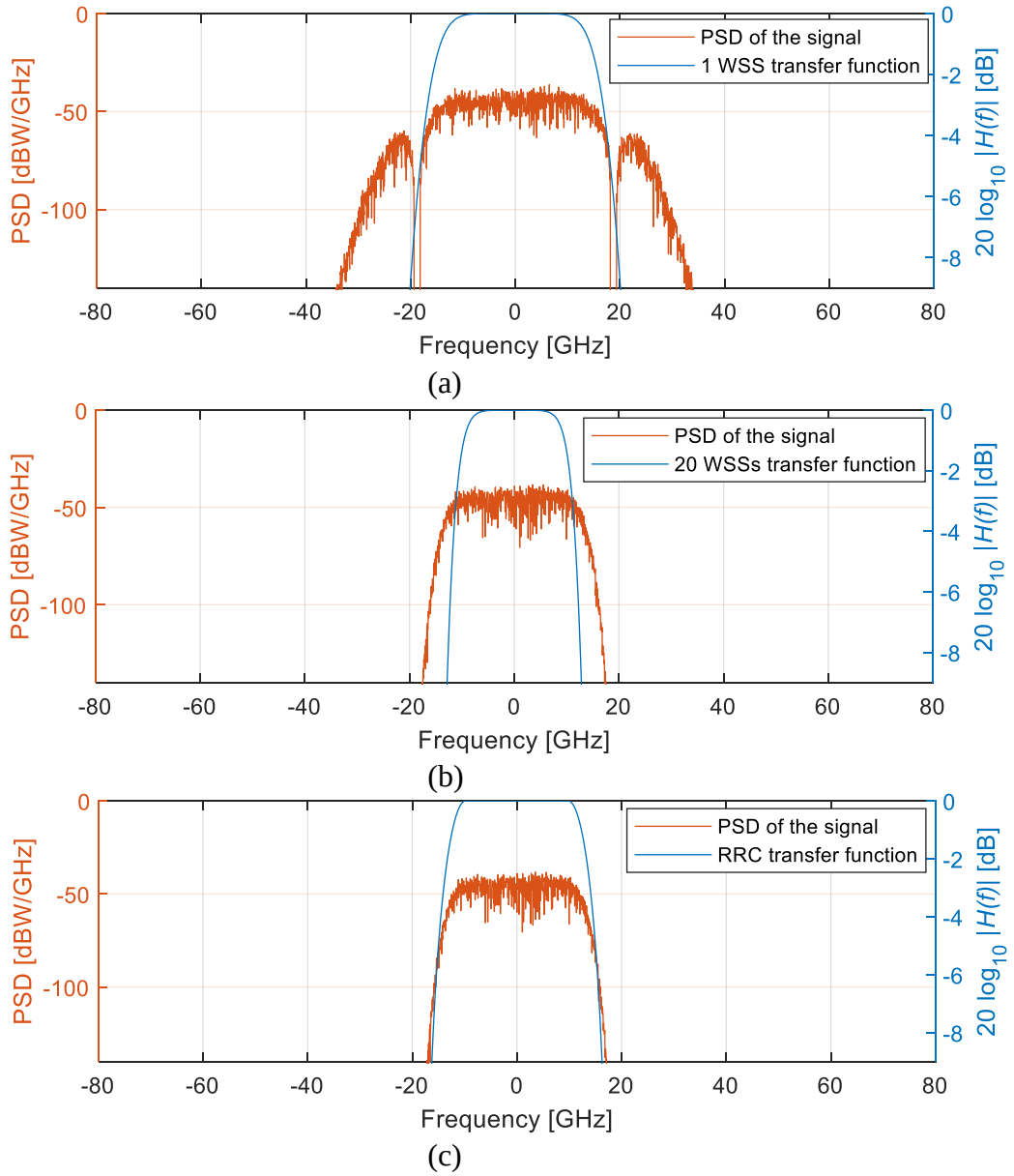

Figure 3.22 *PSD of the signal with side-channels for the 4-QAM modulation format. The R_S =28 GBd with ρ=0.3 and Δf =37.5 GHz. The -6 dB bandwidth of each WSS is 37.5 GHz. In (a) the PSD of the signal and the filter transfer function after the first WSS, (b) the PSD of the signal at the optical receiver input and also the transfer function of 20 cascaded WSSs. In (c) the PSD of the signal after the RRC filter at the receiver, and the transfer function of the RRC filter.*

If we compare Figures 3.22 (a) and 3.22 (b), we notice that the PSD of the signal is clipped in its edge frequencies by the cascade of WSSs. This result can be compared with Figures 3.19 (a) and 3.19 (b), where the clipping is less intense. The explanation for this effect is the larger bandwidth of the signal with ρ=0.3.

Figure 3.23 shows the penalties results for a 4-QAM, 8-QAM and 16-QAM modulation formats, and again we observe a higher penalty for the modulation format with higher order. If we compare Figure 3.23 with Figures 3.10-3.12, we conclude that

the estimated OSNR penalties are practically the same, because the side-channels spectra do not overlap with the center channel spectrum. If we compare Figures 3.23 and 3.20, we observe an increase of the penalties due to the increase of the roll-off factor from ρ=0.1 to ρ=0.3. For example, for the 4-QAM, 28 GBd, 37.5 GHz, after 15 WSSs, the OSNR penalty increase is 0.6 dB. For the 8-QAM, after 10 WSSs, the OSNR penalty increase is 1.8 dB. For the 16-QAM, after 5 WSSs, the OSNR penalty increase is 1.0 dB.

To keep the OSNR penalty below 1.5 dB, from Figure 3.23 and for 4-QAM, 8-QAM and 16-QAM, the optical path can have, 12, 7 and 4 cascaded WSSs, respectively.

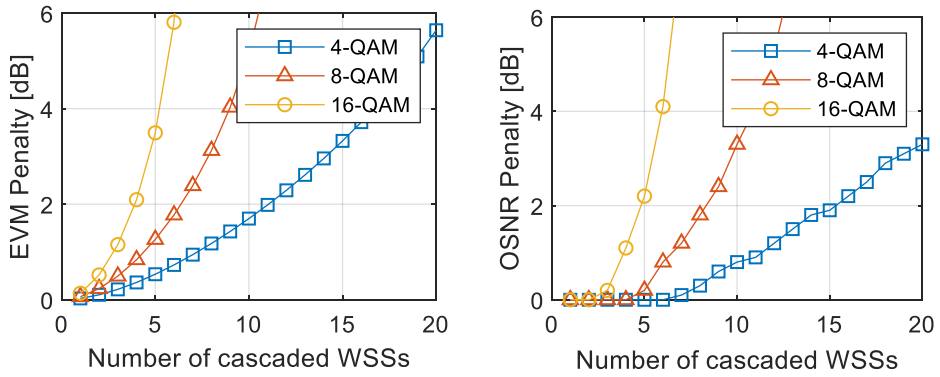

(a) (b)

Figure 3.23 *EVM penalty (a) and OSNR penalty (b) of the center channel as a function of the number of cascaded WSSs. The -6 dB bandwidth of each WSS is 37.5 GHz. The* R_S *=28 GBd with* ρ*=0.3 using the 4-QAM, 8-QAM, and 16-QAM modulation formats and* Δf *=37.5 GHz.*

3.7. Frequency offset for a channel with side-channels

In this section, we study the impact of the existence of a frequency offset, within the ITU-T maximum tolerance, between the channel carrier and the WSS center frequency in the presence of the side-channels. We simulate the scenario where the frequency of the lasers is shifted by +1.5 GHz.

To show the impact of the frequency offset on the EVM penalty and OSNR penalty, we display them in Figure 3.24 as a function of the cascaded WSSs, for the 4-QAM, 8-QAM and 16-QAM modulation formats.

If we compare Figure 3.24 with Figures 3.15-3.17 we conclude that the penalty is practically the same, with or without side-channels, when the frequency offset is applied to all carriers, and since they all have the same frequency shift, there is no increase in the out-of-band crosstalk by the presence of side-channels.

To keep the OSNR penalty below 1.5 dB, from Figure 3.24 and for 4-QAM, 8-QAM and 16-QAM, the optical path can have, 11, 4 and 1 cascaded WSSs, respectively, which are lower values than the ones we obtained without frequency offset in Figure 3.20.

If we compare Figures 3.24 and 3.20, we observe an increase of the OSNR penalties due to the frequency offset. For example, for the 4-QAM, 28 GBd, ρ=0.1, 37.5 GHz, after 15 WSSs the OSNR penalty increase is 0.8 dB. The increase is even higher for higher order modulation formats. For 8-QAM, after 9 WSSs, the OSNR penalty increase is 3.8 dB. For 16-QAM, after 4 WSSs, the OSNR penalty increase is 4.1 dB. Hence, as the number of WSS increases, also rises the gap between the scenario with and without offset. These results presented in this section are similar to the ones obtained in Section 3.5.

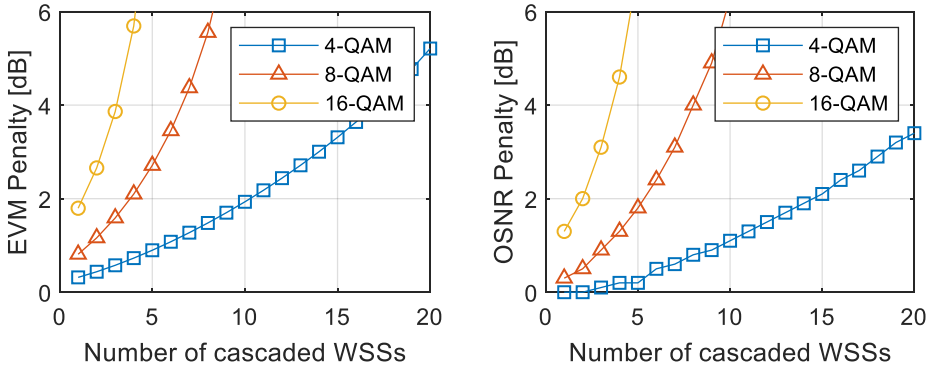

Figure 3.24 *EVM penalty (a) and OSNR penalty (b) of the center channel as a function of the number of cascaded WSSs. The -6 dB bandwidth of each WSS is 37.5 GHz. The R_S =28 GBd with ρ=0.1 using the 4-QAM, 8-QAM and 16-QAM modulation formats and Δf =37.5 GHz. The signal carriers are shifted by +1.5 GHz relative to the WSSs center frequency.*

3.8. Optical Transfer Function (OTF) variance

In this section, we assumed an OTF bandwidth not constant over the frequency range of the WSS. We based the simulations in this section under the assumption that the B_{otf} of the WSSs varies accordingly to a Gaussian distribution [3]. Hence, we consider a standard deviation of 0.1 GHz for the B_{otf}, which is a typical value [3].

We performed the simulations with the same parameters as in Section 3.4 and we did not find a different behavior of the optical communication system for the EVM penalty and OSNR penalty as a function of the number of WSSs in the cascade.

Hence, the variation of the B_{otf} generated from a Gaussian distribution does not affect the optical signal in a noticeable way, after a cascade of 20 WSSs, when

compared to the scenario where the B_{otf} is constant, because the variance of B_{otf} is sufficiently small.

3.9. Conclusions

In this chapter, we presented how the EVM depends on symbol rate and on WSS bandwidth as we change the number of WSSs in the cascade, assuming ASE noise absence. We have concluded that, if we increase the number of cascaded WSSs in the optical path, to maintain the same EVM, then the symbol rate must be reduced. We also concluded that if we increase the number of cascaded WSSs, to maintain the same EVM, the bandwidth of each WSS must be increased.

We used two performance metrics, EVM penalty and OSNR penalty to study the performance of an isolated channel considering the effect of cascading WSS filters. We changed the symbol rate, the roll-off factor, the WSS bandwidth, the modulation format, and the number of WSSs in these studies. In general, we can state that the penalty is higher for the lower 37.5 GHz WSS bandwidth than for the 50 GHz with the same symbol rate. Likewise, for the 37.5 GHz WSS bandwidth, the penalty is higher when the symbol rate is increased. The higher roll-off factor makes the signal spectrum wider below the its -3 dB bandwidth, which also makes the signal experience higher performance penalties for its edge frequencies. For example, for the 4-QAM modulation format of a signal with 28 GBd, ρ=0.1 and each WSS with a -6 dB bandwidth of 37.5 GHz, after 15 WSSs, the OSNR penalty is 1.2 dB. For the 8-QAM, after 10 WSSs, the OSNR penalty is 1.5 dB. For the 16-QAM, after 5 WSSs, the OSNR penalty is 1.2 dB. For the 50 GHz WSS bandwidth, the penalties are practically null, independently of the symbol rate.

We have also concluded that the results from the super-Gaussian model are similar to the results obtained for the analytical model in terms of EVM penalty, OSNR penalty and PSD at the receiver.

In this work, we have also compared the EVM penalty and the OSNR penalty and we have found that they show similar behaviors with the increasing number of WSSs in several scenarios. However, the EVM penalty provides a higher penalty when compared with the OSNR penalty. Nevertheless, we can have a rough estimate of the performance of the signal as it traverses a cascade of WSSs. For example, for the 4-QAM, 28 GBd, ρ=0.1, 37.5 GHz, after 15 WSSs, the difference is 1.1 dB between the two metrics. For

the 8-QAM after 10 WSSs, the difference is 1.2 dB. For the 16-QAM after 5 WSSs, the difference is 0.8 dB.

By assuming that the OSNR penalty must be lower than 1.5 dB, we have observed a reduction on the number of WSSs that can be placed in the optical path as we increase the modulation format order. For a cascaded WSSs having each a -6 dB bandwidth of 37.5 GHz and considering a 28 GBd signal with ρ=0.1, for 4-QAM, 8-QAM and 16-QAM modulation formats, the optical path can have 15, 9 and 5 WSSs in a cascade, respectively. If we increase the roll-off factor to 0.3, these values are reduced to 12, 7 and 4 WSSs, respectively.

We also studied the impact of the existence of a frequency offset between the channel carrier and the WSSs center frequency. We conclude that this offset creates an impact on the edge frequencies of 28 GBd signal by reducing the number of traversed WSSs to keep the OSNR penalty below 1.5 dB, depending on the modulation format. The higher the modulation format order the lower is the number of traversed WSSs.

After studying the isolated channel, we have investigated the effect of a cascade of WSSs in the transmission of a 28 GBd signal in a center channel with side-channels spaced by 37.5 GHz. We changed the modulation format, the roll-off factor and the number of cascaded WSSs, but we have not found any performance degradation in relation to an isolated channel, because the crosstalk between carriers is negligible. We also studied the impact of the existence of a frequency offset between the three carriers and the WSSs center frequency. We conclude that this offset creates a performance degradation of the center channel, increasing the OSNR penalty similarly to the scenario without side-channels.

We have also concluded that the variation of B_{otf} due to not assuming a constant OTF bandwidth over the frequency range of the WSS, does not have any significant impact on the optical signal performance.

References

[1] A.Cartaxo and T. Alves, "Theoretical and experimental performance evaluation methods for DD-OFDM systems with optical amplification," *Journal of Microwaves, Optoelectronics and Electromagnetic Applications,* Vol. 10, No. 1, pp. 84-85, June, 2011.

[2] G. Bosco, V. Curri, A. Carena, P. Poggiolini and F. Forghieri, "On the performance of Nyquist-WDM terabit superchannels based on PM-BPSK, PM-QPSK, PM-8QAM or PM-16QAM subcarriers," *Journal of Lightwave Technology,* Vol. 29, No. 1, pp. 56-57, January 1, 2011.

[3] C. Pulikkaseril, L. A. Stewart, M. A. F. Roelens, G. W. Baxter, S. Poole, and S. Frisken, "Spectral modeling of channel band shapes in wavelength selective switches," *Optics Express,* Vol. 19, No. 9, April 2011.

Chapter 4

Study of the transmission of a superchannel through a cascade of WSSs

4.1. Introduction

In this chapter, we study the transmission of a superchannel with ten subchannels using the EVM and OSNR penalties as performance metrics. In Section 4.2, we characterize the superchannel with its 10 subchannels. For this superchannel, in Section 4.3, we optimize the WSS bandwidth and intercarrier spacing (subchannel frequency spacing) to be used in different scenarios. In Section 4.4, we use the EVM and OSNR penalties as performance metrics to study the performance degradation imposed on center and edge subchannels of the superchannel under study due to optical filtering and due to inter-subchannel crosstalk. In Section 4.5, we study the impact on center and edge subchannels of a frequency offset within ITU-T maximum tolerance between the center frequency of a superchannel and the WSSs center frequency. In Section 4.6, we optimize the WSS bandwidth and the intercarrier spacing that provide the lowest OSNR penalty below 1.5 dB after 20 WSSs for center and edge subchannels, of a superchannel with a number of subchannels between 2 and 10. In Section 4.7, we calculate the spectral efficiency of a superchannel with 10 subchannels and compare with the spectral efficiency of optical channels independently routed. We also calculate the spectral efficiency of a superchannel with a number of subchannels between 2 and 10. In Section 4.8, we compare the transmission a superchannel with 2 subchannels with the transmission of a single channel with twice the symbol rate. Finally, in section 4.9, we present the conclusions of this chapter.

4.2. Superchannel with ten subchannels

We simulated a superchannel with ten subchannels, each transmitting symbols from a difference pseudo-random binary sequence. Since the idea behind superchannels is to increase the spectral efficiency, we tightly packed the 10 subchannels spectrum [1] for 4-QAM, 8-QAM and 16-QAM signals, with R_S =28 GBd and ρ=0.1. We should choose an intercarrier spacing Δf, so that the OSNR penalty due to crosstalk in the

subchannels is below a certain value, which is defined as 0.5 dB in [2] and 1.5 dB in [1]. In this work, we assumed a 1.5 dB limit for the center subchannels due to crosstalk and, in addition, likewise, we assumed the same 1.5 dB limit for the edge subchannels due to crosstalk and filtering, after a cascade of 20 WSSs. In this chapter, we consider 0 dBm as the launch power in each subchannel, the same we used in Chapter 3 for independently routed channels.

Each WSS in the cascade to be studied has a B_{otf}=8.5 GHz in the analytical model, as in the previous chapters. If we want to use the super-Gaussian model, its order can be determined similarly as previously done in Section 2.8. We present two numeric examples: for a -6 dB bandwidth of 300 GHz and 350 GHz, we can match the -6 dB bandwidth of the super-Gaussian model to the -6 dB bandwidth of the analytical model, after 20 WSSs. We concluded that the best match is achieved with the 33.5th and the 39.0th orders, respectively. With these orders, we have obtained similar simulations results with the analytical model and the super-Gaussian model.

In Figure 4.1, we can see the PSD of a superchannel with 10 tightly packed subchannels spaced by 28.9 GHz at the transmitter output. The choice of the intercarrier spacing and the choice of the WSS bandwidth to be used is explained in the next section.

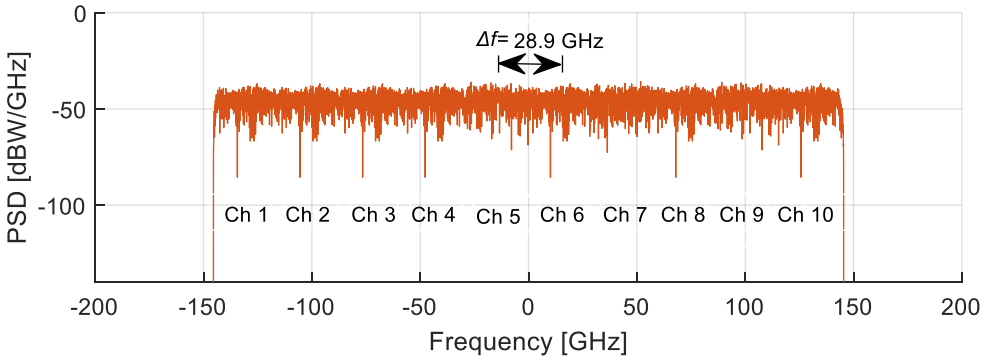

Figure 4.1 *PSD of the transmitted superchannel with 10 subchannels, each with R_S =28 GBd and ρ=0.1, for a 4-QAM modulation format with Δf =28.9 GHz. Each subchannel has been generated with a power of 0 dBm.*

In Figure 4.2 (a), we can see the PSD of the superchannel with 10 tightly packed subchannels after the first WSS and the transfer function of the first WSS filter with a -6 dB bandwidth of 300 GHz. In Figure 4.2 (b), we can see the signal PSD at the input of the optical receiver and the transfer function after 20 cascaded WSSs.

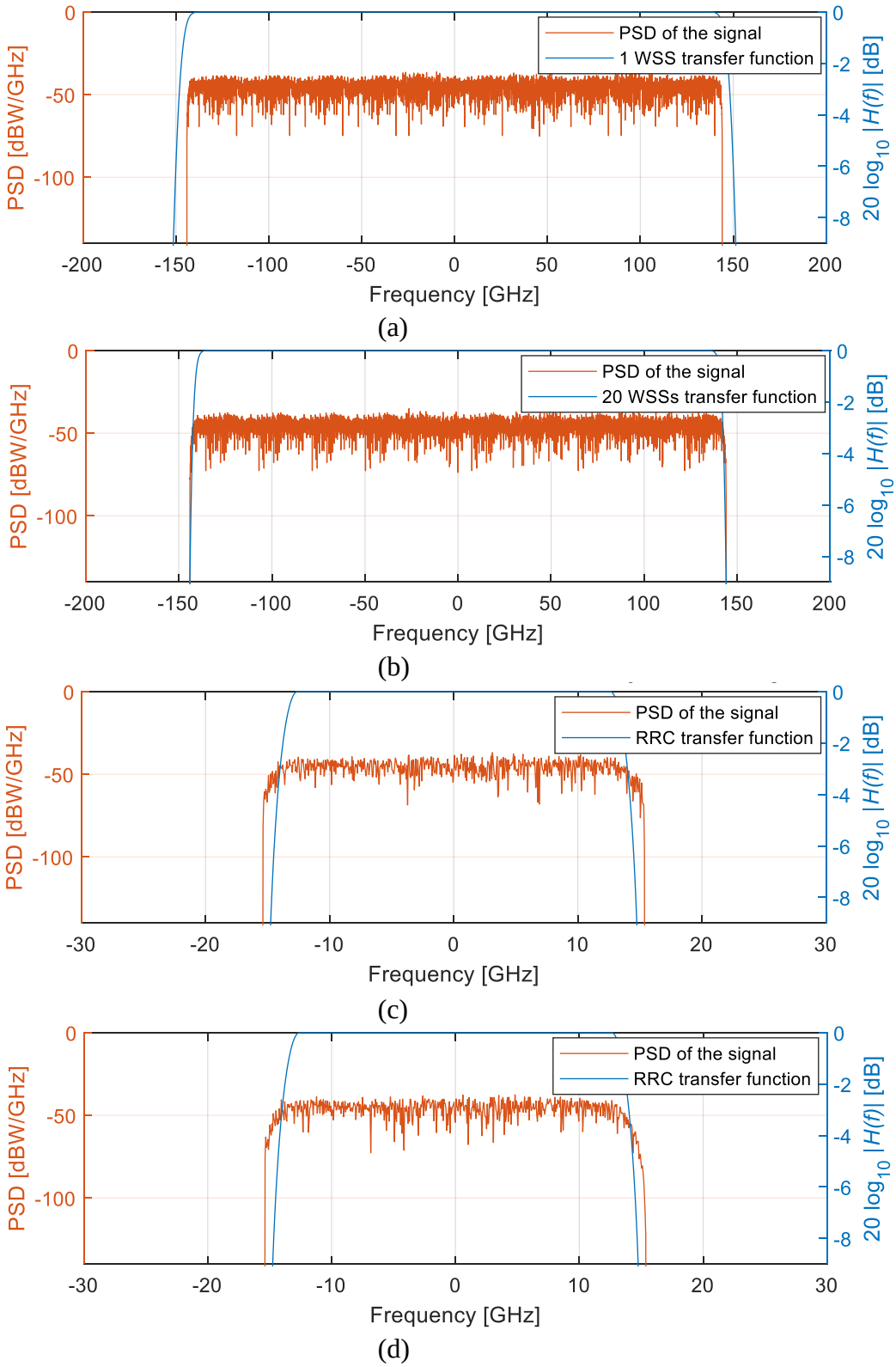

Figure 4.2 *PSD of the superchannel with 10 subchannels, where each subchannel uses 4-QAM modulation, R_S =28 GBd with ρ=0.1 and Δf=28.9 GHz. Each WSS has a -6 dB bandwidth of 300 GHz (a) PSD of the signal and the filter transfer function after the first WSS, (b) PSD of the signal at the optical receiver input and also the transfer function after 20 cascaded WSSs, (c) PSD of the signal after the RRC filter at the receiver and also the transfer function of the RRC filter, for a center subchannel and (d) for the right edge subchannel.*

In Figure 4.2 (c) and (d) we can see a center subchannel and the right edge subchannel, respectively, after being extracted from the superchannel using the RRC filter. The transfer function of the RRC filter is also displayed in Figure 4.2 (c) and (d). It is interesting to see the cascaded filter bandwidth narrowing effect looking at Figure 4.2 (a) and (b). Considering WSSs with a -6 dB bandwidth of 300 GHz, after 20 cascaded WSSs, we observed a narrowing -6 dB bandwidth of 286.8 GHz. The bandwidth narrows to 95.6% of its initial value. In Figure 4.2 (c), we see that the PSD of the signal is symmetrical around the center frequency, while in Figure 4.2 (d), we see that the right side of the signal spectrum has been distorted by the filtering of the WSS cascade.

4.3. Optimization of the intercarrier spacing

For the superchannel considered in the previous section, we now study the impact on the EVM and OSNR penalties when we change the intercarrier spacing. We must keep in mind that lower values of the WSS bandwidth will lead to too high OSNR penalties and larger values of the WSS bandwidth are a waste of the occupied spectrum. Studies are performed for a different number of cascaded WSSs, modulation formats, WSS bandwidths, symbol rates and roll-off factors. The goal of this study is to achieve the optimum intercarrier spacing, which provides the lowest OSNR penalty below a defined threshold, *e.g.* 1.5 dB, and after a specified number of WSSs, *e.g.* 20 WSSs.

Firstly, we perform the simulation for an edge subchannel, then for a center subchannel and, finally, we combine the results from the two subchannels and we find which is the optimum intercarrier spacing. Hence, the procedure has 3 steps:

1. We start by selecting a WSS bandwidth that is equal to the number of subchannels multiplied by the bandwidth of a single subchannel. Then, we change the intercarrier spacing using an interval of values around the bandwidth of a single subchannel and, for each intercarrier spacing in this interval, we investigate for an edge subchannel, if the OSNR penalty is below 1.5 dB, after 20 WSSs. Then, we decrease (or increase) the WSS bandwidth by 12.5 GHz (which is the frequency slot granularity of the flexible grid), until we achieve the lowest WSS bandwidth that guarantees OSNR penalties below a 1.5 dB after 20 WSSs for an edge subchannel. Hence, we find the lowest WSS bandwidth and an interval of acceptable intercarrier spacings. In the 2 subchannels case, we choose the intercarrier spacing from this interval, which delivers the lowest OSNR penalty and the procedure ends. If the superchannel

has more than 2 subchannels the procedure continues while retaining (for later use in step 3) the interval of acceptable intercarrier spacings just found.

2. For the WSS bandwidth selected in the previous step and for a center subchannel, we change the intercarrier spacing using the same values we used at the beginning of the previous step, and we obtain (for later use in step 3) the interval of acceptable intercarrier spacings that provides OSNR penalties below 1.5 dB after 20 WSSs.
3. The intersection of the two intervals obtained in the previous steps provides a new interval. Then, and only for intercarrier spacings in this interval, we add the OSNR penalties for the edge and center subchannels to obtain an added OSNR penalty for each intercarrier spacing. Finally, we select the intercarrier spacing that provides the lowest added OSNR penalty. Hence, we find the intercarrier spacing that provides the lowest OSNR penalty (below 1.5 dB) for all subchannels, after 20 WSSs.

With this procedure, all subchannels have the lowest OSNR penalty, below 1.5 dB, after 20 WSSs and the superchannel uses the lowest WSS bandwidth and, subsequently, has the highest spectral efficiency.

Figure 4.3 presents the EVM and OSNR penalties for subchannels with 28 GBd and ρ=0.1 with -6 dB bandwidth of 300 GHz for each WSS, for the 4-QAM, 8-QAM and 16-QAM modulation formats, for the right edge subchannel of a 10 subchannels superchannel. The EVM and OSNR penalties are presented for 5, 10, 15 and 20 WSSs, in Figure 4.3, as a function of the intercarrier spacing, which illustrates the step 1 of the procedure. From Figure 4.3, we can see that the penalty due to crosstalk increases as we lower the intercarrier spacing. On the other hand, the penalty increases due to WSS filtering for higher intercarrier spacings. An optimum intercarrier spacing for an edge subchannel is found at the lowest OSNR penalty due to a balance between these two effects, for a specified number of cascaded WSSs. Another result is that, for low intercarrier spacing, as we increase the number of WSSs, the penalty remains practically constant and independent of the number of WSSs. However, if we cross the optimum OSNR penalty value to higher intercarrier spacings, the effect of filtering start degrading the performance and the penalty becomes dependent on the number of WSSs traversed. The dependence of the EVM and OSNR penalties on the modulation format becomes evident for these larger intercarrier spacings. The penalty degradation becomes enhanced with higher modulation orders.

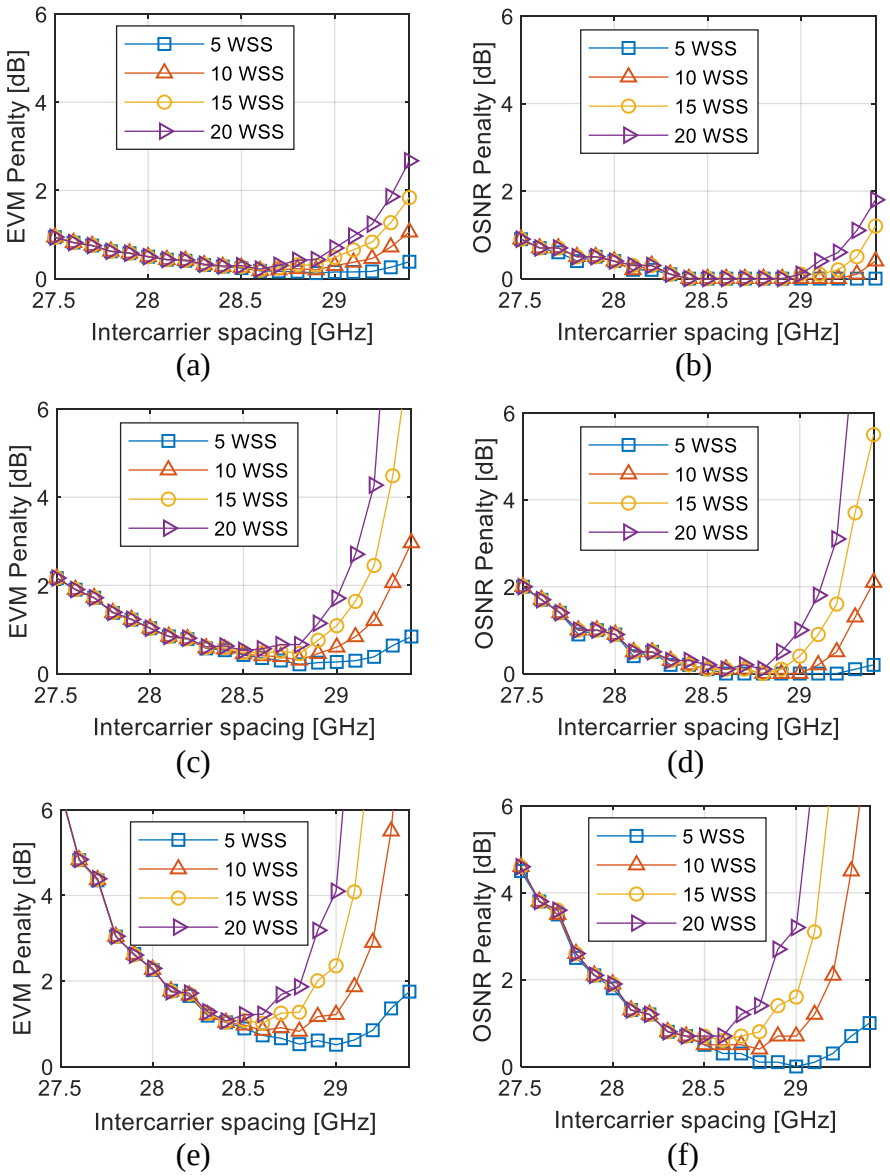

Figure 4.3 *EVM penalty (a), (c), (e) and OSNR penalty (b), (d), (f) dependence on the intercarrier spacing on the right edge subchannel after 5, 10, 15 and 20 WSSs. R_S =28 GBd with ρ=0.1 and a -6 dB bandwidth of 300 GHz, for each WSS in the cascade, for (a)(b) 4-QAM, (c)(d) 8-QAM and (e)(f) 16-QAM modulation formats.*

In Tables 4.1 and 4.2, we present the WSS bandwidth and intercarrier spacing that provides the lowest OSNR penalty below 1.5 dB, after 20 cascaded WSSs, considering only the edge subchannels, for 4-QAM, 8-QAM and 16-QAM for ρ=0.1 and ρ=0.3, respectively. In these two tables, we do not consider the penalty obtained in the center subchannels, which is analyzed next.

When we increase the modulation format order in Table 4.1, the intercarrier spacing stays constant or decreases by 0.1 GHz, but from Figure 4.3 we see that the OSNR penalty increases significantly, as expected. Also, from Tables 4.1 and 4.2, a higher roll-off factor of 0.3 demands higher -6 dB WSSs bandwidths and larger

intercarrier spacings that can achieve a difference of 2.4 GHz, for the 8-QAM and 16-QAM modulation format, than the ones obtained with a roll-off factor of 0.1.

Table 4.1 Optimum intercarrier spacing for R_S =28 GBd with ρ=0.1 using 20 cascaded WSSs considering the lowest OSNR penalties below 1.5 dB in the edge subchannels.

Modulation format	WSS bandwidth [GHz]	Intercarrier spacing [GHz]
4-QAM	300	28.6
8-QAM	300	28.6
16-QAM	300	28.5

Table 4.2 Optimum intercarrier spacing for R_S =28 GBd with ρ=0.3 using 20 cascaded WSSs considering the lowest OSNR penalties below 1.5 dB in the edge subchannels.

Modulation format	WSS bandwidth [GHz]	Intercarrier spacing [GHz]
4-QAM	312.5	29.9
8-QAM	325	31.0
16-QAM	325	31.0

Next, we perform a similar study for the center subchannels. Figure 4.4 presents the EVM and OSNR penalties for ρ=0.1 with -6 dB bandwidth of 300 GHz for each WSS, for the 4-QAM, 8-QAM and 16-QAM modulation formats, for a center subchannel. The EVM and OSNR penalties are presented for 5, 10, 15 and 20 WSSs in Figure 4.4, as a function of the intercarrier spacing, which illustrates the step 2 of the procedure. If we compare Figures 4.4 and 4.3, we see a completely different behavior due to the impact of the intercarrier spacing. For the center subchannels, the penalty decreases as we put the subchannels more far away in the frequency, which results in crosstalk reduction. Since the subchannel is not at the edge of the superchannel, it is not affected by the WSS filtering effect.

The difference between the EVM penalty and OSNR penalty for center and edge subchannels can attain 0.2 dB for penalties below 1.5 dB and otherwise can attain 1 dB.

Next, we add the penalties from the center and edge subchannels to find the lowest OSNR penalty for all subchannels.

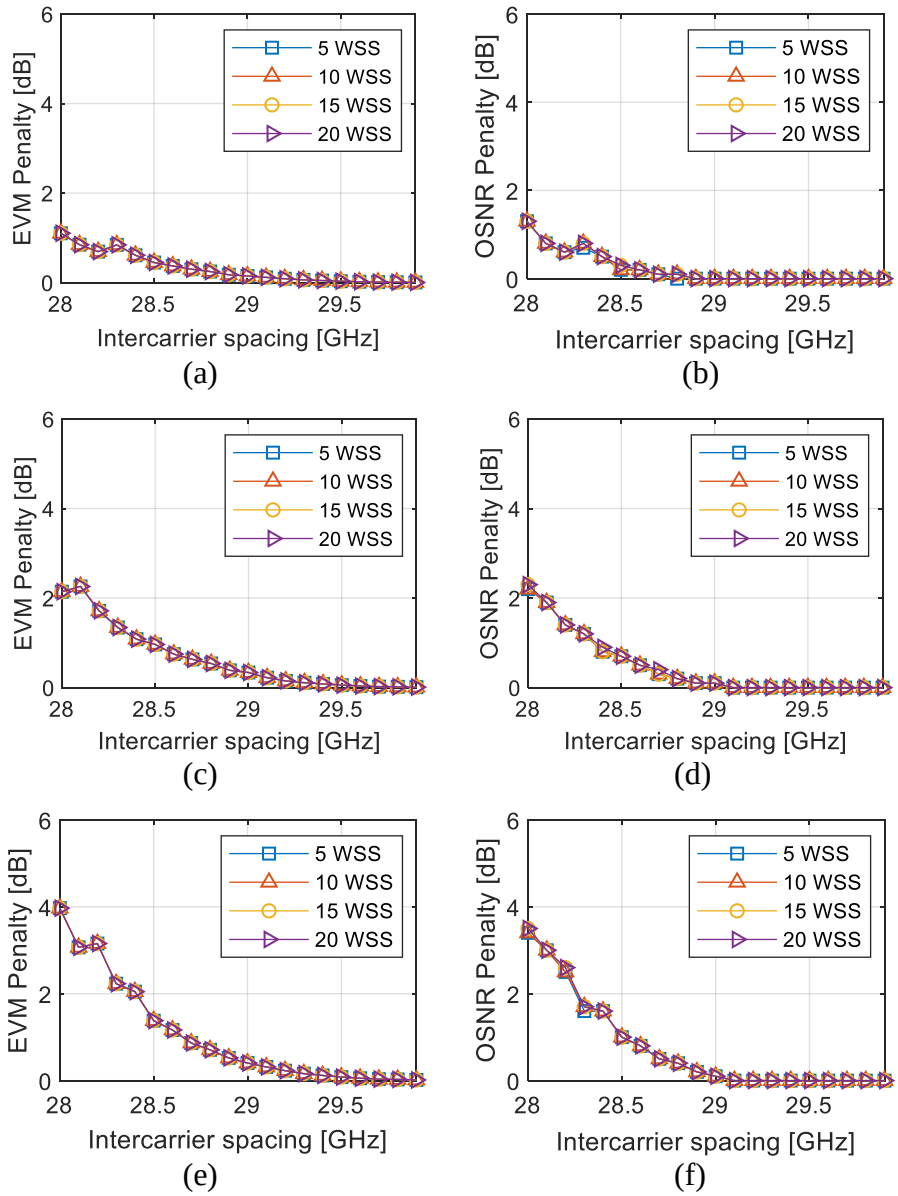

Figure 4.4 *EVM penalty (a) (c) (e) and OSNR penalty (b) (d) (f) dependence on the intercarrier spacing on a center subchannel after 5, 10, 15 and 20 WSSs. R_S =28 GBd with ρ=0.1 and a -6 dB WSS bandwidth of 300 GHz, for each WSS in the cascade, for (a)(b) 4-QAM, (c)(d) 8-QAM and (e)(f) 16-QAM modulation formats.*

Figure 4.5 shows the added EVM and OSNR penalties from the edge and center subchannels we obtained above, which illustrates the step 3 of the procedure.

From Figure 4.5, we see that for 8-QAM and 16-QAM the EVM penalty indicates the same optimum intercarrier spacing as the OSNR penalty, which is remarkable. For 4-QAM the difference is only 0.3 GHz.

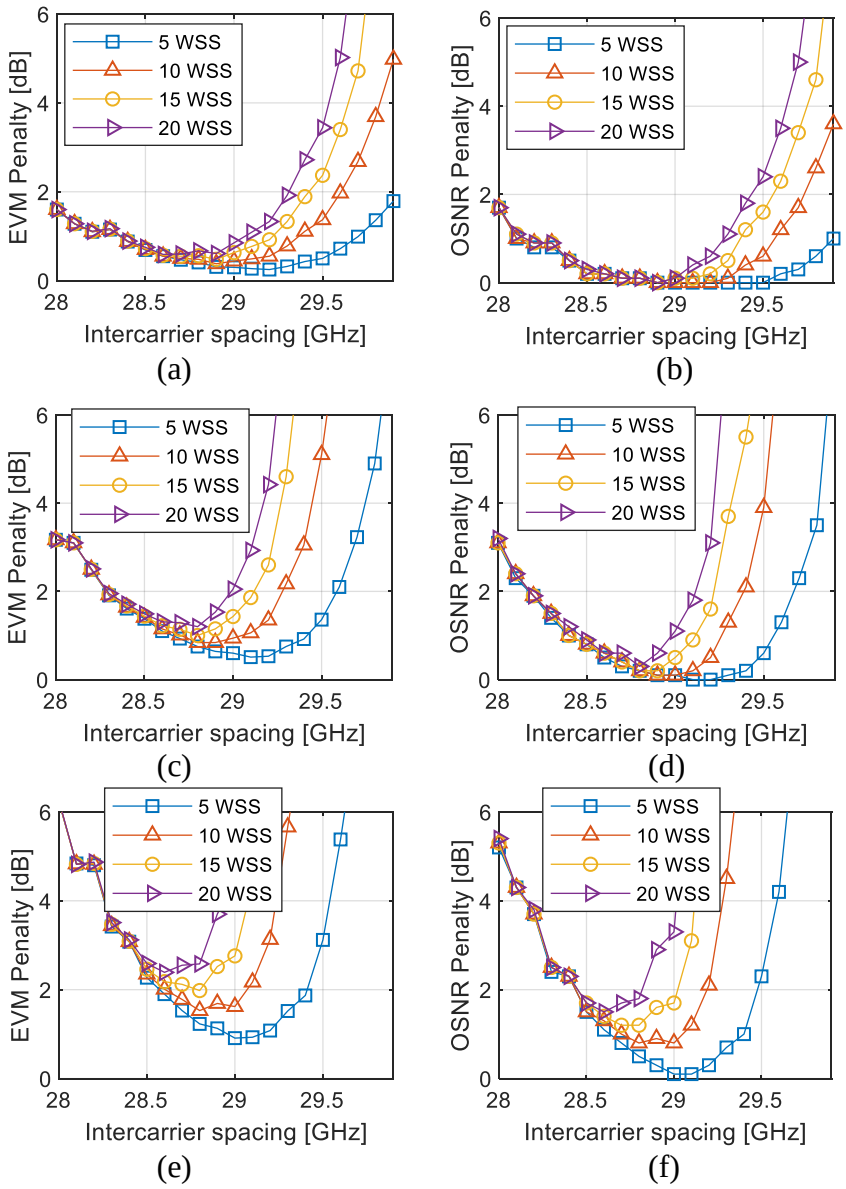

Figure 4.5 *Added EVM penalty (a) (c) (e) and added OSNR penalty (b) (d) (f) dependence on the intercarrier spacing. Added penalties from the penalties on a right edge and a center subchannels after 5, 10, 15 and 20 WSSs. R_S =28 GBd with ρ=0.1 and a -6 dB WSS bandwidth of 300 GHz, for each WSS in the cascade, for (a)(b) 4-QAM, (c)(d) 8-QAM and (e)(f) 16-QAM modulation formats.*

The optimized intercarrier spacings obtained are summarized in Tables 4.3 and 4.4, for ρ=0.1 and ρ=0.3, respectively, showing the optimum intercarrier spacings that achieves the lowest OSNR penalties below 1.5 dB after 20 WSSs for both edge and center subchannels.

Table 4.3 Optimum intercarrier spacing for R_S =28 GBd with ρ=0.1 using 20 cascaded WSSs, considering the lowest OSNR penalties below 1.5 dB in all subchannels.

Modulation format	WSS bandwidth [GHz]	Intercarrier spacing [GHz]
4-QAM	300	28.9
8-QAM	300	28.8
16-QAM	300	28.6

Table 4.4 Optimum intercarrier spacing for R_S =28 GBd with ρ=0.3 using 20 cascaded WSSs, considering the lowest OSNR penalties below 1.5 dB in all subchannels.

Modulation format	WSS bandwidth [GHz]	Intercarrier spacing [GHz]
4-QAM	312.5	30.3
8-QAM	325	31.3
16-QAM	325	31.3

When we increase the modulation format order in Tables 4.3 and 4.4, for the same WSS bandwidth, the intercarrier spacing stays constant or decreases by 0.1 or 0.2 GHz, but from Figure 4.5 we see that the OSNR penalty increases significantly, as expected. When we compare Tables 4.3 and 4.4 with Tables 4.1 and 4.2, we see that, in all scenarios, for the same WSS bandwidth we have to increase the intercarrier spacing so that for both center and edge subchannels, the lowest OSNR penalty is below 1.5 dB, after 20 WSSs. From Tables 4.3 and 4.4, we can also see that if we change the roll-off factor from ρ=0.1 to ρ=0.3, we have to choose a higher WSS bandwidth and intercarrier spacing, which is understandable because the signal occupies more bandwidth.

4.4. EVM and OSNR penalties for a superchannel

After optimizing the intercarrier spacing, we now use the performance metrics, EVM and OSNR penalties to study the superchannel performance in presence of crosstalk and signal distortion due to filtering in the cascade of WSSs. For a -6 dB WSS bandwidth of 300 GHz, we use subchannels using 4-QAM with Δf=28.9 GHz, 8-QAM with Δf=28.8 GHz and 16-QAM with Δf=28.6 GHz, which are extracted from Table 4.3. Figures 4.6 and 4.7 show the EVM and OSNR penalties as a function of the number of WSSs for a center and edge subchannels, respectively, for ρ=0.1 and a -6 dB WSS bandwidth of 300 GHz. In Figure 4.6, the OSNR penalty is always below 1.5 dB for the center subchannel for the three modulation formats. In Figure 4.6, we can observe that the OSNR penalty is practically constant due to the crosstalk between adjacent

subchannels along the cascaded WSSs. This penalty is not affected by the filtering and it is only related to the crosstalk between the subchannels. In any center subchannel of the superchannel, we obtain similar results. Figure 4.7 shows that the OSNR penalty is below 1.5 dB for the edge subchannel, even after the cascade of 20 WSSs.

For the edge subchannel, we observe in Figure 4.7, that the OSNR increases with the number of cascaded WSSs. This effect is especially notorious for the 16-QAM. As we have already observed in Chapters 2 and 3, higher modulation formats are more sensitive to the effect of narrow optical filtering.

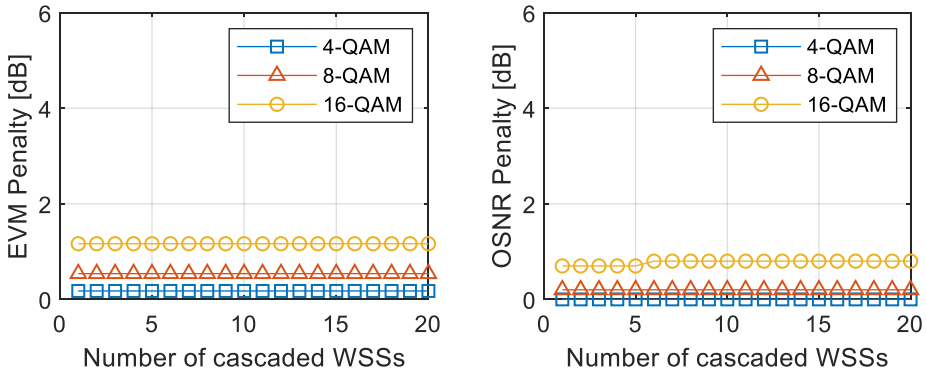

(a) (b)

Figure 4.6 *EVM penalty (a) and OSNR penalty (b) of a center subchannel as a function of the number of cascaded WSSs. R_S =28 GBd with ρ=0.1 and the -6 dB WSS bandwidth is 300 GHz, using 4-QAM with Δf=28.9 GHz, 8-QAM with Δf=28.8 GHz and 16-QAM with Δf=28.6 GHz.*

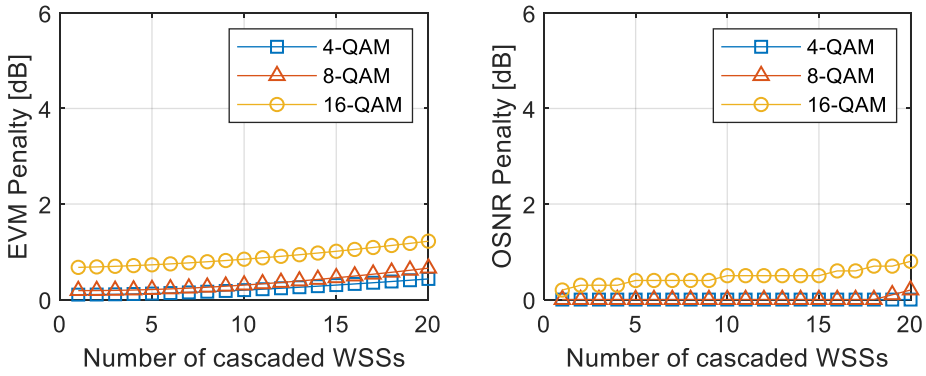

(a) (b)

Figure 4.7 *EVM penalty (a) and OSNR penalty (b) of an edge subchannel as a function of the number of cascaded WSSs. The R_S =28 GBd with ρ=0.1 and the -6 dB WSS bandwidth is 300 GHz, using the 4-QAM with Δf=28.9 GHz, 8-QAM with Δf=28.8 GHz and 16-QAM with Δf=28.6 GHz.*

In Figure 4.8 (a), we can see the PSD of the superchannel with the 10 tightly packed subchannels after the first WSS. Also displayed is the transfer function of the first WSS filter with -6 dB bandwidth of 312.5 GHz. Each subchannel considers R_S =28

GBd with ρ=0.3, 4-QAM and Δf=30.3 GHz. In Figure 4.8 (b), we can see the PSD at the input of the optical receiver and the equivalent filters transfer function after a cascade of 20 WSSs. In Figure 4.8 (c), we can see a center subchannel after being extracted from the superchannel and in Figure 4.8 (d) we can see the right edge subchannel after being extracted from the superchannel. The transfer function of the RRC filter is also displayed in Figure 4.8 (c) and (d).

If we compare Figures 4.8 (a) and 4.2 (a), we can see that the transmitted signal with ρ= 0.3 uses more bandwidth and that the signal spectrum has less frequency margin with respect to the filter response in the cut-off bandwidth. When we compare Figures 4.8 (c) and 4.2 (c), it is clear that the increase of the roll-off factor has a more detrimental effect on the PSD of the signal, since more signal frequencies are removed after WSS filtering.

We can also see the filter bandwidth narrowing effect looking at Figure 4.8 (a) and (b), with each WSS having a -6 dB bandwidth of 312.5 GHz after 20 cascaded WSSs, we observed a narrowing of the equivalent filter -6 dB bandwidth of 299.4 GHz. The bandwidth narrows to 95.8% of its initial value. It should be emphasized that, in absolute values, the narrowing is similar to the single channel case, for the 37.5 GHz or 50 GHz channel spacings. In relative values, the impact is much higher for a single channel in which the bandwidth narrowing are 64.9 % for 37.5 GHz and 73.6% for 50 GHz, as we saw in Chapter 3, which is much less than 95.8% for 312.5 GHz or 95.6% for 300 GHz -6 dB bandwidths. If we select the appropriate WSS bandwidth and intercarrier spacing, we can achieve less severe impairments for the edge subchannels in comparison with the single channel as in [3].

In Figure 4.8 (c), we see that PSD of the received signal is symmetrical around the center frequency while in Figure 4.8 (d), we see that the right side of the spectrum has been distorted by the WSS filtering.

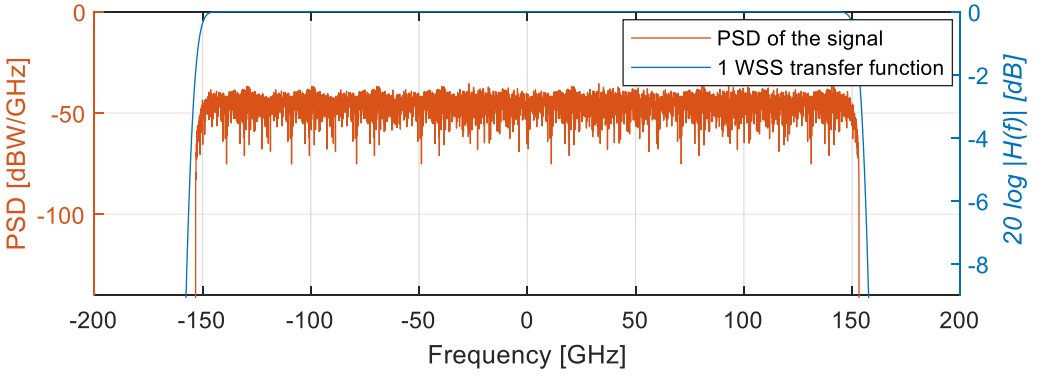

(a)

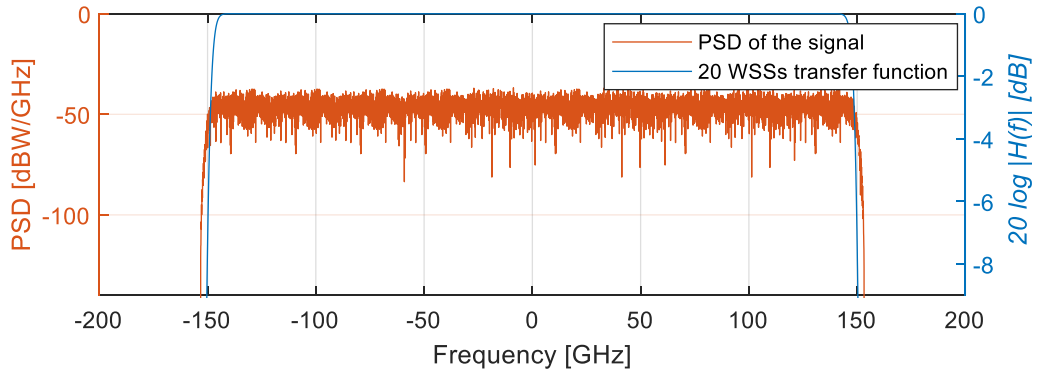

(b)

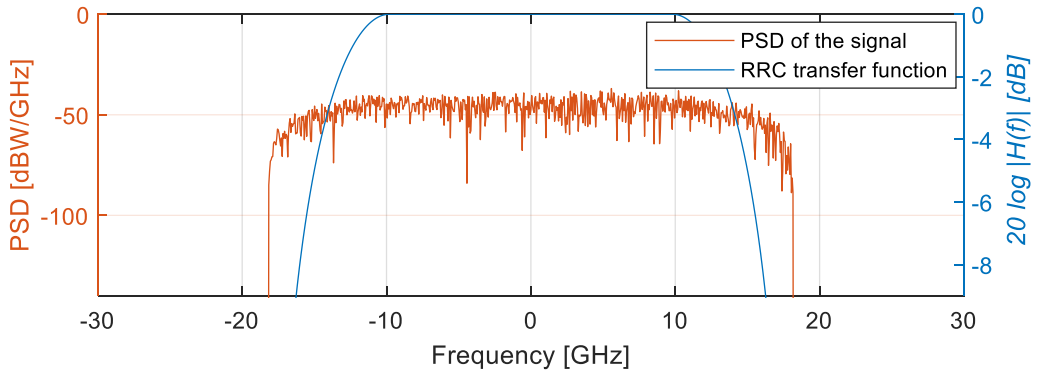

(c)

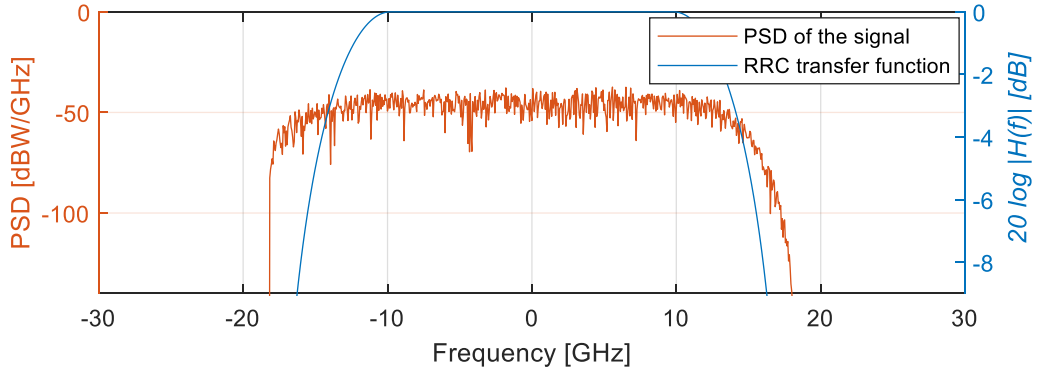

(d)

Figure 4.8 *PSD of a superchannel, with 10 subchannels using 4-QAM for R_S =28 GBd, ρ=0.3 and Δf =30.3 GHz. Each WSS has a -6 dB bandwidth is 312.5 GHz (a) the PSD of the signal and the filter transfer function after the first WSS, (b) the PSD of the signal at the optical receiver input and also the transfer function, both after 20 cascaded WSSs, (c) the PSD of the signal after the RRC filter at the receiver and also the transfer function of the RRC filter, for a center subchannel and (d) for the right edge subchannel.*

Next, we present the performance metrics, EVM and OSNR penalties obtained for ρ=0.3. In Figure 4.9, we see the results for a center subchannel, where the OSNR penalty is below 1.5 dB and the -6 dB WSS bandwidth is 312.5 GHz, using 4-QAM with Δf=30.3 GHz. The -6 dB WSS bandwidth is 325 GHz when using 8-QAM and 16-QAM both with Δf=31.3 GHz. In Figure 4.9, it should be noted that the OSNR penalty is practically constant along the whole cascade. This conclusion is similar to the scenario with ρ=0.1.

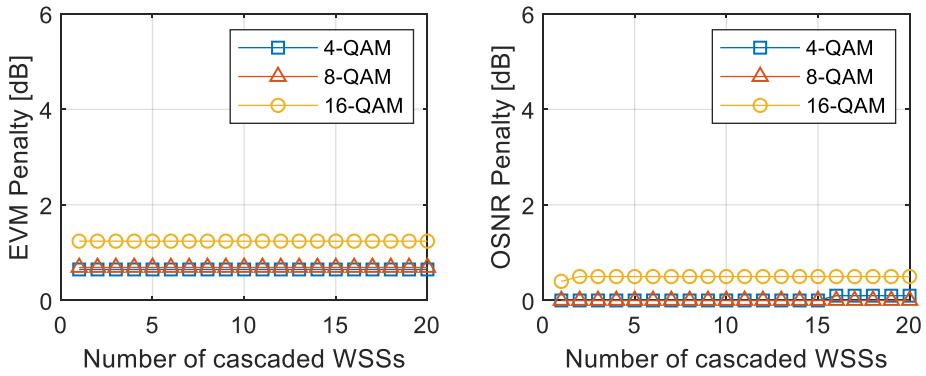

Figure 4.9 *EVM penalty (a) and OSNR penalty (b) of a center subchannel as a function of the number of cascaded WSSs, R_S =28 GBd, ρ=0.3, -6 dB WSS bandwidth of 312.5 GHz, using 4-QAM with Δf=30.3 GHz. The -6 dB WSS bandwidth is 325 GHz when using 8-QAM and 16-QAM both with Δf=31.3 GHz.*

In Figure 4.10, we show the results obtained for the edge subchannel, where the OSNR penalty is below 1.5 dB even after 20 WSSs.

For a signal in the edge subchannel, we observe in Figure 4.10, that the OSNR penalty increases for a higher number of WSSs. Again, this conclusion is similar to the one found with ρ=0.1.

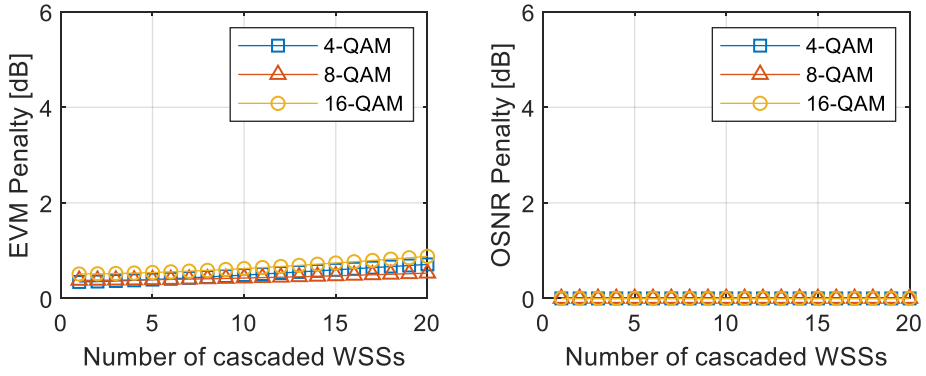

Figure 4.10 *EVM penalty (a) and OSNR penalty (b) of the edge subchannel as a function of the number of cascaded WSSs, R_S =28 GBd, ρ=0.3, -6 dB WSS bandwidth of 312.5 GHz, using 4-QAM with Δf=30.3 GHz. The -6 dB WSS bandwidth is 325 GHz when using 8-QAM and 16-QAM both with Δf=31.3 GHz.*

In Figures 4.6, 4.7, 4.9, 4.10, we must keep in mind that the WSS bandwidth changes with the modulation format.

In Tables 4.5 and 4.6 we present the OSNR penalties in the center and edge subchannels after 20 cascaded WSSs for the optimized intercarrier spacing, for R_S =28 GBd and ρ=0.1 and ρ=0.3, respectively.

Table 4.5 Intercarrier spacing and the lowest OSNR penalty after 20 cascaded WSSs, for R_S =28 GBd, ρ=0.1, considering OSNR penalties below 1.5 dB in all subchannels.

Modulation format	WSS bandwidth [GHz]	Intercarrier spacing [GHz]	Center subchannel OSNR penalty [dB]	Edge subchannel OSNR penalty [dB]
4-QAM	300	28.9	0	0
8-QAM	300	28.8	0.2	0.2
16-QAM	300	28.6	0.8	0.8

Table 4.6 Intercarrier spacing and the lowest OSNR penalty after 20 WSSs for R_S =28 GBd, ρ=0.3, considering OSNR penalties below 1.5 dB in all subchannels.

Modulation format	WSS bandwidth [GHz]	Intercarrier spacing [GHz]	Center subchannel OSNR penalty [dB]	Edge subchannel OSNR penalty [dB]
4-QAM	312.5	30.3	0.1	0
8-QAM	325	31.3	0	0
16-QAM	325	31.3	0.5	0

When we compare Tables 4.5 and 4.6, we see that when we change from ρ=0.1 to 0.3, we have a larger bandwidth used by the superchannel. To keep the penalties below 1.5 dB, for 4-QAM, we need to increase the WSS bandwidth by 1 slot of 12.5 GHz, from 300 GHz to 312.5 GHz, but for 8-QAM and 16-QAM, we need to increase it by 2 slots of 12.5 GHz, from 300 GHz to 325 GHz to deal with the narrowing effect of the WSS cascade.

Then, we have also increased the symbol rate from 28 to 32.5 GBd and performed similar studies. The results are summarized in Tables 4.7 and 4.8, for ρ=0.1 and ρ=0.3, respectively, and considering a center subchannel and an edge subchannel, both with OSNR penalties below 1.5 dB after 20 WSSs. When we compare Tables 4.7 and 4.8 we observe a significant increase in the WSS bandwidth and intercarrier spacing due to a higher roll-off factor and, consequently, more used bandwidth. When we compare Tables 4.7 and 4.8 with Tables 4.5 and 4.6, we observe that an increase in the symbol rate imposes an increase on the -6 dB WSS bandwidth and on the intercarrier spacing, because each subchannel occupies more bandwidth.

Table 4.7 Intercarrier spacing and the lowest OSNR penalty after 20 cascaded WSSs for R_S =32.5 GBd with ρ=0.1, considering OSNR penalties below 1.5 dB in all subchannels.

Modulation format	WSS bandwidth [GHz]	Intercarrier spacing [GHz]	Center subchannel OSNR penalty [dB]	Edge subchannel OSNR penalty [dB]
4-QAM	337.5	32.7	0.3	0.4
8-QAM	337.5	32.6	1.1	0.9
16-QAM	350	33.5	0	0

Table 4.8 Intercarrier spacing and the lowest OSNR penalty after 20 cascaded WSSs for R_S =32.5 GBd with ρ=0.3, considering OSNR penalties below 1.5 dB in all subchannels.

Modulation format	WSS bandwidth [GHz]	Intercarrier spacing [GHz]	Center subchannel OSNR penalty [dB]	Edge subchannel OSNR penalty [dB]
4-QAM	350	34.0	0.6	0.2
8-QAM	362.5	35.3	0.3	0.2
16-QAM	375	36.4	0	0

4.5. Frequency offset for a superchannel

Now we study the impact of the existence of a frequency offset, within the ITU-T maximum tolerance, between the superchannel and the WSSs center frequency. As in Chapter 3, the frequency of all the lasers is shifted by +1.5 GHz, but now we have to consider center and edge subchannels.

As a summary of the results obtained, Tables 4.9 and 4.10 show, for ρ=0.1 and ρ=0.3, respectively, the lowest OSNR penalties below 1.5 dB obtained after 20 cascaded WSSs, for a center and an edge subchannels.

Table 4.9 Intercarrier spacing and the lowest OSNR penalty for a center and an edge subchannel after 20 WSSs and R_S =28 GBd with ρ=0.1 with a frequency offset of +1.5 GHz.

Modulation format	WSS bandwidth [GHz]	Intercarrier spacing [GHz]	Center subchannel OSNR penalty [dB]	Edge subchannel OSNR penalty [dB]
4-QAM	300	28.6	0.1	0
8-QAM	300	28.5	0.6	0.6
16-QAM	312.5	29.2	0	0

Table 4.10 Intercarrier spacing and the lowest OSNR penalty for a center and an edge subchannel after 20 WSSs and R_S =28 GBd with ρ=0.3 with a frequency offset of +1.5 GHz.

Modulation format	WSS bandwidth [GHz]	Intercarrier spacing [GHz]	Center subchannel OSNR penalty [dB]	Edge subchannel OSNR penalty [dB]
4-QAM	312.5	30.3	0	0.6
8-QAM	325	31.1	0.1	0
16-QAM	325	30.9	0.9	0.2

If we compare Tables 4.9 and 4.10 with Tables 4.5 and 4.6, after the 20 cascaded WSSs, there is a difference between the scenarios with offset and without offset. For the 16-QAM with ρ=0.1 there is an increase on the WSS bandwidth GHz because, in the edge subchannel, the frequency offset leads to the OSNR penalties above 1.5 dB. For the other cases, there is an increase of the lowest OSNR penalties and a change in the intercarrier spacings.

It is interesting to see that the OSNR penalty on the center subchannels increase although center subchannels are not affected by the WSS filtering. The explanation is because the intercarrier spacing was changed so that we can achieve the lowest OSNR penalty in all subchannels. This also explains why for the 4-QAM with ρ=0.1 and the 8-QAM with ρ=0.3, the OSNR penalty on the edge subchannel do not change but the OSNR penalty for the center subchannel increases.

4.6. Superchannels with a different number of subchannels

In this section, we change the number of subchannels in the superchannel from 2 to 10. In each case, we optimized the WSS bandwidth and intercarrier spacing with the goal of having a OSNR penalty of less than 1.5 dB, in all subchannels after a cascade of 20 WSSs. In this section, we consider that all superchannels have subchannels with roll-off factor of 0.1. The results obtained are presented in Tables 4.11 and 4.12, for R_S =28 GBd and R_S =32.5 GBd, respectively, with the corresponding lowest OSNR penalties for a center and an edge subchannels, for the 4-QAM modulation format.

Table 4.11 Intercarrier spacing and the lowest OSNR penalty after 20 cascaded WSSs for R_S =28 GBd with ρ=0.1, 4-QAM modulation format and considering OSNR penalties below 1.5 dB in all subchannels, for a different number of subchannels.

Number of subchannels	WSS bandwidth [GHz]	Intercarrier spacing [GHz]	Center subchannel OSNR penalty [dB]	Edge subchannel OSNR penalty [dB]
2	75	28.3	-	0
3	100	28.6	0	0
4	125	28.6	0.1	0.1
5	150	28.3	0.3	1.2
6	187.5	28.7	0	0
7	212.5	28.6	0	0
8	237.5	28.6	0.1	0.6
9	262.5	28.1	0.7	1.1
10	300	28.9	0	0

The average intercarrier spacing is 28.5 GHz for a superchannel with each subchannel with a 28 GBd, 4-QAM signal with ρ=0.1.

Table 4.12 Intercarrier spacing and the lowest OSNR penalty after 20 cascaded WSSs for R_S =32.5 GBd with ρ=0.1, 4-QAM modulation format and considering OSNR penalties below 1.5 dB in all subchannels, for a different number of subchannels.

Number of subchannels	WSS bandwidth [GHz]	Intercarrier spacing [GHz]	Center subchannel OSNR penalty [dB]	Edge subchannel OSNR penalty [dB]
2	75	33.1	-	0.3
3	112.5	33.1	0	0
4	137.5	32.6	0.6	1.4
5	175	32.8	0.1	0.1
6	212.5	33.1	0	0
7	237.5	32.8	0.2	0.7
8	275	32.9	0.1	0
9	300	32.1	0.9	0.8
10	337.5	32.7	0.3	0.4

The average intercarrier spacing is 32.8 GHz for a superchannel with each subchannel with a 32.5 GBd, 4-QAM signal with ρ=0.1.

From Tables 4.11 and 4.12 we can see that the intercarrier spacing is slight larger than the symbol rate. The OSNR penalties are equal between edge and center channel in almost all cases.

In Tables 4.13 and 4.14, we can see the results for the optimized WSS bandwidths, intercarrier spacing and the corresponding lowest OSNR penalties for a center and an edge subchannels for the 16-QAM modulation format.

When we compare with the 4-QAM scenario, we can observe an increase in the optimized intercarrier spacing that leads to the lowest OSNR penalty below 1.5 dB, because the 16-QAM signal is less robust in the presence of crosstalk and filtering. We have already seen that 16-QAM signal has a higher required OSNR at the receiver. So, in almost all cases, we have to increase the WSS bandwidth to ensure that the lowest OSNR penalty remains below 1.5 dB, since the 16-QAM modulation format is less tolerant to out-of-band crosstalk. For the 2 subchannels case, not only the intercarrier spacing increases, but also the WSS bandwidth has to be increased by 12.5 GHz to ensure the OSNR penalty limit.

Table 4.13 Intercarrier spacing and the lowest OSNR penalty after 20 cascaded WSSs for R_S =28 GBd with ρ=0.1, 16-QAM modulation format and considering OSNR penalties below 1.5 dB in all subchannels, for a different the number of subchannels.

Number of subchannels	WSS bandwidth [GHz]	Intercarrier spacing [GHz]	Center subchannel OSNR penalty [dB]	Edge subchannel OSNR penalty [dB]
2	87.5	28.9	-	0
3	100	29.1	0	0.3
4	137.5	29.0	0	0
5	162.5	29.1	0	0
6	187.5	29.0	0	0
7	225	28.8	0	0
8	250	29.0	0	0
9	275	29.1	0	0.2
10	300	28.6	0.8	0.8

The average intercarrier spacing is 29.0 GHz for a superchannel with each subchannel with a 28 GBd, 16-QAM signal with ρ=0.1.

Table 4.14 Intercarrier spacing and the lowest OSNR penalty after 20 cascaded WSSs for R_S =32.5 GBd with ρ=0.1, 16-QAM modulation format and considering OSNR penalties below 1.5 dB in all subchannels, for a different the number of subchannels.

Number of subchannels	WSS bandwidth [GHz]	Intercarrier spacing [GHz]	Center subchannel OSNR penalty [dB]	Edge subchannel OSNR penalty [dB]
2	87.5	33.2	-	0
3	112.5	33.5	0	0.2
4	150	33.5	0	0
5	187.5	33.5	0	0
6	212.5	33.5	0	0.5
7	250	33.5	0	0
8	287.5	33.4	0	0
9	312.5	33.0	0.7	0.3
10	350	33.5	0	0

The average intercarrier spacing is 33.4 GHz for a superchannel with each subchannel with a 32.5 GBd, 16-QAM signal with ρ=0.1.

From Tables 4.13 and 4.14 we can see that the intercarrier spacing is slight larger than the symbol rate. The OSNR penalties are equal between center and edge subchannels in all cases.

When we increase the modulation format order from 4-QAM to 16-QAM , for 28 GBd, the average intercarrier spacing increases from 28.6 to 29.1 GHz, and for 32.5 GBd, the average intercarrier spacing increases from 32.8 to 33.6 GHz.

4.7. Spectral efficiency

The spectral efficiency is defined by

$$SE = \frac{R_b}{B} \qquad (5.1)$$

where R_b is maximum binary information transmission capacity and B is the total bandwidth of the signal being either a superchannel or a single channel [4].

To transmit signals with 100 Gb/s in each independent channel with dual polarization (DP) 4-QAM, using a frequency slot of 37.5 GHz, we have a SE of 100/37.5=2.67 bit/s/Hz. If we increase the modulation format order to 8-QAM to transmit signals with 150 Gb/s in each channel, we obtain a SE of 150/37.5=4 bit/s/Hz. If we increase the modulation format order to 16-QAM to transmit signals with 200 Gb/s in each channel, we attain a SE of 200/37.5=5.33 bit/s/Hz. If we consider a frequency slot of 50 GHz, for 4-QAM, 8-QAM and 16-QAM, we obtain SE=2, 3 and 4 bit/s/Hz, respectively.

Since the idea behind the use of superchannels is to increase the SE, we now calculate the SE of the superchannel with 10 subchannels, we have been studying in this chapter. To transmit 10 subchannels at 100 Gb/s each, using DP 4-QAM, 28 GBd signal with ρ=0.1 and to ensure an OSNR penalty lower than 1.5 dB in all subchannels after 20 cascaded WSSs, each WSS must have a -3 dB bandwidth of 300 GHz, which gives a SE of 10x100/300=3.33 bit/s/Hz. If we increase the modulation order to 8-QAM to transmit 10 subchannels at 150 Gb/s, we obtain a SE of 10x150/300=5 bit/s/Hz. If we increase the modulation order to 16-QAM to transmit 10 subchannels of 200 Gb/s each, we attain a SE of 10x200/300=6.67 bit/s/Hz.

The SEs obtained for four scenarios are shown in Tables 4.15 and 4.16 for R_S =28 GBd and R_S =32.5 GBd, respectively. In the first scenario, the channels with a frequency slot of 50 GHz are not aggregated in a superchannel, *i.e.*, they are individually routed along the optical network. In the second scenario, the channels with a frequency slot of 37.5 GHz, are not aggregated. The third scenario is for superchannels with 10 subchannels and ρ=0.1 and the fourth scenario is for superchannels with ρ=0.3.

Table 4.15 Spectral efficiency values in bit/s/Hz for a superchannel with 10 subchannels, independently routed channels and R_S =28 GBd.

Modulation format	50 GHz grid	37.5 GHz grid	Superchannel with ρ=0.1	Superchannel with ρ=0.3
4-QAM	2.00	2.67	3.33	3.20
8-QAM	3.00	4.00	5.00	4.62
16-QAM	4.00	5.33	6.67	6.15

Table 4.16 Spectral efficiency values in bit/s/Hz for a superchannel with 10 subchannels, independently routed channels and R_S =32.5 GBd.

Modulation format	50 GHz grid	37.5 GHz grid	Superchannel with ρ=0.1	Superchannel with ρ=0.3
4-QAM	2.00	2.67	2.96	2.86
8-QAM	3.00	4.00	4.44	4.14
16-QAM	4.00	5.33	5.71	5.33

In Tables 4.17 and 4.18, for R_S =28 GBd and R_S =32.5 GBd, respectively, we calculate the transmission capacity attained in a single optical fiber, assuming that all C-band is available with its 4.8 THz bandwidth.

Table 4.17 Transmission capacity of C-band in Tb/s using superchannels with 10 subchannels and R_S =28 GBd.

Modulation format	50 GHz grid	37.5 GHz grid	Superchannel with ρ=0.1	Superchannel with ρ=0.3
4-QAM	9.6	12.8	16.0	15.4
8-QAM	14.4	19.2	24.0	22.2
16-QAM	19.2	25.6	32.0	29.5

From the comparison of these four scenarios, we see how a superchannel can increase the SE and capacity of transmission. If we compare the transmission capacity of the whole C-band using a scenario with 28 GBd, ρ=0.1 in a 37.5 GHz grid with the scenario using superchannels, we obtain for 4-QAM, 8-QAM and 16-QAM, an increased capacity of around 25%, which is substantial. If we compare the transmission capacity of scenario with 32.5 GBd, ρ=0.1, in a 50 GHz grid with the scenario using superchannels, we obtain for 4-QAM, 8-QAM and 16-QAM, an increase capacity of 48%, 48% and 43%, respectively, which is remarkable.

Table 4.18 Transmission capacity of C-band in Tb/s using superchannels with 10 subchannels and R_S =32.5 GBd.

Modulation format	50 GHz grid	37.5 GHz grid	Superchannel with ρ=0.1	Superchannel with ρ=0.3
4-QAM	9.6	12.8	14.2	13.7
8-QAM	14.4	19.2	21.3	19.9
16-QAM	19.2	25.6	27.4	25.6

Of course, we can increase even more these transmission capacities if we use a higher order modulation formats (32-QAM, 64-QAM) but at the cost of a reduced reach and the consequent increase in the number of regenerators [5].

Another way of increasing the SE is to reduce the FEC, which implies reducing the symbol rate and reducing the consumed bandwidth. This has a severe drawback because it imposes a lower BER at the receiver and, consequently, a higher required OSNR at the optical receiver input, which leads again to a reduced reach.

The reach could be increased, *e.g.*, if we lower the modulation format order from 16-QAM to 4-QAM and double the symbol rate, but the downside is the need to use optical and electrical components with twice the bandwidth, which are top-of-the-shelf and very expensive.

Now, we are going to calculate the spectral efficiency of the superchannels as a function of the number of subchannels. We consider all superchannels with subchannels having a 4-QAM modulation format with ρ=0.1. The results are presented in Tables 4.19 and 4.20, for R_S =28 GBd and R_S =32.5 GBd, respectively, with the corresponding -6 dB WSS bandwidths optimized previously, to guarantee the lowest OSNR penalties below 1.5 dB in all subchannels, after 20 cascaded WSSs.

Table 4.19 Spectral efficiency of a superchannel with a different number of subchannels, each with R_S =28 GBd with ρ=0.1, 4-QAM modulation format and considering OSNR penalties below 1.5 dB in all subchannels after 20 WSSs.

Number of subchannels	WSS bandwidth [GHz]	Spectral efficiency [bit/s/Hz]
2	75	2.67
3	100	3.00
4	125	3.20
5	150	3.33
6	187.5	3.20
7	212.5	3.29
8	237.5	3.37
9	262.5	3.43
10	300	3.33

The average spectral efficiency is 3.20 bit/s/Hz for a superchannel with each subchannel with a 28 GBd, 4-QAM signal with ρ=0.1.

Table 4.20 Spectral efficiency for a superchannel with a different number of subchannels, each with R_S =32.5 GBd with ρ=0.1, 4-QAM modulation format and considering OSNR penalties below 1.5 dB in all subchannels after 20 WSSs.

Number of subchannels	WSS bandwidth [GHz]	Spectral efficiency [bit/s/Hz]
2	75	2.67
3	112.5	2.67
4	137.5	2.91
5	175	2.86
6	212.5	2.82
7	237.5	2.95
8	275	2.91
9	300	3.00
10	337.5	2.96

The average spectral efficiency is 2.86 bit/s/Hz for a superchannel with each subchannel with a 32.5 GBd, 4-QAM signal with ρ=0.1.

Tables 4.19 and 4.20 are represented graphically in Figures 4.11 and 4.12. From Tables 4.19 and 4.20 or from Figures 4.11 and 4.12, we can see that almost all values of SE are higher for the 28 GBd case than for the 32.5 GBd case, for the same payload bit rate. The average value of the SE with respect to the number of subchannels is higher for the 28 GBd than for the 32.5 GBd. We should bear in mind that, for the 28 GBd case, we are requiring that the OSNR at the optical receiver input be higher than for the 32.5 GBd case, because the signal uses a smaller FEC and, consequently, a lower BER is required. Hence, the higher SE comes at the cost of a smaller link reach.

In this study, we selected the WSS bandwidth so that all subchannels have the lowest OSNR penalty below 1.5 dB after a cascade of 20 WSSs. Another possibility would be to choose WSS bandwidths that are integer multiples of 37.5 GHz or 50 GHz as in [6], where the authors did this choice to accommodate a less complex management of the routing and wavelength assignment than the one that would result from assigning integer multiples of 12.5 GHz. However, nowadays, the network operators try to avoid this dynamic number of subchannels [7] with its complex management. Hence, the SE presented in this work is a more pragmatic approach of the current network situation and it allows to offer an higher SE.

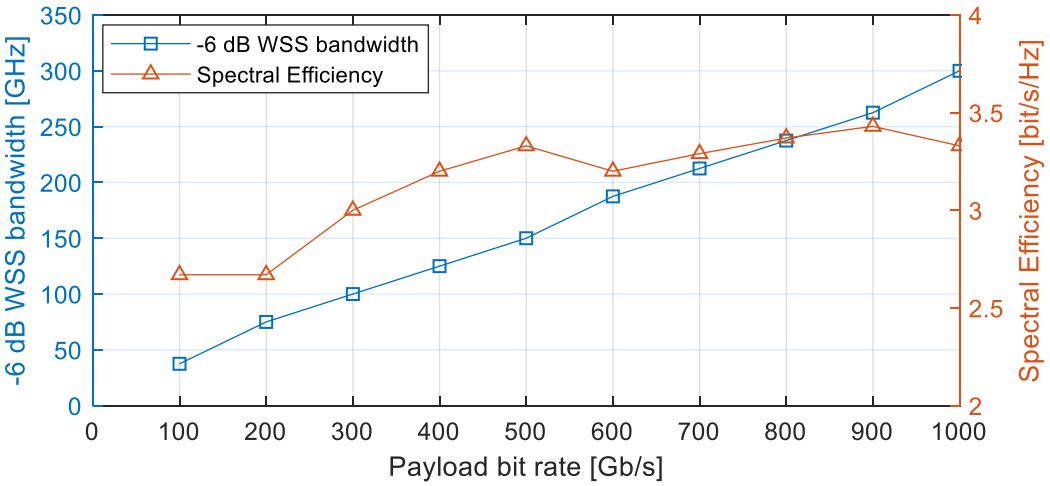

Figure 4.11 *Spectral efficiency and -6 dB WSS bandwidth as a function of the payload rate in each superchannel with a different number of subchannels, each with R_S =28 GBd with ρ=0.1, 4-QAM modulation format and guaranteeing OSNR penalties below 1.5 dB in all subchannels.*

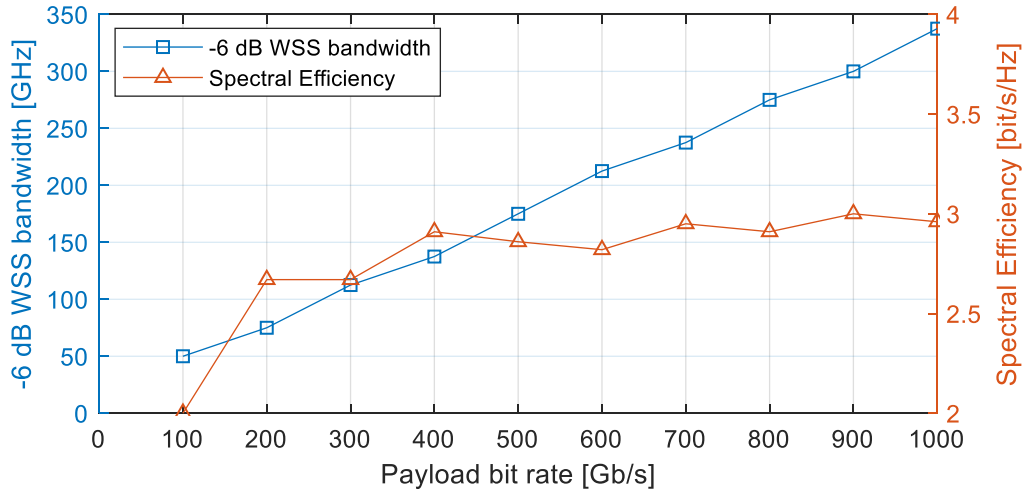

Figure 4.12 *Spectral efficiency and -6 dB WSS bandwidth as a function of the payload rate in each superchannel with a different number of subchannels, each with R_S =32.5 GBd with ρ=0.1, 4-QAM modulation format and guaranteeing OSNR penalties below 1.5 dB in all subchannels.*

4.8. Single channel with twice the symbol rate

Recently, the industry offers the possibility of doubling the usual symbol rates to values up to 69 GBd [8]. Moreover, the rate of implementation of superchannels by the network operators are slower than expected a few years ago, mainly because the difficulty in finding the most appropriated optical path through the optical network, since the superchannels need a spectral contiguity so that its bandwidth can be adapted to the traffic volume [7].

In this section, we compare two alternatives: using a channel with a 65 GBd signal and a superchannel with 2 subchannels, each with 32.5 GBd, both in a 75 GHz frequency slot. All signals have the same the FEC allowing the same pre-FEC BER=10^{-2}. The signals have the same 4-QAM modulation format and a roll-off factor of 0.1.

First, we need to have the reference values of BER, SNR and OSNR for 4-QAM modulation format with 65 GBd. From Table 2.5, we see that the theoretical result for the SNR is 7.33 dB for a BER= 10^{-2} and the 4-QAM modulation format. For R_s= 32.5 GBd the OSNR is 11.48 dB. Using Equation (2.22) we obtain the theoretical OSNR of 14.49 dB for R_s= 65 GBd to reach a BER=10^{-2}. Next, we checked the BER, SNR and OSNR estimation implemented in the simulator in a B2B configuration. The simulated results are 7.32 dB for SNR and 14.47 dB for OSNR, which are very close to the theoretical values. In Figure 4.13, we see the EVM and OSNR penalties results for the two scenarios, one channel with R_s= 65 GBd and a superchannel with 2 subchannels each with 32.5 GBd, ρ=0.1, 4-QAM modulation format, as a function of the number of cascaded WSSs, each with a -6 dB WSS bandwidth of 75 GHz. The superchannel has a intercarrier spacing of 33.1 GHz.

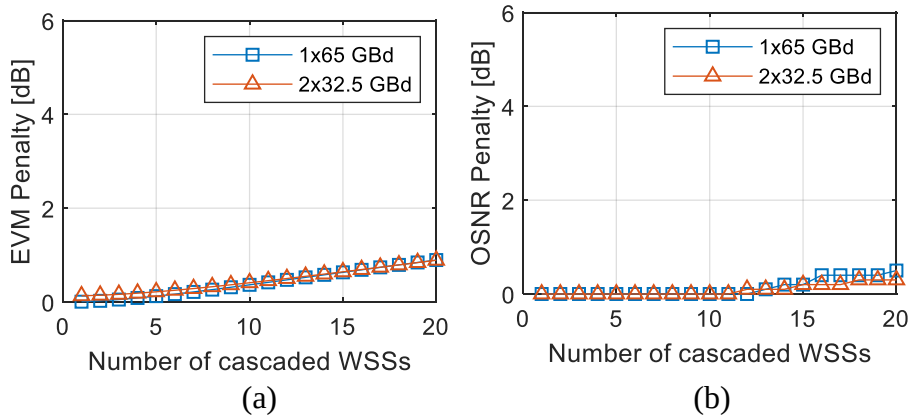

(a) (b)

Figure 4.13 *EVM penalty (a) and OSNR penalty (b) of a channel with 65 GBd and a superchannel with 2 subchannels each with 32.5 GBd, 4-QAM, ρ=0.1 as a function of the number of cascaded WSSs. The -6 dB WSS bandwidth is 75 GHz. The superchannel has Δf=33.1 GHz.*

Table 4.21 OSNR penalty after 20 cascaded WSSs for signals that have ρ=0.1, 4-QAM modulation format and Δf=33.1 GHz.

	OSNR penalty [dB]
Channel 1x65 GBd	0.5
Superchannel 2x32.5 GBd	0.3

From Figure 4.13, we extracted the OSNR penalties in both scenarios after 20 cascaded WSSs and we show them in Table 4.21. From Figure 4.13 and Table 4.21 we

see that the superchannel provides a 0.2 dB lower OSNR penalty than the single channel with 65 GBd, after 20 cascaded WSSs.

If we compare a 65 GBd signal using a frequency slot of 75 GHz, with two 32.5 GBd signals using two independently routed channels with 50 GHz each (studied in Chapter 2), we see a clear advantage in doubling the symbol rate, because it provides a better SE. We have 200 Gb/s in a 75 GHz frequency slot instead of 200 Gb/s in a 2x50=100 GHz frequency slot. However, when we compare the 65 GBd signal with the superchannel with two 32.5 GBd signals, using an equal 75 GHz frequency slot, we have the same SE and we see that the 65 GBd signal has only a 0.2 dB higher OSNR penalty.

If we increase the modulation format order to 16-QAM, we must increase the WSS bandwidth to 87.5 GHz, adjust the intercarrier spacing to 33.2 GHz and then perform the simulation again to obtain the OSNR penalty. After 20 WSSs, we obtain the results presented in Table 4.22. Both scenarios lead to a null OSNR penalty.

Table 4.22 OSNR penalty after 20 cascaded WSSs for signals that have ρ=0.1 and 16-QAM modulation format and Δf =33.2 GHz.

	OSNR penalty [dB]
Channel 1x65 GBd	0
Superchannel 2x32.5 GBd	0

Also for the 4-QAM scenario, the OSNR penalty difference between the two scenarios is negligible after 20 cascaded WSSs. Therefore, other factors should be used to help decide which option is the best. With a 65 GBd channel, it is necessary a single transceiver at each end of the optical path, while with the superchannel two are needed, although probably integrated in a single package. Additionally, the perceived capacity increase of the optical link in the future, the cost and how mature are the products offered by the manufacturers are also parameters to be considered in the design. Hence, both alternatives are valid and the choice remains with the network operator preference.

4.9. Conclusions

In this chapter, we have studied the transmission of a superchannel with ten subchannels along a cascade of 20 WSSs. This study has been performed by obtaining the EVM and OSNR penalties of center and edge subchannels of a superchannel. As a reference, we have set that the OSNR penalty should be below 1.5 dB for all subchannels. We obtained the intercarrier spacing that guarantees the lowest OSNR penalty for the lowest WSS bandwidth. We changed the WSS bandwidth, the intercarrier

spacing, the symbol rate, the modulation format, the roll-off factor, the number of cascaded WSSs and the WSS spectral model in these studies.

We have concluded that by increasing the order of the super-Gaussian filter, we can match accurately the transfer function of the analytical model, and obtain similar results.

We conclude that there is an OSNR penalty on center subchannels due only to crosstalk and that the OSNR penalty on edge subchannels is due to crosstalk and to the filter bandwidth narrowing effect.

When we increase the roll-off factor from 0.1 to 0.3, we have to increase the intercarrier spacing by 1.4 GHz for 4-QAM, 2.5 GHz for 8-QAM and 2.7 GHz for 16-QAM. We have also to increase the WSS bandwidth by one frequency slot of 12.5 GHz for 4-QAM, and 2 slots of 12.5 GHz for 8-QAM and 16-QAM, to reach OSNR penalties below 1.5 dB after 20 WSSs.

The penalty degradation remains practically constant for a center subchannel, as we increase the number of WSSs, while for an edge subchannel, this penalty is always increasing, with the number of cascaded WSSs.

The filter bandwidth narrowing effect of the cascade of WSSs narrows the bandwidth available for the signal, similarly to the scenario were we have one independently routed channel, although, a much lower impact is observed for the superchannels, because the WSS bandwidths are much larger than for an independently routed channel. Moreover, for the superchannel we can adjust the WSS bandwidth and intercarrier spacing to guarantee an OSNR penalty below 1.5 dB after 20 WSSs.

When we increased the symbol rate from 28 to 32.5 GBd, we observed that an increased intercarrier spacing was necessary and a larger WSS bandwidth is required.

We also studied the impact of the existence of a frequency offset within ITU-T maximum tolerance between the subchannels carriers and the WSS center frequency. We concluded that a shift of +1.5 GHz has an impact on the right edge frequencies of the superchannel. For a superchannel with 28 GBd and a roll-off factor of 0.1 in each subchannel, for 16-QAM, we observed an increase of the WSS bandwidth by 12.5 GHz, while for 4-QAM and 8-QAM only the intercarrier spacing is changed because of the frequency offset. The intercarrier spacing may increase or decrease depending on the balancing between the OSNR penalties of center and edge subchannels to achieve the lowest OSNR penalty for all subchannels.

If we select the appropriate WSS bandwidth and intercarrier spacing, we can achieve less severe impairments for the edge subchannels in comparison with the single channel for scenarios with or without frequency offset.

When we changed the number of subchannels from 2 up to 10, while keeping the OSNR penalty below 1.5 dB for all subchannels, using the 4-QAM and 16-QAM modulation formats for 28 GBd and 32.5 GBd, we have concluded that a higher symbol rate required, almost always, an higher WSS bandwidth and always a higher intercarrier spacing. When we increased the modulation format order, we also observed, almost always, an higher intercarrier spacing and higher WSS bandwidth, due to lower tolerance of higher modulation formats to bandwidth narrowing.

We have compared the SE when using superchannels with the scenario with channels not aggregated into superchannels. A superchannel with 10 subchannels, each with 28 GBd and a roll-off factor of 0.1, can attain a SE of 6.67 bit/s/Hz. For 32.5 GBd, a SE of 5.71 bit/s/Hz is possible. This increase in the SE creates a large increase in the transmission capacity, that can attain 32 Tb/s for the 28 GBd or 27.4 Tb/s for the 32.5 GBd scenario, assuming we are using the whole C-band. When we changed the number of subchannels between 2 and 10, we observed an average SE of 3.20 bit/s/Hz, for the 28 GBd case, and 2.86 bit/s/Hz, for the 32.5 GBd case.

At the end of the chapter, we have compared a superchannel with 2 subchannels of 32.5 GBd to the scenario with a single channel with twice the bandwidth, *i.e.*, 65 GBd. We observed a marginally lower OSNR penalty in the superchannel scenario. We can conclude that the best solution regarding the two scenarios depends on other factors and on the network operator design preferences.

References

[1] G. Bosco, V. Curri, A. Carena, P. Poggiolini and F. Forghieri, "On the performance of Nyquist-WDM terabit superchannels based on PM-BPSK, PM-QPSK, PM-8QAM or PM-16QAM subcarriers," *Journal of Lightwave Technology*, Vol. 29, No. 1, pp. 56-57, January 1, 2011.

[2] J. Pedro, "Designing transparent flexible-grid optical networks for maximum spectral efficiency (Invited)," *Journal of Optical Communications and Networking*, Vol. 9, No. 4, pp. C35-C40, April, 2017.

[3] J. M. Fabrega, "On the filter narrowing issues in elastic optical networks," *Journal of Optical Communications and Networking*, Vol. 8, No. 7, pp. 1-2, July, 2016.

[4] J. M. Simmons, "Optical Network Design and Planning", Springer, 2nd Edition, 2014, pp. 404-405.

[5] T. Rahman *et al.*, "Long-haul transmission of PM-16QAM-,PM-32QAM-, and PM-64QAM-based terabit superchannels over a field deployed legacy fiber," *Journal of Lightwave Technology*, Vol. 34, No. 13, pp. 3071-3076, July 1, 2016.

[6] M. Jinno, "Elastic optical networking: roles and benefits in beyond 100-Gb/s era (Invited Tutorial)," *Journal of Lightwave Technology*, Vol. 35, No. 5, pp. 1119-1120, March 1, 2017.

[7] T. Zami, B. Lavigne, and M. Bertolini, "How 64 GBaud optical carriers maximize the capacity in core elastic WDM networks with fewer transponders per Gb/s," *Journal of Optical Communications and Networking*, Vol. 11, No. 1, pp. A20-A30, January 2019.

[8] Coriant Inc., "The role of higher baud rates in evolving coherent transport", white paper, Coriant Inc., 2018, pp. 6-15.

Chapter 5

Conclusions and Future Work

In this chapter, the dissertation final conclusions and some suggestions for future work are presented.

5.1. Final conclusions

In Chapter 2 we have described the simulation model of an optical channel and we have compared the analytical and the super-Gaussian models to characterize the WSS filter used in ROADMs. We have shown how to set correctly the order of the super-Gaussian filter to achieve a good match of its transfer function with the analytical model. By choosing that both transfer functions have the same -6 dB bandwidth, the filter order that allows the best fitting can be more accurately established. We have also found that for a certain OTF bandwidth, the best filter order depends on the WSS bandwidth and also on the number of the cascaded WSSs. We observed that the higher the WSS bandwidth, the higher the order of the super-Gaussian transfer function.

We saw that the filter bandwidth narrowing effect due to a cascade of WSSs, having each a -6 dB bandwidth of 37.5 GHz leads to higher distortion on the signal edge frequencies than for a 50 GHz bandwidth filter. For a 32.5 GBd signal, this effect is more pronounced, because its bandwidth is larger than for a 28 GBd signal. We have shown that higher modulation format orders are less tolerant to the filtering effect, which limits the number of traversed WSSs.

Also in Chapter 2, we have presented the performance metrics used in this work, BER, EVM and OSNR. We have also showed a method to estimate the EVM penalty due to filtering and crosstalk in the simulation, without the need of generating ASE noise sample functions and we compared it with the OSNR penalty from Monte Carlo simulation.

In Chapter 3, we have studied the performance of an independently routed channel, with and without side-channels, as it traverses a cascaded of WSSs using the EVM and OSNR penalties as performance metrics. We have performed these studies by

changing the symbol rate, the roll-off factor, the WSS bandwidth, the modulation format and the number of cascaded WSSs. We have also concluded that the EVM and OSNR penalties obtained with the super-Gaussian model filter are almost identical to the ones obtained with the analytical model, if the parameters of the super-Gaussian are adequately chosen.

By comparison of the EVM penalty with the OSNR penalty, we have shown that they have similar behaviors with increasing number of WSSs for several different cases. The EVM penalty provides in general a higher penalty when compared with the OSNR penalty. For OSNR penalties below 1.5 dB, the difference can attain 0.8 dB. For higher penalties the difference between the estimates can reach 2 dB. The EVM penalty requires a much shorter computational time, when compared to a Monte Carlo simulation. As a reference, the simulation takes a few seconds to estimate the EVM penalty, while the OSNR penalty estimation can take many hours.

We have also studied the impact of a frequency offset between the frequency of the channel carrier and the WSS center frequency. We have concluded that this offset affects more significantly the edge frequencies of a 28 GBd signal by reducing the number of traversed WSSs, from 15 to 11 in comparison with the case of a null frequency offset for an independently routed channel with 4-QAM modulation format and a roll-off of 0.1, to keep an acceptable OSNR penalty below 1.5 dB. We have shown that this effect is more pronounced for higher modulation format orders, since the number of traversed WSSs is reduced from 9 to 4 for 8-QAM and from 5 to 1 for 16-QAM.

In Chapter 4, we have studied the transmission of a superchannel with ten subchannels, as it traverses a cascaded of WSSs using the EVM and OSNR penalties to estimate the performance of center and edge subchannels of a superchannel. We have chosen that all subchannels should have an OSNR penalty below 1.5 dB to ensure the system quality. We have changed the WSS bandwidth, the intercarrier spacing, the symbol rate, the modulation format, the roll-off factor, the number of cascaded WSSs and the WSS spectral model to perform these studies. We have noticed that the subchannels performance is significantly dependent on the intercarrier spacing. If too large, the edge subchannels suffer a higher distortion from the filtering cascade. If too narrow, it creates a considerable intercarrier crosstalk between the subchannels.

Furthermore, when we increase the signal roll-off factor from 0.1 to 0.3, for a 28 GBd signal with 4-QAM modulation format, we have to increase the intercarrier

spacing by 1.4 GHz and the WSS bandwidth by 12.5 GHz to achieve the lowest WSS bandwidth and the lowest OSNR penalty below 1.5 dB after 20 WSSs.

The filter bandwidth narrowing effect of the cascade of WSSs limits the bandwidth available for the superchannel, as in the scenario of one independently routed channel, although, we have observed a much lower impact on the performance of the superchannel, because the bandwidth of each WSS is much larger, more than 300 GHz, while for the independently routed channel it is only 37.5 GHz. Moreover, for the superchannel we can adjust the WSS bandwidth and intercarrier spacing to guarantee an OSNR penalty below 1.5 dB after 20 WSSs.

We have also studied the impact of a frequency offset within ITU-T maximum tolerance between the subchannels carriers of the superchannel and the WSSs center frequency. We have concluded that a frequency offset of +1.5 GHz distorts the right edge frequencies of the superchannel and to guarantee an OSNR penalty below 1.5 dB, the WSSs bandwidth may have to be increased and the intercarrier spacing adjusted, depending on the modulation format. As an example, for 28 GBd, 16-QAM with ρ=0.1, we had to increase the WSS bandwidth from 300 to 312.5 GHz and increase the intercarrier spacing from 28.6 to 29.2 GHz. However, for the 4-QAM and 8-QAM only the intercarrier spacing is changed because of the frequency offset. The intercarrier spacing may increase or decrease depending on the balancing between the OSNR penalties of center and edge subchannels to achieve the lowest OSNR penalty for all subchannels.

If we select the appropriate WSS bandwidth and intercarrier spacing, we can achieve less severe impairments for the edge subchannels in comparison with the single channel for scenarios with or without frequency offset.

Then, we have studied the influence of the number of subchannels from 2 to 10 on the cascaded filters performance, using the 4-QAM and 16-QAM modulation formats for 28 GBd and 32.5 GBd. We have optimized the intercarrier spacing for all these superchannels with the aim of having the lowest OSNR penalty below 1.5 dB for all subchannels after 20 WSSs. When we increased the modulation format order and the symbol rate, we have also observed in almost all situations, a higher intercarrier spacing and a higher WSS bandwidth to maintain the OSNR penalty below the 1.5 dB reference.

Then, we have also studied the SE of the optimized superchannels in relation to the scenario of independently routed channels. A superchannel with 10 subchannels, each with 28 GBd, 16-QAM and roll-off factor of 0.1, has a SE of 6.67 bit/s/Hz. For

32.5 GBd, a SE of 5.71 bit/s/Hz is attainable. The higher SE comes at the cost of a smaller number of WSSs, and possibly, a smaller link reach. We have concluded that the increase in the SE creates a significant growth in the transmission capacity of an optical fiber communication system. Assuming, we are using the whole C-band, the superchannels can attain 32 Tb/s for the 28 GBd case or 27.4 Tb/s for the 32.5 GBd case in comparison with the independently routed channels, which attain only 19.2 Tb/s or 25.6 Tb/s for a 50 GHz or 37.5 GHz grid, respectively.

Finally, we have compared the performance of a superchannel with 2 subchannels of 32.5 GBd to the performance of a single channel with twice the symbol rate, *i.e.*, 65 GBd. We have observed a negligible difference in the OSNR penalties obtained for both cases.

5.2. Future Work

Here some future work proposals are suggested:

- Improvement of the simulator by including a more realistic model of the receiver with its imperfections.
- Study the effects of signal propagation in the optical fiber.
- Investigation of the performance improvement of using a wave shaper to perform a pre-emphasis on the transmitted optical signal in order to compensate for the distortion induced by the bandwidth narrowing effect of the cascaded WSSs.
- Improvement of the simulator by including fiber nonlinear propagation effects using the simplified Gaussian noise model, which models signal distortion arising from fiber propagation as nonlinear interference noise.
- Study the influence of having subchannels with different QAM modulation formats in the same superchannel.
- Upgrade the simulator to include WDM superchannels in order to study the inter-superchannel interference.
- Improvement of the node model by using typical ROADM architectures, such as Broadcast & Select and Route & Select and considering specific add-drop features in such architectures.

Appendix A

Mathematical deduction of the bit error probability for 4-QAM over a AWGN channel

We present in this appendix the mathematical deduction of the bit error probability for symbols using the 4-QAM modulation format. The mapping used to convert groups of 2 bits into symbols is the Gray mapping, so that only one bit changes when we go from one signal point to another in its immediate neighborhood, as can be seen in detail in Chapter 2. The symbols are considered as equiprobables and are transmitted over a channel with AWGN.

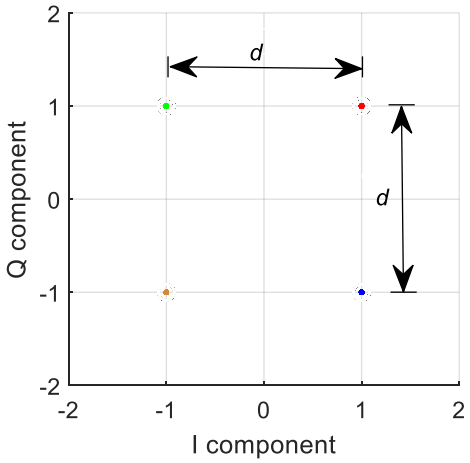

Figure A.1 *Modulation format: 4-QAM. In-phase and quadrature components of the constellation where each symbol has a color which is different from neighboring symbols and it is superimposed with the Euclidian distance between signal points.*

We represent, in Figure A.1, by d the minimum Euclidian distance between the signal points. We represent the energy of a symbol in the constellation by

$$E = \left(\frac{d}{2}\right)^2 + \left(\frac{d}{2}\right)^2 = \frac{d^2}{2} \tag{A.1}$$

We represent the average energy per symbol by

$$E_s = \frac{E + E + E + E}{4} = \frac{d^2}{2} \tag{A.2}$$

We represent the average energy per bit by

$$E_b = \frac{E_s}{log_2 M} = \frac{1}{2}\frac{d^2}{2} = \frac{d^2}{4} \tag{A.3}$$

where $M = 4$ is the number of symbols in the constellation.

If we consider a channel with AWGN, characterized by a variance $\sigma_N^2 = N_o/2$, the probability of a bit being wrongly detected can be shown to be given by [1]

$$P_b = Q\left(\frac{d_{th}}{\sigma_N}\right) \tag{A.4}$$

where $Q(\,)$ is the Q-function, which gives the area below the Gaussian probability density function (PDF) in the wrong decision region and d_{th} is the threshold distance which is the distance between the location of the highest value of Gaussian PDF and the wrong decision region.

If the received symbol crosses the decision threshold to another symbol decision region it is detected as another symbol. With the Gray mapping this means that only a wrong bit is received. We represent the symbol error probability of the 4-QAM symbols by

$$P = 2\,Q\left(\frac{d_{th}}{\sigma_N}\right) \tag{A.5}$$

considering an AWGN channel, σ_N^2 is the average noise power and d_{th} in our case is d/2. The factor 2 in Equation (A.5) is because we consider that are only 2 possible error detection scenarios.

We represent the average symbol error probability by

$$P_s = \frac{P + P + P + P}{4} = 2\,Q\left(\frac{d_{th}}{\sigma_N}\right) \tag{A.6}$$

We represent the average bit error probability by

$$P_b = \frac{P_s}{log_2 M} = \frac{1}{2}2\,Q\left(\frac{d_{th}}{\sigma_N}\right) = Q\left(\frac{d_{th}}{\sigma_N}\right) = Q\left(\sqrt{\frac{d_{th}^2}{\sigma_N^2}}\right) \tag{A.7}$$

From Figure A.1 and using Equation (A.3), we now calculate d_{th}^2

$$d_{th}^2 = \left(\frac{d}{2}\right)^2 = \frac{d^2}{4} = E_b \tag{A.8}$$

and E_b is also given by

$$E_b = \frac{s}{R_b} \tag{A.9}$$

where s is the signal power and R_b is the bit rate. We also know that

$$\sigma_N^2 = \frac{N_o}{2} \tag{A.10}$$

The noise power *n* can be related to the noise-equivalent bandwidth B_{eq} by

$$n = \frac{N_o}{2} B_{eq} \tag{A.11}$$

where N_o is the power spectral density of noise, and

$$B_{eq} = 2 R_s \tag{A.12}$$

where R_s is the symbol rate. Hence

$$\frac{N_o}{2} = \frac{n}{2 R_s} \tag{A.13}$$

Since for the *M*-ary modulation format we have

$$R_b = R_s log_2 M \tag{A.14}$$

where R_b is the bit rate. Hence

$$\frac{N_o}{2} = \frac{n}{R_b} \tag{A.15}$$

Using Equations (A.8) and (A.10) we can rewrite (A.7) as shown by

$$P_b = Q\left(\sqrt{\frac{E_b}{N_o/2}}\right) = Q\left(\sqrt{\frac{2\,E_b}{N_o}}\right) \tag{A.16}$$

Finally, using Equations (A.9) and (A.15) we can express (A.16) in the form

$$P_b = Q\left(\sqrt{\frac{s}{n}}\right) \tag{A.17}$$

The Q-function relates with the *erfc()* by

$$Q(x) = \frac{1}{2}\operatorname{erfc}\left(\frac{x}{\sqrt{2}}\right) \tag{A.18}$$

Using (A.18) we can express (A.17) in the alternative form

$$P_b = \frac{1}{2}\operatorname{erfc}\left(\sqrt{\frac{s}{2\,n}}\right) \tag{A.19}$$

Appendix B

Mathematical deduction of the bit error probability for 8-QAM (2-ASK/4-PSK) over a AWGN channel

We present in this appendix the mathematical deduction of the bit error probability for symbols using the 8-QAM (2-ASK/4-PSK) modulation format. The mapping used to convert groups of 3 bits into symbols is the Gray mapping, whenever possible. With the Gray mapping, only one bit changes when we go from one signal point to another in its immediate neighborhood. With this modulation format, we can not have a Gray mapping for all the signal points. As can be seen in detail in Chapter 2, there are four symbol pairs where more than one bit changes. The symbols are considered as equiprobables and are transmitted over a channel with AWGN.

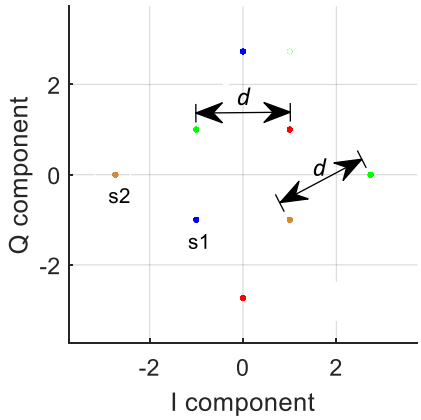

Figure B.1 *Modulation format: 8-QAM (2-ASK/4-PSK). In-phase and quadrature components of the constellation where each symbol has a color which is different from neighboring symbols and it is superimposed with the Euclidian distance between signal points.*

We represent, in Figure B.1, by d the minimum Euclidian distance between the signal points. We represent the energy of a symbol in the internal square of the constellation by

$$E_{s1} = \left(\frac{d}{2}\right)^2 + \left(\frac{d}{2}\right)^2 = \frac{d^2}{2} \tag{B.1}$$

We represent the energy of a symbol in the external square of the constellation by

$$E_{s2} = \left(\frac{d}{2} + \sqrt{d^2 - \left(\frac{d}{2}\right)^2} \right)^2 \tag{B.2}$$

We represent the average energy per symbol by

$$E_s = \frac{4\,E_{s1} + 4\,E_{s2}}{8} \tag{B.3}$$

$$E_s = \left(\frac{4 \cdot \frac{d^2}{2} + 4 \cdot \left(\frac{d}{2} + \sqrt{d^2 - \left(\frac{d}{2}\right)^2} \right)^2}{8} \right) = 3 + \sqrt{3} \tag{B.4}$$

since we use *d*=2.

We represent the average energy per bit by

$$E_b = \frac{E_s}{log_2 M} = \frac{3 + \sqrt{3}}{3} \tag{B.5}$$

where $M = 8$ is the number of symbols in the constellation.

If we consider a channel with AWGN, characterized by a variance $\sigma_N^2 = N_o/2$, the probability of a bit being wrongly detected can be shown to be given by [1]

$$P_b = Q\left(\frac{d_{th}}{\sigma_N}\right) \tag{B.6}$$

where $Q(\,)$ is the Q-function, which gives the area below the Gaussian probability density function (PDF) in the wrong decision region and d_{th} is the threshold distance which is the distance between the location of the highest value of Gaussian PDF and the wrong decision region.

If the received symbol crosses the decision threshold to another symbol decision region it is detected as another symbol. With the Gray mapping this would mean that only a wrong bit is received. However, for the 8-QAM (2-ASK/4-PSK) we can not have the advantage of the Gray mapping.

With the mapping used in Chapter 2, each symbol in the external square can have 2 erroneous transitions, one of them with only 1 wrong bit and the other with 2 wrong bits and we represent the symbol error probability by

$$P_{s2} = Q\left(\frac{d_{th}}{\sigma_N}\right) + 2\,Q\left(\frac{d_{th}}{\sigma_N}\right) = 3\,Q\left(\frac{d_{th}}{\sigma_N}\right) \tag{B.7}$$

In Equation (B.7), the 1st term is because of the 1 wrong bit and the 2nd term is because of the 2 wrong bits, which explains the factor 2. We are considering an AWGN channel, σ_N^2 is the average noise power and d_{th} in our case is *d/2*.

Each symbol in the internal square can have 4 erroneous transitions, 3 of them with only 1 wrong bit and the 4th with 2 wrong bits and we represent the symbol error probability by

$$P_{s1} = Q\left(\frac{d_{th}}{\sigma_N}\right) + Q\left(\frac{d_{th}}{\sigma_N}\right) + Q\left(\frac{d_{th}}{\sigma_N}\right) + 2\,Q\left(\frac{d_{th}}{\sigma_N}\right) = 5\,Q\left(\frac{d_{th}}{\sigma_N}\right) \tag{B.8}$$

We represent the average symbol error probability by

$$P_s = \frac{4\,P_{s1} + 4\,P_{s2}}{8} \tag{B.9}$$

$$P_s = \frac{4 \cdot 3\,Q\left(\frac{d_{th}}{\sigma_N}\right) + 4 \cdot 5\,Q\left(\frac{d_{th}}{\sigma_N}\right)}{8} = 4\,Q\left(\frac{d_{th}}{\sigma_N}\right) \tag{B.10}$$

We represent the average bit error probability by

$$P_b = \frac{P_s}{log_2 M} = \frac{1}{3}4\,Q\left(\frac{d_{th}}{\sigma_N}\right) = \frac{4}{3}Q\left(\frac{d_{th}}{\sigma_N}\right) = \frac{4}{3}Q\left(\sqrt{\frac{d_{th}^2}{\sigma_N^2}}\right) \tag{B.11}$$

From Figure B.1, we now calculate d_{th}^2

$$d_{th}^2 = \left(\frac{d}{2}\right)^2 = \frac{d^2}{4} = 1 \tag{B.12}$$

because we use *d*=2.

Rewriting Equation (B.5)

$$d_{th}^2 = 1 = \frac{3\,E_b}{3+\sqrt{3}} \tag{B.13}$$

and E_b is given by

$$E_b = \frac{s}{R_b} \tag{B.14}$$

where s is the signal power and R_b is the bit rate. We also know that

$$\sigma_N^2 = \frac{N_o}{2} \tag{B.15}$$

The noise power *n* can be related to the noise-equivalent bandwidth B_{eq} by

$$n = \frac{N_o}{2}\,B_{eq} \tag{B.16}$$

where N_o is the power spectral density of noise, and

$$B_{eq} = 2\,R_s \tag{B.17}$$

where R_s is the symbol rate. Hence

$$\frac{N_o}{2} = \frac{n}{2\,R_s} \tag{B.18}$$

Since for the *M*-ary modulation format we have

$$R_b = R_s log_2 M \tag{B.19}$$

where R_b is the bit rate. Hence

$$\frac{N_o}{2} = \frac{3\,n}{2\,R_b} \tag{B.20}$$

Using Equations (B.13) and (B.15) we can rewrite (B.11) as shown by

$$P_b = \frac{4}{3} Q\left(\sqrt{\frac{\frac{3\,E_b}{3+\sqrt{3}}}{N_o/2}}\right) = \frac{4}{3} Q\left(\sqrt{\frac{6}{3+\sqrt{3}}\frac{E_b}{N_o}}\right) \tag{B.21}$$

Finally, using Equations (B.14) and (B.20) we can express (B.21) in the form

$$P_b = \frac{4}{3} Q\left(\sqrt{\frac{2}{3+\sqrt{3}}\,\frac{s}{n}}\right) \tag{B.22}$$

The Q-function relates with the *erfc()* by

$$Q(x) = \frac{1}{2}\mathrm{erfc}\left(\frac{x}{\sqrt{2}}\right) \tag{B.23}$$

Using (B.23) we can express (B.22) in the alternative form

$$P_b = \frac{2}{3}\mathrm{erfc}\left(\sqrt{\frac{1}{3+\sqrt{3}}\,\frac{s}{n}}\right) \tag{B.24}$$

Appendix C

Mathematical deduction of the bit error probability for 16-QAM over a AWGN channel

We present in this appendix the mathematical deduction of the bit error probability for symbols using the 16-QAM modulation format. The mapping used to convert groups of 4 bits into symbols is the Gray mapping, so that only one bit changes when we go from one signal point to another in its immediate neighborhood, as can be seen in detail in Chapter 2. The symbols are considered as equiprobables and are transmitted over a channel with AWGN.

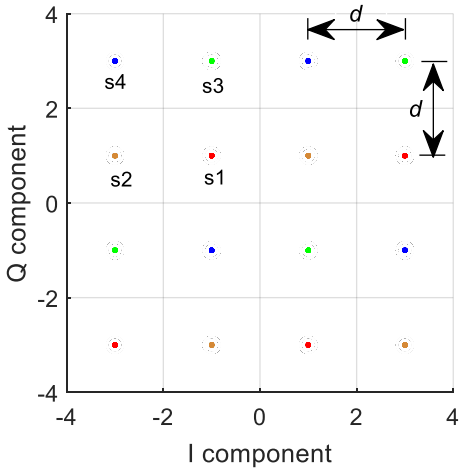

Figure C.1 *Modulation format: 16-QAM. In-phase and quadrature components of the constellation where each symbol has a color which is different from neighboring symbols and it is superimposed with the Euclidian distance between signal points.*

We represent, in Figure C.1, by d the minimum Euclidian distance between the signal points. We represent the energy of a symbol s1 in the constellation by

$$E_{s1} = \left(\frac{d}{2}\right)^2 + \left(\frac{d}{2}\right)^2 = \frac{d^2}{2} \tag{C.1}$$

We represent the energy of a symbol s2 by

$$E_{s2} = \left(\frac{3d}{2}\right)^2 + \left(\frac{d}{2}\right)^2 = \frac{5d^2}{2} \tag{C.2}$$

We represent the energy of a symbol s3 by

$$E_{s3} = \left(\frac{d}{2}\right)^2 + \left(\frac{3d}{2}\right)^2 = \frac{5d^2}{2} \quad \text{(C.3)}$$

We represent the energy of a symbol s4 by

$$E_{s4} = \left(\frac{3d}{2}\right)^2 + \left(\frac{3d}{2}\right)^2 = \frac{9d^2}{2} \quad \text{(C.4)}$$

We represent the average energy per symbol by

$$E_s = \frac{4\,E_{s1} + 4\,E_{s2} + 4\,E_{s3} + 4\,E_{s4}}{16} = \frac{5d^2}{2} \quad \text{(C.5)}$$

We represent the average energy per bit by

$$E_b = \frac{E_s}{log_2 M} = \frac{1}{4}\frac{5d^2}{2} = \frac{5d^2}{8} \quad \text{(C.6)}$$

where $M = 16$ is the number of symbols in the constellation.

If we consider a channel with AWGN, characterized by a variance $\sigma_N^2 = N_o/2$, the probability of a bit being wrongly detected can be shown to be given by [1]

$$P_b = Q\left(\frac{d_{th}}{\sigma_N}\right) \quad \text{(C. 7)}$$

where $Q(\,)$ is the Q-function, which gives the area below the Gaussian probability density function (PDF) in the wrong decision region and d_{th} is the threshold distance which is the distance between the location of the highest value of Gaussian PDF and the wrong decision region.

If the received symbol crosses the decision threshold to another symbol decision region it is detected as another symbol. With the Gray mapping this means that only a wrong bit is received. We represent the symbol error probability of the symbols s1 by

$$P_{s1} = 4\,Q\left(\frac{d_{th}}{\sigma_N}\right) \quad \text{(C.8)}$$

considering an AWGN channel, σ_N^2 is the average noise power and d_{th} in our case is *d/2*. The factor 4 in Equation (C.8) is because we consider that are only 4 possible error detection scenarios for symbol s1.

We represent the symbol error probability of the symbols s2 by

$$P_{s2} = 3\,Q\left(\frac{d_{th}}{\sigma_N}\right) \tag{C.9}$$

The factor 3 in Equation (C.9) is because we consider that are only 3 possible error detection scenarios for symbol s2.

We represent the symbol error probability of the symbols s3 by

$$P_{s3} = 3\,Q\left(\frac{d_{th}}{\sigma_N}\right) \tag{C.10}$$

The factor 3 in Equation (C.10) is because we consider that are only 3 possible error detection scenarios for symbol s3.

We represent the symbol error probability of the symbols s4 by

$$P_{s4} = 2\,Q\left(\frac{d_{th}}{\sigma_N}\right) \tag{C.11}$$

The factor 2 in Equation (C.11) is because we consider that are only 2 possible error detection scenarios for symbol s4.

We represent the average symbol error probability by

$$P_s = \frac{4\,P_{s1} + 4\,P_{s2} + 4\,P_{s3} + 4\,P_{s4}}{16} \tag{C.12}$$

$$P_s = \frac{4 \cdot 4\,Q\left(\frac{d_{th}}{\sigma_N}\right) + 4 \cdot 3\,Q\left(\frac{d_{th}}{\sigma_N}\right) + 4 \cdot 3\,Q\left(\frac{d_{th}}{\sigma_N}\right) + 4 \cdot 2\,Q\left(\frac{d_{th}}{\sigma_N}\right)}{16} = 3\,Q\left(\frac{d_{th}}{\sigma_N}\right) \tag{C.13}$$

We represent the average bit error probability by

$$P_b = \frac{P_s}{log_2 M} = \frac{1}{4}3\,Q\left(\frac{d_{th}}{\sigma_N}\right) = \frac{3}{4}Q\left(\frac{d_{th}}{\sigma_N}\right) = \frac{3}{4}Q\left(\sqrt{\frac{d_{th}^2}{\sigma_N^2}}\right) \tag{C.14}$$

From Figure C.1 and using Equation (C.6) we now calculate d_{th}^2

$$d_{th}^2 = \left(\frac{d}{2}\right)^2 = \frac{d^2}{4} = \frac{2}{5}E_b \tag{C.15}$$

and E_b is also given by

$$E_b = \frac{s}{R_b} \tag{C.16}$$

where s is the signal power and R_b is the bit rate. We also know that

$$\sigma_N^2 = \frac{N_o}{2} \tag{C.17}$$

The noise power *n* can be related to the noise-equivalent bandwidth B_{eq} by

$$n = \frac{N_o}{2} B_{eq} \tag{C.18}$$

where N_o is the power spectral density of noise, and

$$B_{eq} = 2 R_s \tag{C.19}$$

where R_s is the symbol rate. Hence

$$\frac{N_o}{2} = \frac{n}{2 R_s} \tag{C.20}$$

Since for the *M*-ary modulation format we have

$$R_b = R_s log_2 M \tag{C.21}$$

where R_b is the bit rate. Hence

$$\frac{N_o}{2} = \frac{2 n}{R_b} \tag{C.22}$$

Using Equations (C.15) and (C.17) we can rewrite (C.14) as shown by

$$P_b = \frac{3}{4} Q\left(\sqrt{\frac{\frac{2}{5} E_b}{N_o/2}}\right) = \frac{3}{4} Q\left(\sqrt{\frac{4}{5}\,\frac{E_b}{N_o}}\right) \tag{C.23}$$

Finally, using Equations (C.16) and (C.22) we can express (C.23) in the form

$$P_b = \frac{3}{4} Q\left(\sqrt{\frac{1}{5}\,\frac{s}{n}}\right) \tag{C.24}$$

The Q-function relates with the *erfc()* by

$$Q(x) = \frac{1}{2}\operatorname{erfc}\left(\frac{x}{\sqrt{2}}\right) \tag{C.25}$$

Using Equation (C.25) we can express (C.24) in the alternative form

$$P_b = \frac{3}{8}\operatorname{erfc}\left(\sqrt{\frac{s}{10\,n}}\right) \tag{C.26}$$

References

[1] J. G. Proakis, M. Salehi, “Chapter 7, Digital transmission through the additive white gaussian noise channel,” em *Communication Systems Engineering*, Prentice Hall, 2nd Edition, 2002, pp. 405-413.